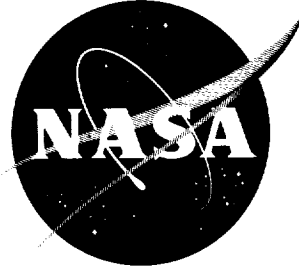


*80p.*

N 63 16 99 1

*code-1*



# TECHNICAL NOTE

D-1811

LONGITUDINAL RANGE ATTAINABLE BY THE CONSTANT-ALTITUDE  
VARIABLE-PITCH REENTRY MANEUVER INITIATED AT  
VELOCITIES UP TO ESCAPE VELOCITY

By E. Brian Pritchard

Langley Research Center  
Langley Station, Hampton, Va.

NATIONAL AERONAUTICS AND SPACE ADMINISTRATION  
WASHINGTON

June 1963

Code-1

CHOL 1 ME COPY

NATIONAL AERONAUTICS AND SPACE ADMINISTRATION

TECHNICAL NOTE D-1811

LONGITUDINAL RANGE ATTAINABLE BY THE CONSTANT-ALTITUDE

VARIABLE-PITCH REENTRY MANEUVER INITIATED AT

VELOCITIES UP TO ESCAPE VELOCITY

By E. Brian Pritchard

SUMMARY

The longitudinal range, traversed by a vehicle which maintains a constant-altitude flight path by pitch-angle modulation on both the low- and high-drag sides of the vehicle drag polar, is defined for initial maneuver velocities up to parabolic velocity. The vehicles considered operate on Newtonian drag polars and vary in maximum lift-drag-ratio capability from 0 to 2 and vehicle ballistic parameter from 10 to 200 pounds per square foot. The maneuver altitude variation was 150,000 to 240,000 feet.

As is to be expected, operation either at high altitude or high maximum lift-drag-ratio capability is required for appreciable longitudinal ranges to be achieved by the present maneuver. Approximately global ranges are found to be attainable by a vehicle having a maximum lift-drag ratio of 2.0 initiating the constant-altitude maneuver at parabolic velocity. Considerably longer ranges are shown to be available if the constant-altitude maneuver is controlled by pitch variation rather than by roll variation with the vehicle trimmed at maximum lift-drag ratio.

For vehicles having maximum lift-drag-ratio capabilities of less than 0.8, a good approximation to the problem is obtained by assuming an elliptic variation of drag coefficient with time. The time average value of the drag coefficient is then used in the range equation as developed for constant drag coefficient to obtain the approximate longitudinal range.

The angle-of-attack rates required for the successful operation of a vehicle which carries out a constant-altitude maneuver by pitch modulation were defined to yield some insight into the piloting problems associated with the maneuver. Infinite values of angle-of-attack rate were indicated at values of the lift coefficient of negative and positive maximum lift coefficient and zero lift coefficient which correspond to maximum start and end maneuver velocities and satellite velocity. It is believed that the infinite angle-of-attack rate occurring at zero lift is a local discontinuity. Also, the infinite values obtained at positive and negative maximum lift coefficients should cause only a slight deviation in the planned flight path.

## INTRODUCTION

Aerodynamic control of range is necessary during the reentry period following a deep space mission at velocities near escape speed if the vehicle is to land at a preselected site. Deviations from the desired entry conditions will occur because of guidance and control system inaccuracies encountered during the mission. Therefore, the atmospheric trajectory must be modified by aerodynamic maneuvering to negate these errors and reach the desired landing site. In general, little maneuver capability is available to the reentry vehicle during the initial reentry pullup. Range control maneuvers are therefore primarily initiated at the pullout point. Of the many conceivable maneuvers associated with control of the longitudinal range traversed by the reentry vehicle, the constant-altitude maneuver is commonly considered since it is a comparatively simple one. This maneuver requires that the vehicle be controlled so as to maintain the vector sum of the lift and centrifugal forces equal to the vehicle weight.

Many reentry studies (refs. 2 to 7) have considered the constant-altitude maneuver utilizing the variable roll mode of control. A closed form solution to the equations of motion is easily obtained for the usual assumption of a spherical, nonrotating earth, since the vehicle drag coefficient remains constant throughout the maneuver. The variable-pitch mode of control has been studied only briefly. (See refs. 8 and 9.) These studies indicate that an appreciable longitudinal range increase may be attained by utilization of this control mode rather than the variable roll mode for the same vehicle and reentry conditions.

The purpose of the present report is to present, in a systematic manner, the longitudinal range attainable during a constant-altitude maneuver for vehicles utilizing Newtonian drag polars with maximum lift-drag-ratio capabilities up to 2 and values of the ballistic parameter  $W/C_D A$  of 10 to 200 pounds per square foot. The maximum velocity at which the maneuver is considered to be initiated is 36,500 feet per second.

It should be noted that future space vehicles having  $L/D$  capabilities greater than one-half will probably be unsymmetrical in shape. Therefore, in this investigation it is assumed that the vehicle is rolled  $180^\circ$  at initiation of the constant-altitude maneuver and thus negative lift is obtained with positive angle of attack. When the vehicle reaches satellite speed, the vehicle is again rolled  $180^\circ$  to achieve positive lift with positive angle of attack. Therefore, major thermal protection is required on only one side of the vehicle.

The equations of motion were solved by using a high-speed digital computer at the Langley Research Center.

## SYMBOLS

A	reference area, sq ft
$C_D$	drag coefficient

$C_D(C_L)_{\max}$	drag coefficient corresponding to maximum lift coefficient
$C_L$	lift coefficient
$D$	drag force, lb
$g$	earth's gravitational acceleration, ft/sec <sup>2</sup>
$h$	altitude, ft
$K$	constant
$L$	lift force, lb
$L/D$	lift-drag ratio
$r$	radial distance from earth center to vehicle, ft
$r_o$	earth radius, 3,957 miles
$R$	longitudinal range, ft
$t$	time, measured from initiation of maneuver, sec
$V$	velocity, ft/sec
$V_s$	satellite velocity, $\sqrt{rg}$ , ft/sec
$\bar{V} = V/V_s$	
$W$	vehicle weight, lb
$\alpha$	angle of attack, deg
$\gamma$	entry angle, deg
$\rho$	atmospheric density, slug-ft <sup>-3</sup>

Subscripts:

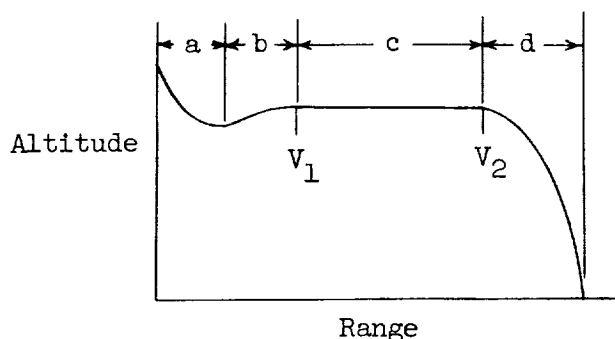
max	maximum value
min	minimum value
o	earth
t	time average value
l	maneuver initial conditions

2           maneuver end conditions  
 l           low drag  
 h           high drag

Dots over symbols denote differentiation with respect to time.

## ANALYSIS

The nominal reentry trajectory traversed by a vehicle on its return from a deep space mission may be divided into four distinct regions (see sketch): the initial pullout (a), the transitional maneuver (b), the constant-altitude maneuver (c), and the final glide to the desired landing point (d). The present investigation was concerned only with the constant-altitude portion of the reentry trajectory and the longitudinal ranges attainable with this maneuver.



obtained from Newtonian aerodynamics with an assumed maximum drag coefficient of 1.7. The drag polars for the vehicles considered in the present report are presented in figure 1.

The variation of parameters considered herein was chosen so as to cover adequately the probable range of conditions at initiation of the constant-altitude maneuver. The range traversed between entry and pullout at altitudes less than 150,000 feet is at least of the same magnitude as the range attainable in constant-altitude flight. Thus, any range analysis involving these low altitudes must include a study of the transition maneuver which is beyond the scope of the present investigation. For this reason, altitudes less than 150,000 feet have not been considered here. Utilizing presently envisioned guidance and control systems, it is very difficult to maneuver a vehicle accurately from the region of the initial pullout to high-altitude low-density regions. For this reason, the upper limit on maneuver altitude was taken as 240,000 feet for the present investigation. This limit has been shown to be a reasonable one in reference 7.

The upper limit on initial maneuver velocity was taken as escape velocity, 36,500 feet per second, since even at the reentry velocities associated with hyperbolic interplanetary flight a significant amount of the vehicle's kinetic energy must be dissipated in performing the initial pullout maneuver and the transitional maneuver to the desired altitude at which the constant-altitude maneuver

is to be initiated. Thus, this velocity appears to be a reasonable upper boundary for presently envisioned space missions.

Vehicle wing loadings were obtained by selecting values of the ballistic parameter from 10 to 200 pounds per square foot at the drag coefficient for maximum lift-drag ratio. This range appears to cover the range of wing loadings for reentry vehicles.

By utilizing the general reentry equations of motion in conjunction with the Newtonian flat-plate lift and drag coefficient expressions of reference 1, the equations of motion may be developed for the constant-altitude variable-pitch maneuver. The reentry equations of motion for this case may be written in the form:

$$\frac{d\gamma}{dt} = \frac{g_0}{V} \left\{ \frac{L}{W_0} - \left[ 1 - \frac{V^2}{r_0 g_0} \left( 1 + \frac{h}{r_0} \right) \right] \frac{\cos \gamma}{\left( 1 + \frac{h}{r_0} \right)^2} \right\} \quad (1)$$

$$- \frac{dV}{dt} = \frac{Dg}{W} + g \sin \gamma \quad (2)$$

$$\frac{dh}{dt} = V \sin \gamma \quad (3)$$

$$\frac{d\left(\frac{R}{r_0}\right)}{dt} = \frac{V}{r_0} \cos \gamma \quad (4)$$

The conditions for a vehicle flying a constant-altitude maneuver are:

$$\left. \begin{array}{l} \gamma = 0 \\ \frac{dh}{dt} = 0 \end{array} \right\} \quad (5)$$

Therefore, equations (1), (2), and (4) become for the constant-altitude maneuver:

$$\frac{L}{W} = 1 - \bar{V}^2 \quad (6)$$

$$\frac{dV}{dt} = - \frac{Dg}{W} = - \frac{C_D \rho V^2}{2} \frac{A}{W} g \quad (7)$$

$$\frac{d\left(\frac{R}{r_0}\right)}{dt} = \frac{v}{r_0} \quad (8)$$

From Newtonian aerodynamics for a flat plate, the vehicle lift and drag coefficients may be defined, as in reference 1, as:

$$C_L = (C_{D,max} - C_{D,min}) \sin^2 \alpha \cos \alpha \quad (9)$$

and

$$C_D = C_{D,min} + (C_{D,max} - C_{D,min}) \sin^3 \alpha \quad (10)$$

Equation (9) may be written in the form

$$C_L = (C_{D,max} - C_{D,min}) (\cos \alpha - \cos^3 \alpha) \quad (11)$$

Solution of this equation for  $\cos \alpha$  results in the expression

$$\cos \alpha = -\frac{2}{\sqrt{3}} \cos \left[ \frac{\phi}{3} + (120)K \right] \quad (K = 0, 1, \text{ or } 2) \quad (12)$$

where

$$\cos \phi = \frac{\sqrt{27} C_L}{2(C_{D,max} - C_{D,min})} \quad \left( 0 \leq \phi \leq \frac{\pi}{2} \right)$$

It is seen from equation (10) that

$$\cos \alpha = \sqrt{1 - \left( \frac{C_D - C_{D,min}}{C_{D,max} - C_{D,min}} \right)^{2/3}} \quad (13)$$

Now, equating equations (12) and (13) and solving for  $C_D$  to obtain the desired explicit relation between  $C_L$  and  $C_D$  yields:



$$C_D = C_{D,\min} + (C_{D,\max} - C_{D,\min}) \left( 1 - \frac{4}{3} \cos^2 \left\{ \frac{\cos^{-1} \left[ \frac{\sqrt{27} C_L}{2(C_{D,\max} - C_{D,\min})} \right]}{3} + (120)K \right\} \right)^{3/2} \quad (14)$$

The two values of  $K$  which are of interest are  $K = 1$  and  $K = 2$ . Setting  $K = 1$  yields the relation between  $C_D$  and  $C_L$  for that region of the drag polar between  $C_{L,\max}$  and  $C_{D,\min}$ . For  $K = 2$  equation (14) yields the relation between  $C_D$  and  $C_L$  for the region between  $C_{L,\max}$  and  $C_{D,\max}$ .

Substitution of equation (14) into equation (7) does not yield a closed form solution. Therefore, solution of the equations of motion by numerical means is necessitated. Equations (6), (7), (8), and (14) were programed for a high-speed digital computer to obtain the solution to the problem. For simplicity in carrying out the numerical integration,  $C_L$  is always considered positive in equation (14).

## RESULTS AND DISCUSSION

### Longitudinal Range

The longitudinal ranges attainable during a constant-altitude pitch-controlled maneuver by the several vehicles considered here with the Newtonian drag polars of figure 1 are presented in figures 2 to 5 as a function of the velocity at which the maneuver is initiated. In figures 2 to 5, for values of  $W/C_D A$  of 10, 50, 100, and 200, respectively, the altitudes are varied from 150,000 feet to 240,000 feet in 10,000-foot increments. These curves were obtained for operation of the vehicle on the low-drag side of the drag polar ( $C_{L,\max}$  to  $C_{D,\min}$ ). The longitudinal range thus attained is therefore the maximum which a vehicle having the prescribed drag polar may achieve in constant-altitude flight for the given initial conditions. As is to be expected, longitudinal range is increased by increasing the initial altitude,  $W/C_D A$ , maximum lift-drag-ratio capability, or initial velocity.

The regions to the right of the indicated boundaries of these figures are those velocities for which the constant-altitude maneuver may not be initiated since the negative lift capability of the vehicle is insufficient to offset the centrifugal force acting on the vehicle. Thus the vehicle would tend to skip outside the atmosphere under this condition.

It should be noted that the velocity for which the range is zero is the velocity at which the vehicle is unable to generate sufficient lift to overcome the earth's gravitational attraction and thus maintain constant altitude.

These velocities are presented in figure 6 as a function of the vehicle maximum lift-drag-ratio capability. As shown, small increases in lift capability yield a large reduction in the maneuver end velocity for values of the vehicle  $(L/D)_{\max}$  capability near zero, diminishing returns occurring for increasing  $(L/D)_{\max}$ .

It is believed that figures 2 to 6 may be of use in the design of future space vehicles wherein it is necessary to have a complete knowledge of the vehicle's range capability during the various atmospheric maneuvers.

Obviously, a predetermined reentry reference trajectory will be required for any manned space mission. This trajectory will consist of a reference midcorridor entry angle, entry velocity, and nominal maneuver to be flown to the landing site. The nominal maneuver to be carried out after reentry is initiated must be chosen after extensive study of all practical maneuvers. With the presumption that the constant-altitude maneuver is to be utilized, it would be required to define a nominal altitude and velocity at which the maneuver is to be initiated. For the present study, velocities of initiation of 36,500 and 26,000 feet per second were selected.

In figures 7 and 8, the longitudinal range attainable in constant-altitude flight for these initial velocities is shown as a function of the vehicle maximum lift-drag-ratio capability. Obviously, a ballistic vehicle is incapable of maneuvering; hence, the curves are extended to zero range at zero maximum lift-drag ratio.

If it is first considered that the constant-altitude maneuver is initiated at satellite velocity, as indicated in figure 7, it is seen that maximum ranges of the order of 3,000 to 9,500 miles are attainable for a vehicle having a maximum lift-drag-ratio capability of 2 and an operational altitude of 240,000 feet. These range values, of course, depend on the value of the weight parameter. Decreasing the lift-drag-ratio capability of the vehicle to 1 is shown to reduce the attainable range (1,700 to 4,000 miles) for operation at the same altitude. Note also the slope of the curve for range plotted against  $(L/D)_{\max}$  increases with increasing altitude. This increase is primarily due to the increase in the time spent at drag coefficients near the minimum value at the higher altitudes wherein the higher  $(L/D)_{\max}$  vehicles have a large advantage.

In figure 8, wherein the maneuver is initiated at parabolic velocity, the boundary lines indicate the maximum range attainable in constant-altitude flight. That is, the maneuver is initiated at negative maximum lift coefficient and ended at positive maximum lift coefficient, and thereby utilizes the full lift capability of the vehicle.

Significant range capability is available to the high  $L/D$  vehicles initiating the maneuver at satellite velocity. Utilizing this velocity as the nominal

velocity of initiation of the maneuver allows a considerable amount of the vehicle kinetic energy to be expended during the initial reentry pullup for lateral range corrections, peak deceleration load reduction, and exact control of the altitude at which the constant-altitude maneuver is to be carried out. Of course, considerable benefits are to be obtained by utilizing higher initial maneuver velocities as is shown by comparing figures 7 and 8. Note, however, that the initial reentry velocity, vehicle position in the reentry corridor, required range to landing, and the required kinetic energy expenditure to reach the desired maneuver altitude must be considered for any mission and vehicle before a desired initial maneuver velocity may be selected. Since this investigation was not concerned with any particular mission or vehicle requirements, no definite conclusions may be drawn here as to the desired nominal altitudes and velocities.

As has been demonstrated in figures 2 to 8, the vehicle weight parameter greatly influences the range attainable by a vehicle engaged in a constant-altitude maneuver. The effect of this parameter is indicated in figure 9 for vehicles having maximum lift-drag-ratio capabilities of 0.18 and 2.0. In each case, the maneuver is initiated either at parabolic velocity or the velocity for which maximum vehicle negative lift capability is required at initiation of the maneuver. As shown in figure 9(a), the attainable longitudinal range increases with an increase in  $W/C_{DA}$  up to a maximum range of 0.2336 earth radii, at which point the maneuver is initiated at parabolic velocity and negative maximum lift coefficient. A further increase in  $W/C_{DA}$  requires a reduction in initial velocity so that the constant-altitude maneuver may be initiated. This necessary decrease in velocity more than offsets any increase in range due to higher values of  $W/C_{DA}$  and results in decreasing range with increasing  $W/C_{DA}$ . The tick marks at the side of the figure indicate lines of constant initial velocity at negative maximum lift coefficient and hence constant range. Note that maximum range is not necessarily attained at an altitude of 240,000 feet. For instance, at a value of  $W/C_{DA}$  of 120 pounds per square foot, maximum range is attained by maintaining a constant-altitude maneuver at 190,000 feet.

As shown in figure 9(b), the lift capability of the  $(L/D)_{\max} = 2.0$  vehicle is such that the maneuver is not initiated at negative maximum lift coefficient for the range of altitude and  $W/C_{DA}$  considered here. Thus the longitudinal range attainable continuously increases with increasing altitude and/or ballistic weight parameter.

It is of interest to compare the longitudinal range attainable by operation of the reentry vehicle on the low-drag side of its drag polar with that attainable by operation on the high-drag side. These ranges are compared in figure 10 for an initial maneuver velocity of 36,500 feet per second. Those maneuvers are not shown wherein the initial velocity must be less than the parabolic value in order to maintain the clarity of the plots. Lines of constant altitude and vehicle maximum lift-drag-ratio capability are as shown. The limit for which the constant-altitude maneuver may be initiated at parabolic velocity is shown by the shaded regions.

Generally, on the high-drag side of the polar, greater range is attainable with decreasing  $(L/D)_{\max}$  capability for the same initial maneuver altitude.

This trend reverses for values of  $(L/D)_{\max}$  less than about 0.35. Increasing high-drag range with decreasing  $(L/D)_{\max}$  between 2.0 and 0.35 is due to the fact that the vehicle is operating at lower values of drag coefficient for the same values of the lift coefficient, as may be seen from the drag polar of figure 1. However, for values of the maximum lift-drag ratio less than 0.35, the effect of decreased lift capability more than offsets the decrease in drag coefficient, and results in a reversal of the trend.

Comparison of figures 10(a) to 10(d) shows, with respect to the ballistic parameter, the expected results of increasing range with increasing weight parameter for operation on the high- as well as the low-drag side of the drag polar.

Note also that the ratio of low-drag range to high-drag range varies from approximately 1.5 at  $(L/D)_{\max} = 0.18$  to 40 at  $(L/D)_{\max} = 2.0$ . This effect is due primarily to fixing the maximum drag coefficient at a value of 1.7 and allowing the minimum vehicle drag coefficient to decrease with increasing lift-drag-ratio capability so that very low values of minimum drag coefficient result for the high-lift vehicles.

The maximum range which a vehicle can attain in constant-altitude flight was demonstrated in figure 9 to be dependent only on the velocity at which the maneuver is initiated with the further restriction that the maneuver be initiated at negative maximum lift coefficient and ended at the maximum positive value. This maximum range is presented in figure 11, for an initial velocity equal to the parabolic value, as a function of the maximum lift-drag-ratio capability of the vehicle. Approximately global longitudinal range is available for an  $(L/D)_{\max} = 2.0$  vehicle operating on the low-drag side of its drag polar. Operation on the high-drag side of the polar yields little increase in maximum range with increasing  $(L/D)_{\max}$  capability for values of  $(L/D)_{\max} > 0.8$ . Rolling the vehicle about the wind axis with the vehicle trimmed at the attitude for maximum lift-drag ratio results in much less attainable range than the low-drag pitch maneuver but a significant advantage over the high-drag pitch maneuver.

If it is assumed that the vehicle drag coefficient varies elliptically with time during the low-drag maneuver, the dashed curve is obtained. This approximation (developed in appendix A) is seen to yield very good results for vehicles having lift-drag-ratio capabilities of less than about 0.8. Although not shown, this approximation is less accurate for values of the initial lift coefficient other than the maximum value. However, the approximation is quite sufficient to obtain a first-order solution to the longitudinal range attainable in constant-altitude flight for vehicles with  $(L/D)_{\max} \leq 0.8$ .

This figure also indicates that a large degree of range control is available to a vehicle utilizing the pitch-control mode. That is, by alternately operating on the low- and high-drag sides of the drag polar, any range between the maximum for the high-drag mode and the low-drag mode is attainable. This procedure would, of course, result in some variation in the flight altitude during the transition from the low-drag to the high-drag side of the polar or vice versa. The resultant range overlap between the low-drag and high-drag pitch maneuvers is approximately

23,000 miles for the  $(L/D)_{\max} = 2$  vehicle to 280 miles for the  $(L/D)_{\max} = 0.18$  vehicle. A vehicle having a maximum lift-drag-ratio capability of 0.5, as in the proposed lunar vehicle, is seen to have a range overlap of 2,150 miles. Of course, a vehicle returning from a lunar mission would require lower initial velocities and hence would have a range overlap less than that shown in figure 11. Note also that, if the vehicle is capable of operation at a combination of the low-drag and high-drag pitch maneuvers, it may utilize the same nominal maneuver altitude without regard to its initial position in the reentry corridor. Large errors in either the initial reentry conditions or the location of the point of reentry may thus be negated without the pilot being required to choose another altitude or reentry maneuver.

As far as the lateral-range capability of a vehicle making a constant-altitude maneuver is concerned, the variable-pitch maneuver may be coupled with a roll maneuver to achieve at least as much lateral-range capability as the roll-only maneuver.

#### Angle-of-Attack Rate

In investigating any reentry maneuver, it is necessary to determine, if possible, the feasibility of the maneuver from the guidance and control standpoint. Generally, this problem requires a pilot simulation study wherein the pilot attempts to fly and evaluate a maneuver. A rough estimate of the feasibility of a maneuver may be obtained, however, by analytically defining the angular rates and so forth required of the vehicle to carry out the particular maneuver in question. In the case of the variable-pitch constant-altitude maneuver the primary quantity to be considered is the angle-of-attack rates necessary to maintain the maneuver.

Angle-of-attack rates, as obtained by the method of appendix B, are shown in figure 12 for the  $(L/D)_{\max} = 0.18$  and  $(L/D)_{\max} = 2$  vehicles having a weight parameter of 10 pounds per square foot and flying at an altitude of 150,000 feet. Here,  $\dot{\alpha}$  is always positive since the vehicle is rolled  $180^\circ$  to attain negative lift with positive angle of attack. It may be seen from the governing equation that infinite values of  $\dot{\alpha}$  occur at values of the lift coefficient of zero and positive and negative  $C_{L,\max}$ . It is felt that the infinite value obtained at  $C_L = 0$  is a local discontinuity in the equation and will not affect the piloting of the vehicle during this maneuver. In addition, the infinite values of  $\dot{\alpha}$  obtained at  $\pm C_{L,\max}$  should not affect the vehicle flight path other than to cause a slight variation in altitude in these regions. However, it appears that pilot simulation studies should be carried out to define the vehicle handling qualities in these regions.

## CONCLUDING REMARKS

Control of the constant-altitude maneuver by pitch modulation was found to yield very large increases in longitudinal range over the roll-control mode if the low-drag side of the drag polar is utilized. Operation on the high-drag side of the drag polar was found to be relatively inefficient in attaining significant longitudinal ranges and very efficient in attaining short ranges.

The longitudinal distance traversed by any vehicle having a drag polar which may be approximated by the Newtonian aerodynamics with maximum lift-drag ratio less than or equal to 2 and a ballistic parameter  $W/C_D A$  of 0 to 200 pounds per square foot initiating constant-altitude flight between the altitudes of 150,000 and 240,000 feet at velocities  $\leq 36,500$  feet per second is obtainable.

The effect of increasing the vehicle weight parameter is to increase the attainable range up to the maximum value. After this point is reached, the range decreases slightly with a further increase in  $W/C_D A$ .

A reasonable approximation to the range attainable during constant-altitude flight is available for values of maximum lift-drag ratio less than about 0.8 if it is assumed that the drag coefficient varies elliptically with time.

The infinite angle-of-attack rates indicated during operation at maximum lift coefficient should cause only a slight variation in altitude and are not believed to constitute a major problem.

Langley Research Center,  
National Aeronautics and Space Administration,  
Langley Station, Hampton, Va., April 3, 1963.

## APPENDIX A

### ELLIPTIC APPROXIMATION

It may be seen from the equations of motion that an analytic solution to the longitudinal range attainable in constant-altitude flight is available if a simple relation between drag coefficient and time can be found. It was noted from the results of the machine program that, during the constant-altitude pitch-controlled maneuver, the variation of vehicle drag coefficient with time was essentially an elliptic variation. This phenomenon was particularly pronounced for the low maximum lift-drag-ratio vehicles; therefore, the following elliptic relation was chosen for the approximate analysis:

$$\frac{(t - m)^2}{a^2} + \frac{(C_D - n)^2}{b^2} = 1 \quad (A1)$$

where

$$a = \frac{t_2}{1 + \sqrt{1 - \left[ \frac{C_{D,1} - C_{D(C_L)_{\max}}}{C_{D(C_L)_{\max}} - C_{D,\min}} \right]^2}}$$

$$b = C_{D(C_L)_{\max}} - C_{D,\min}$$

$$n = C_{D(C_L)_{\max}}$$

$$m = \frac{t_2}{1 + \frac{1}{\sqrt{1 - \left[ \frac{C_{D,1} - C_{D(C_L)_{\max}}}{C_{D(C_L)_{\max}} - C_{D,\min}} \right]^2}}}$$

and  $C_{D,1}$  is the drag coefficient at initiation of the maneuver. For example, figure 13 compares the machine results with the elliptic variation of drag coefficient with time given by equation (A1) for a vehicle having a maximum lift-drag ratio of 0.5. A maximum error in  $C_D$  of approximately 7 percent is obtained for this case.

Unfortunately, substitution of equation (A1) into equation (7) does not yield a closed form solution for the longitudinal range traversed during the constant-altitude maneuver. To obtain a closed form solution, a second assumption is therefore required. This assumption is: the range equation as developed for constant altitude and drag coefficient (the roll-control maneuver) may be employed, with small error, if a time average value of the drag coefficient is utilized. For any initial maneuver conditions this relationship may be shown to be given by:

$$C_{D,t} = C_{D(C_L)_{\max}} - \frac{\frac{1}{2}[C_{D(C_L)_{\max}} - C_{D,\min}]}{1 + \sqrt{1 - \left[ \frac{C_{D(C_L)_{\max}} - C_{D,l}}{C_{D(C_L)_{\max}} - C_{D,\min}} \right]^2}} \left\{ \pi + \left[ \frac{C_{D(C_L)_{\max}} - C_{D,l}}{C_{D(C_L)_{\max}} - C_{D,\min}} \right] \sqrt{1 - \left[ \frac{C_{D(C_L)_{\max}} - C_{D,l}}{C_{D(C_L)_{\max}} - C_{D,\min}} \right]^2}} - \sin^{-1} \left[ \frac{C_{D(C_L)_{\max}} - C_{D,l}}{C_{D(C_L)_{\max}} - C_{D,\min}} \right] \right\} \quad (A2)$$

For the particular case wherein the maneuver is initiated at negative  $C_{L,\max}$  and ended at positive  $C_{L,\max}$ , equation (A2) reduces to

$$C_{D,t} = C_{D(C_L)_{\max}} - \frac{\pi}{4} [C_{D(C_L)_{\max}} - C_{D,\min}] \quad (A3)$$

The longitudinal range attainable by a vehicle in constant-altitude flight may be obtained approximately by substitution of equation (A2) into the constant-drag-coefficient range relation

$$\frac{R}{r} = \frac{-2W/A}{C_{D,t}^{\text{prg}}} \log_e \frac{V_2}{V_1} \quad (A4)$$



## APPENDIX B

### DETERMINATION OF ANGLE-OF-ATTACK RATES FOR THE CONSTANT-ALTITUDE MANEUVER

The angle-of-attack rates associated with the constant-altitude variable-pitch maneuver may be obtained in closed form. Differentiating equation (9) yields

$$\dot{C}_L = (C_{D,\max} - C_{D,\min})(2 \sin \alpha \cos^2 \alpha - \sin^3 \alpha) \dot{\alpha} \quad (B1)$$

Solving equation (10) for angle of attack in terms of  $C_D$  and substituting the results into equation (B1) yields

$$\begin{aligned} \dot{C}_L = (C_{D,\max} - C_{D,\min}) & \left\{ 2 \left( \frac{C_D - C_{D,\min}}{C_{D,\max} - C_{D,\min}} \right)^{1/3} \left[ 1 - \left( \frac{C_D - C_{D,\min}}{C_{D,\max} - C_{D,\min}} \right)^{2/3} \right] \right. \\ & \left. - \left( \frac{C_D - C_{D,\min}}{C_{D,\max} - C_{D,\min}} \right) \right\} \dot{\alpha} \end{aligned} \quad (B2)$$

which after collecting terms may be written as

$$\dot{C}_L = \left[ 2(C_{D,\max} - C_{D,\min})^{2/3} (C_D - C_{D,\min})^{1/3} - 3(C_D - C_{D,\min}) \right] \dot{\alpha} \quad (B3)$$

From the relation between lift and velocity (eq. (6))

$$C_L = \frac{2W}{\rho g A} \left( \frac{1 - \bar{V}^2}{\bar{V}^2} \right) \quad (B4)$$

Differentiation of equation (B4) with respect to time yields

$$\dot{C}_L = - \frac{4W}{\rho g A} \frac{\dot{\bar{V}}}{\bar{V}^3} \quad (B5)$$

Substitution of equation (7) into equation (B5) results in the expression

$$\dot{C}_L = \frac{2C_D}{\bar{V}} \sqrt{\frac{g}{r}} \quad (B6)$$

Equating equations (B3) and (B6) yields the expression for the rate of angle of attack required to maintain a constant-altitude maneuver by pitch control,

$$\dot{\alpha} = \frac{2C_D}{\bar{V}} \sqrt{\frac{g}{r}} \frac{1}{2(C_{D,\max} - C_{D,\min})^{2/3} (C_D - C_{D,\min})^{1/3} - 3(C_D - C_{D,\min})} \quad (B7)$$

or

$$\dot{\alpha} = \frac{2C_D}{\bar{V}} \sqrt{\frac{g}{r}} \frac{1}{(C_{D,\max} - C_{D,\min}) \sin \alpha (2 - 3 \sin^2 \alpha)} \quad (B8)$$

It may be shown that the minimum value of  $\dot{\alpha}$  occurs at an angle of attack of  $\sin^{-1} \frac{\sqrt{2}}{3}$  or  $28.14^\circ$ . It should also be noted that infinite values of  $\dot{\alpha}$  occur at  $\alpha = 0$  and  $\alpha = \alpha_{C_{L,\max}}$ .

In addition,  $\dot{\alpha}$  is always considered positive since the vehicle is rolled  $180^\circ$  initially to attain negative lift with positive angle of attack and then rolled an additional  $180^\circ$  at satellite velocity to attain positive lift thereafter with positive angle of attack.

## REFERENCES

1. Chapman, Dean R.: An Analysis of the Corridor and Guidance Requirements for Supercircular Entry Into Planetary Atmospheres. NASA TR R-55, 1960.
2. Lees, Lester, Hartwig, Frederic W., and Cohen, Clarence B.: Use of Aerodynamic Lift During Entry Into the Earth's Atmosphere. ARS Jour., vol. 29, no. 9, Sept. 1959, pp. 633-641.
3. Levine, Philip: Analysis of Re-Entry Problems Associated With the Return of Manned Space Vehicles to Earth. Tech. Memo. RAD-TM-62-2, AVCO Res. and Advanced Dev. Div., Feb. 15, 1962.
4. Galman, Barry A.: Direct Re-Entry at Escape Velocity. Preprint No. 60-86, American Astronautical Soc., Aug. 1960.
5. Mandell, Donald S.: A Study of the Maneuvering Performance of Lifting Reentry Vehicles. [Preprint] 1555-60, American Rocket Soc., Dec. 1960.
6. Sommer, Simon C., and Short, Barbara J.: Point Return From a Lunar Mission for a Vehicle That Maneuvers Within the Earth's Atmosphere. NASA TN D-1142, 1961.
7. Moul, Martin T., Schy, Albert A., and Williams, James L.: Dynamic Stability and Control Problems of Piloted Reentry From Lunar Missions. NASA TN D-986, 1961.
8. Becker, J. V., Baradell, D. L., and Pritchard, E. B.: Aerodynamics of Trajectory Control for Re-Entry at Escape Speed. Astronautica Acta, Vol. VII, Fasc. 5-6, 1961, pp. 334-358.
9. Ferri, Antonio, and Ting, Lu: Practical Aspects of the Reentry Problem. PIBAL Report No. 705 (Contract No. AF 49(638)-445), Polytechnic Inst. Brooklyn, July 1961.
10. Minzner, R. A., Champion, K. S. W., and Pond, H. L.: The ARDC Model Atmosphere, 1959. Air Force Surveys in Geophysics No. 115 (AFCRC-TR-59-267), Air Force Cambridge Res. Center, Aug. 1959.

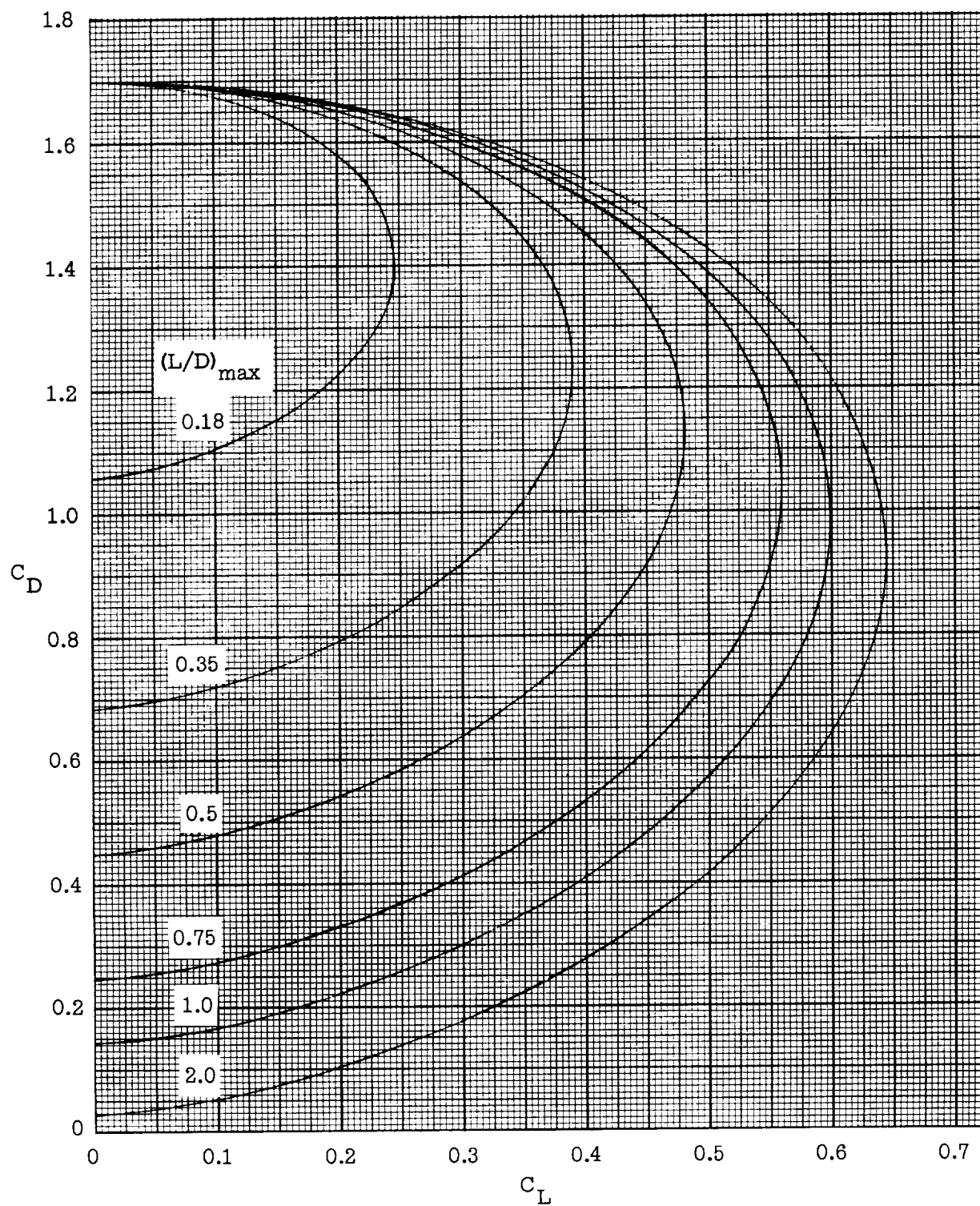
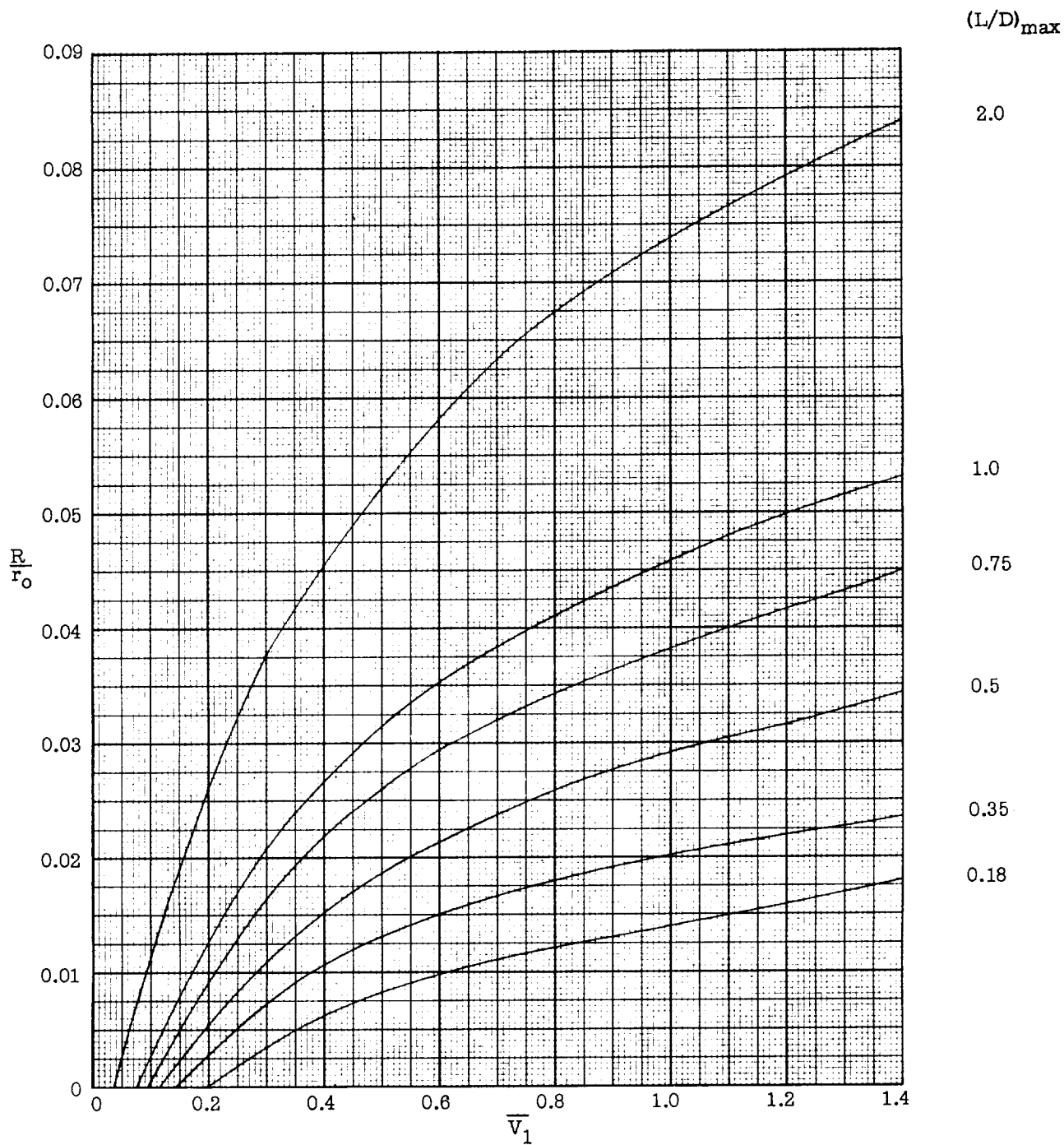
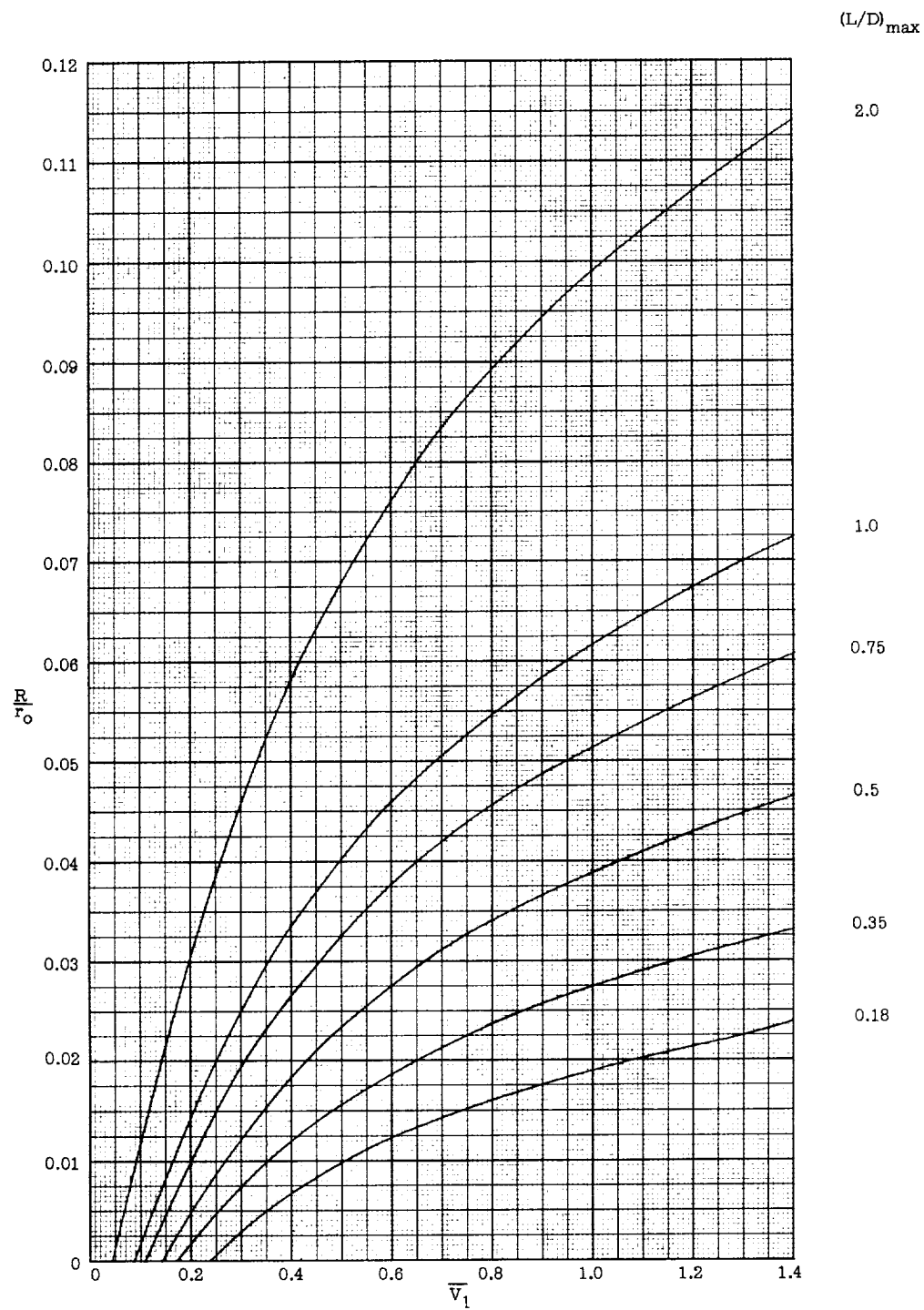


Figure 1.- Newtonian drag polar.



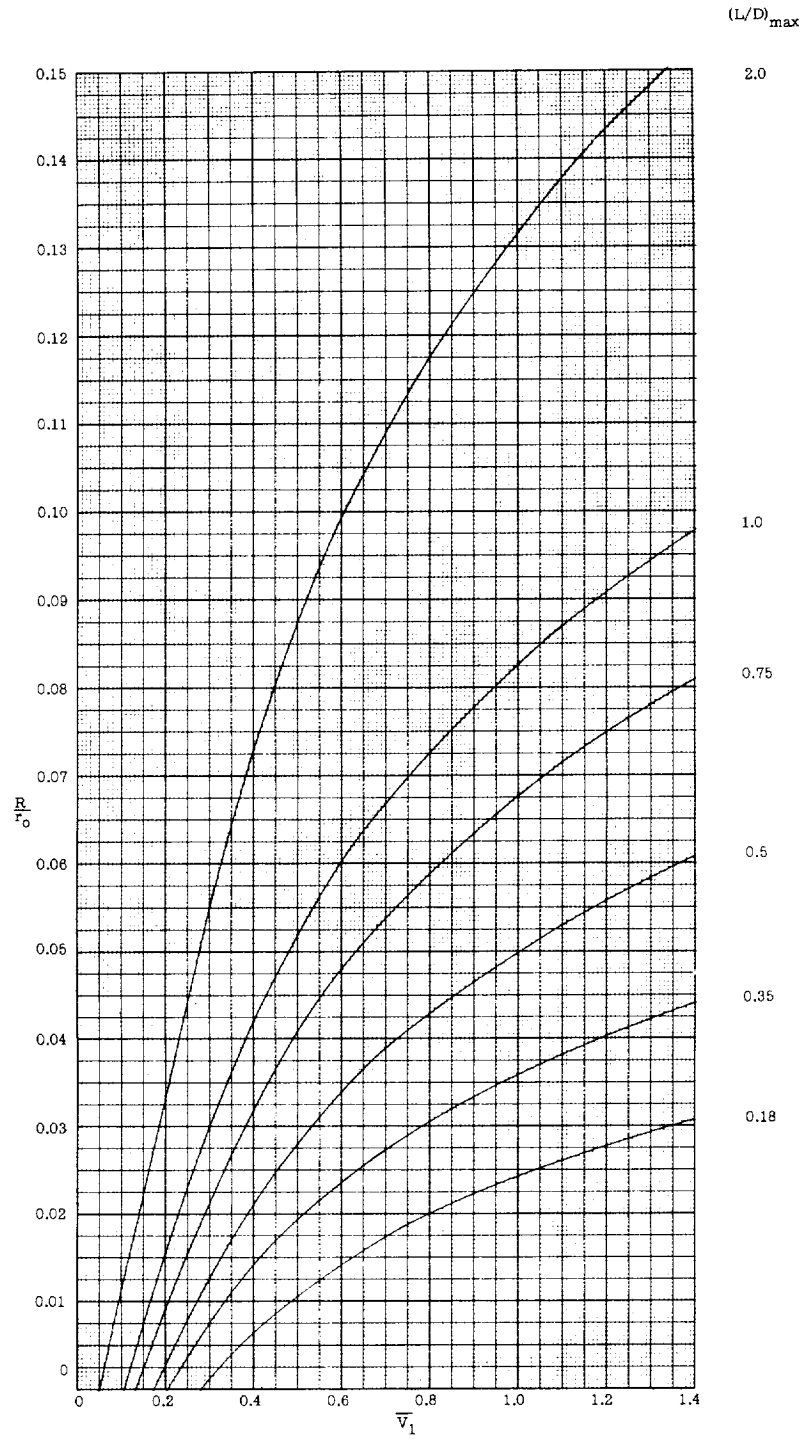
(a)  $h = 150,000$  feet.

Figure 2.- Effect of velocity of initiation on longitudinal range attainable in constant-altitude maneuver.  $W/C_D A = 10$  pounds per square foot.



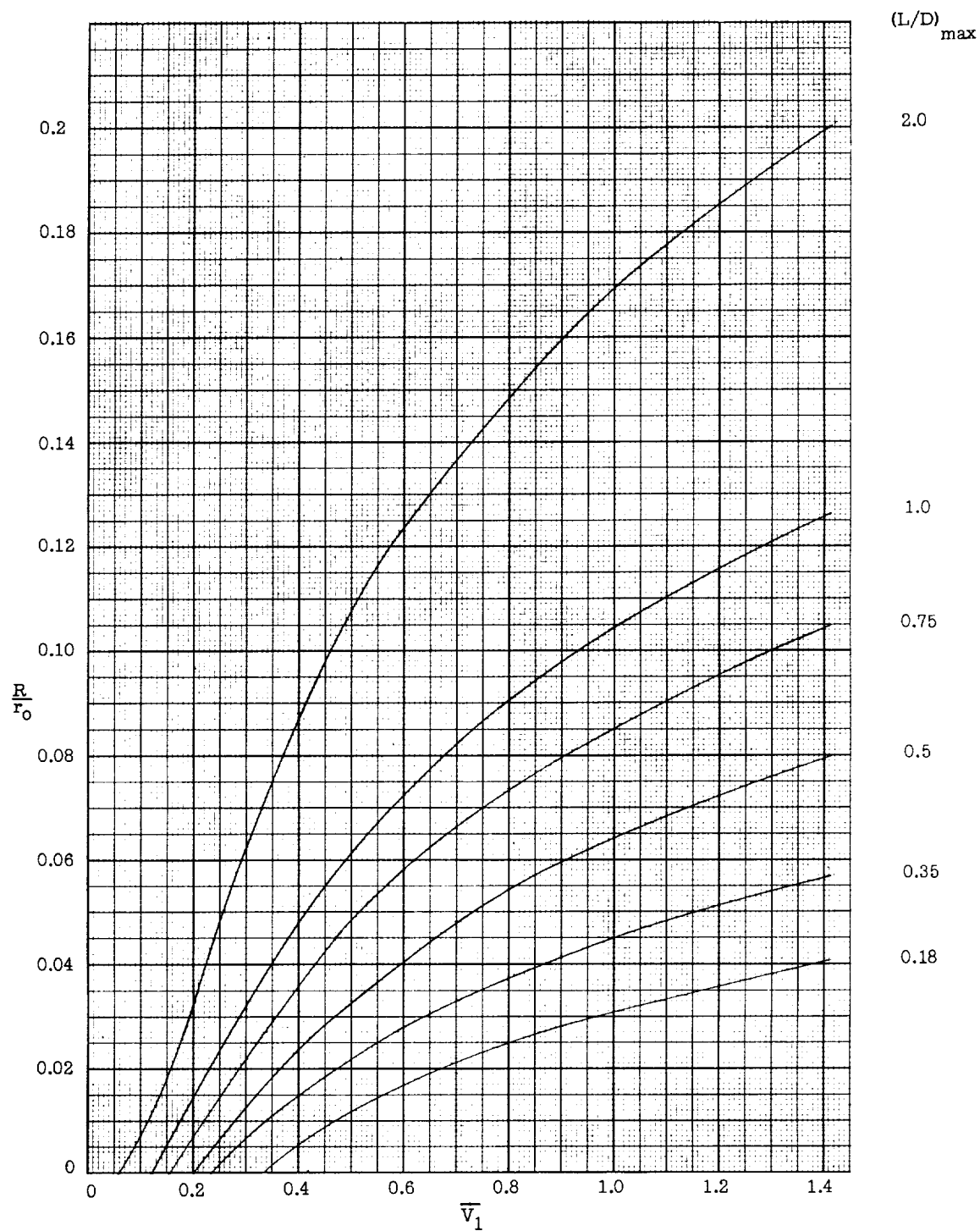
(b)  $h = 160,000$  feet.

Figure 2.- Continued.



(c)  $h = 170,000$  feet.

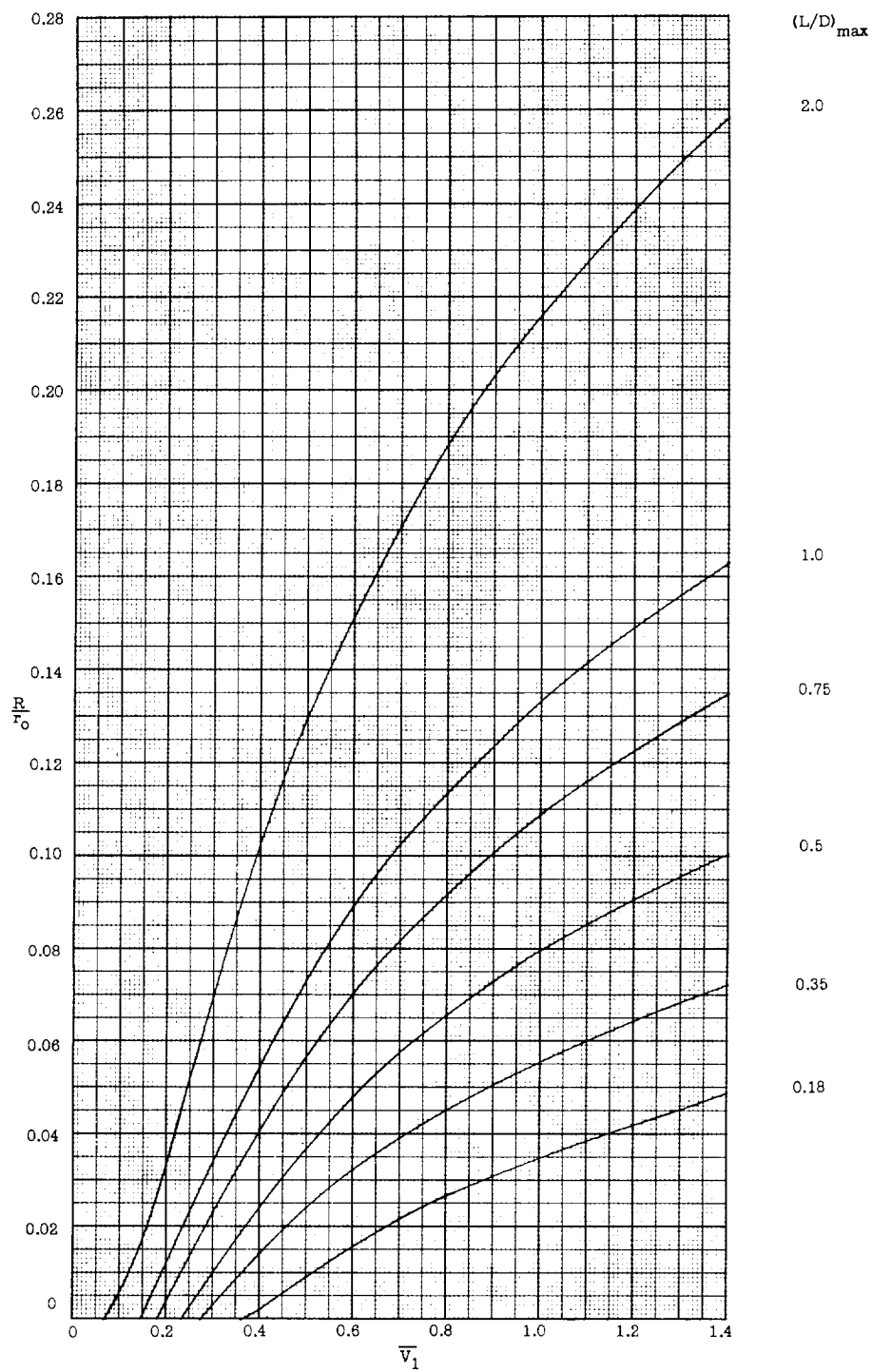
Figure 2.- Continued.



(d)  $h = 180,000$  feet.

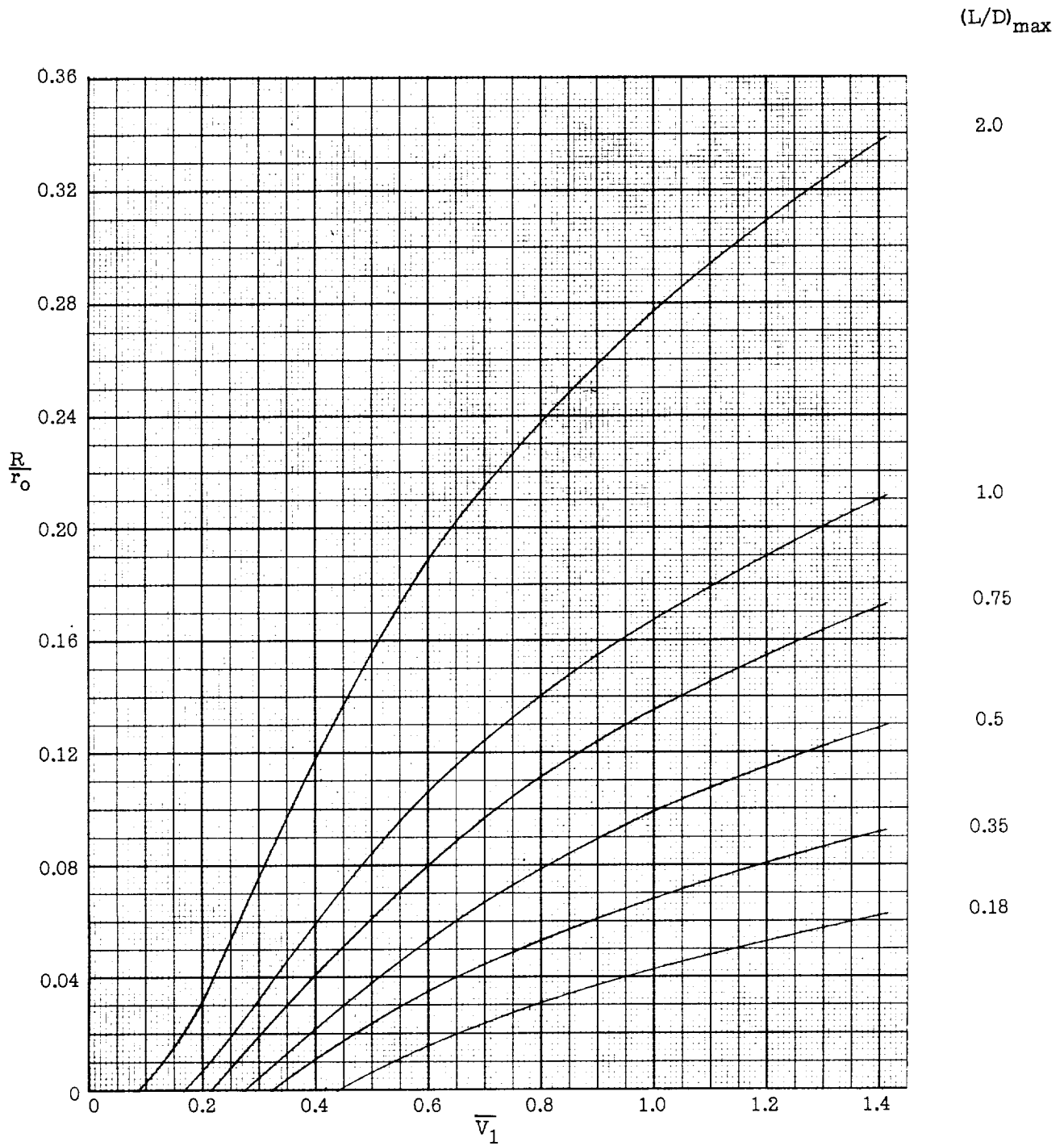
Figure 2.- Continued.





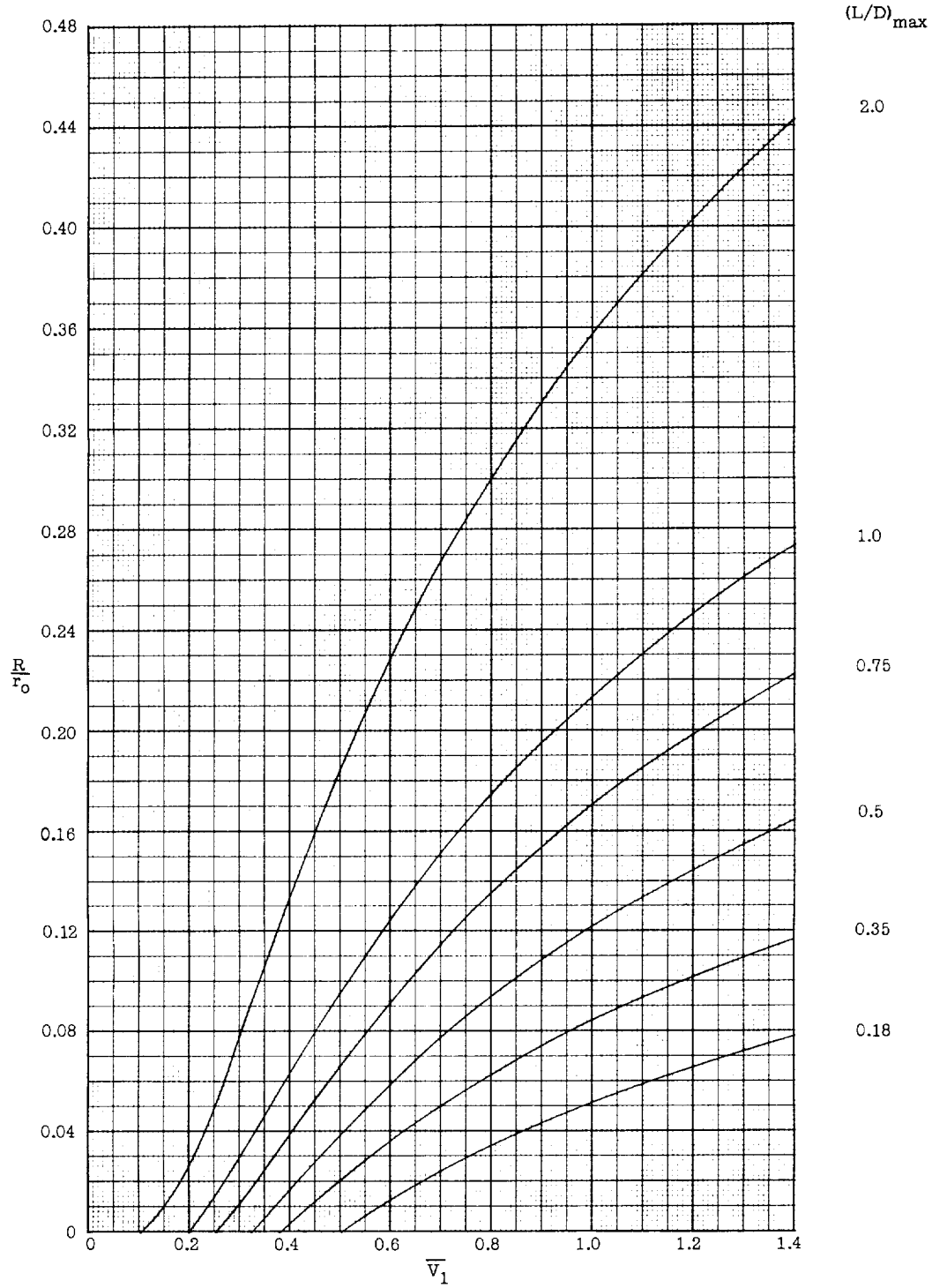
(e)  $h = 190,000$  feet.

Figure 2.- Continued.



(f)  $h = 200,000$  feet.

Figure 2.- Continued.



(g)  $h = 210,000$  feet.

Figure 2.- Continued.

$(L/D)_{\max}$

2.0

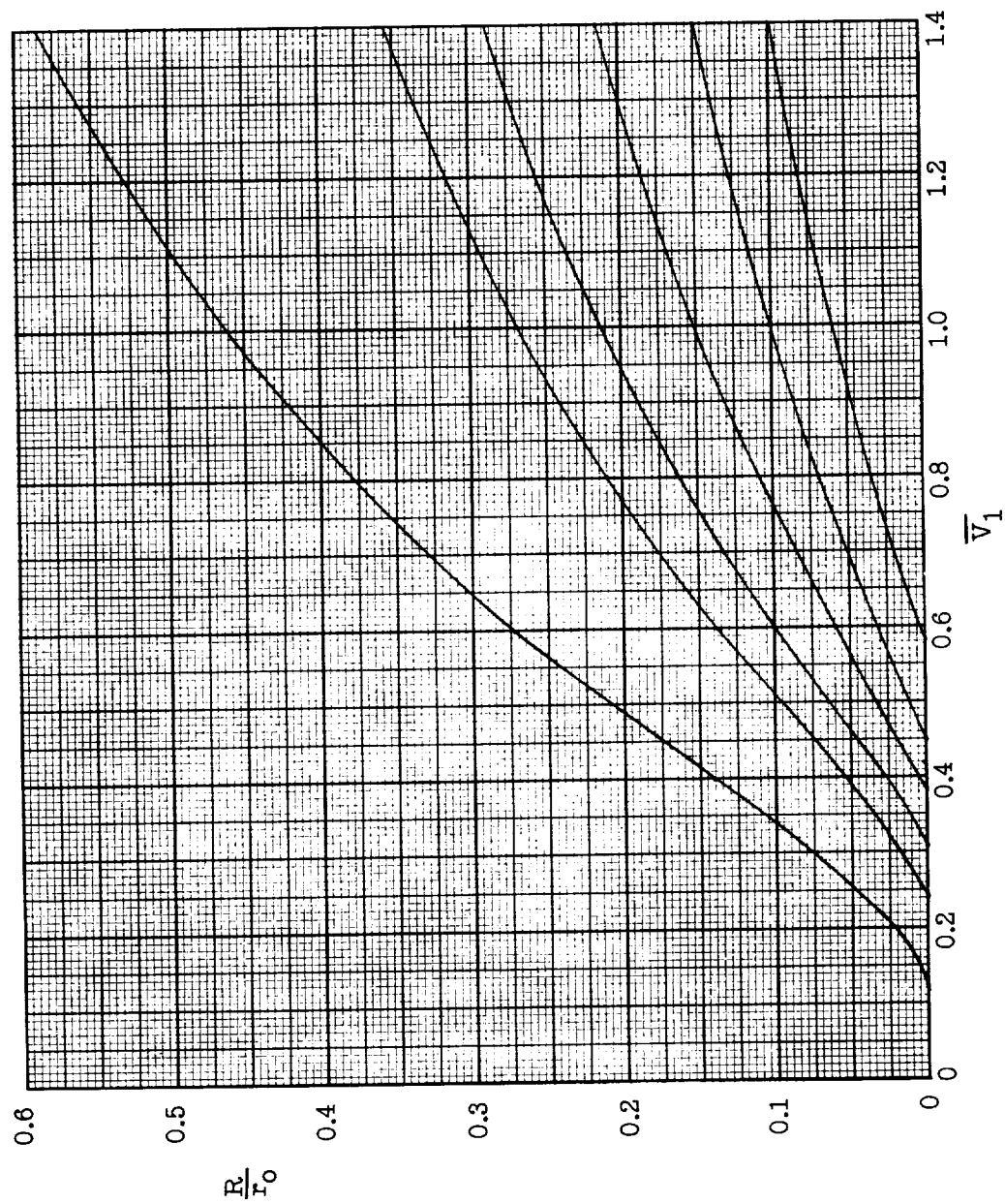
1.0

0.75

0.5

0.35

0.18



(h)  $h = 220,000$  feet.

Figure 2.- Continued.

$(L/D)_{\max}$

2.0

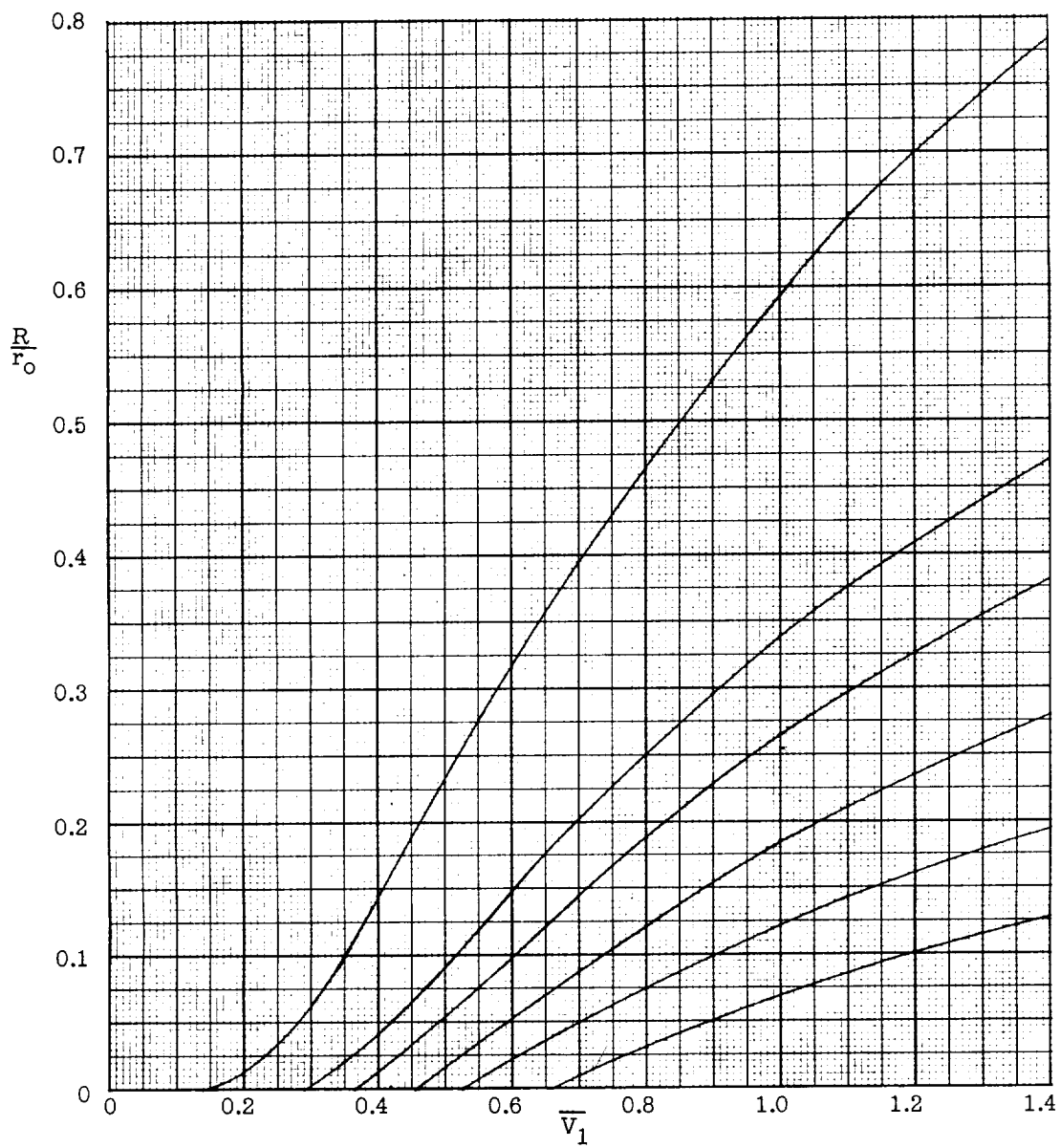
1.0

0.75

0.5

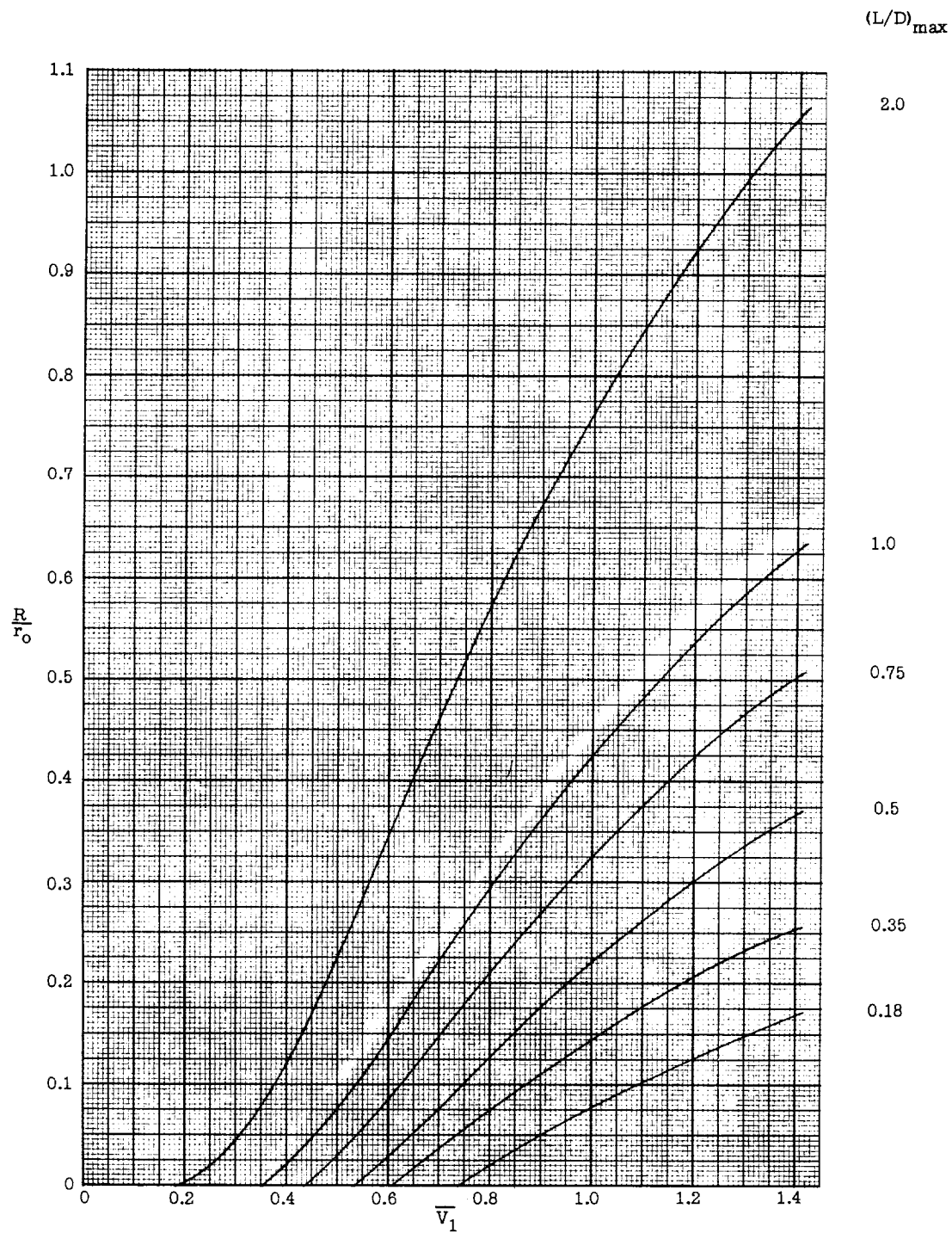
0.35

0.18



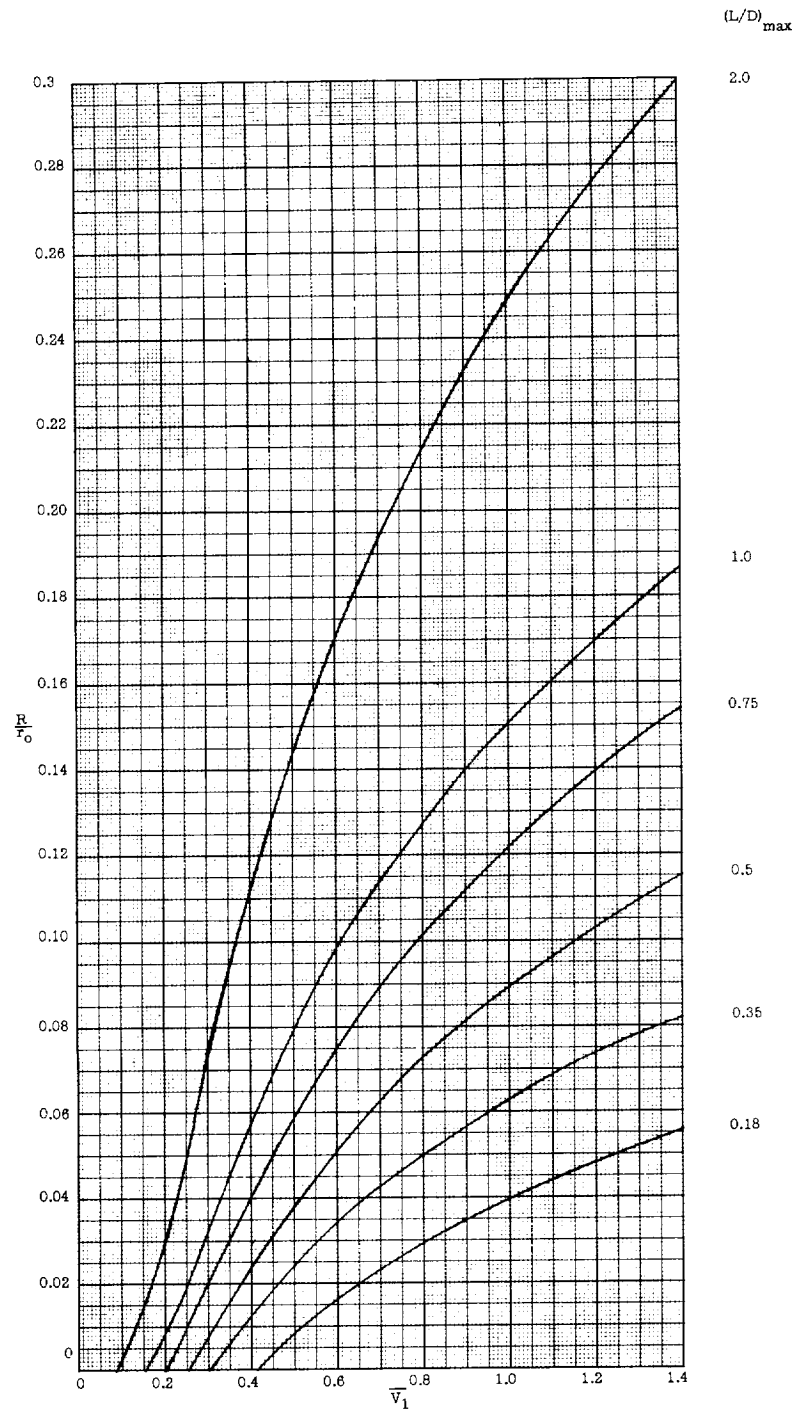
(1)  $h = 230,000$  feet.

Figure 2.- Continued.



(j)  $h = 240,000$  feet.

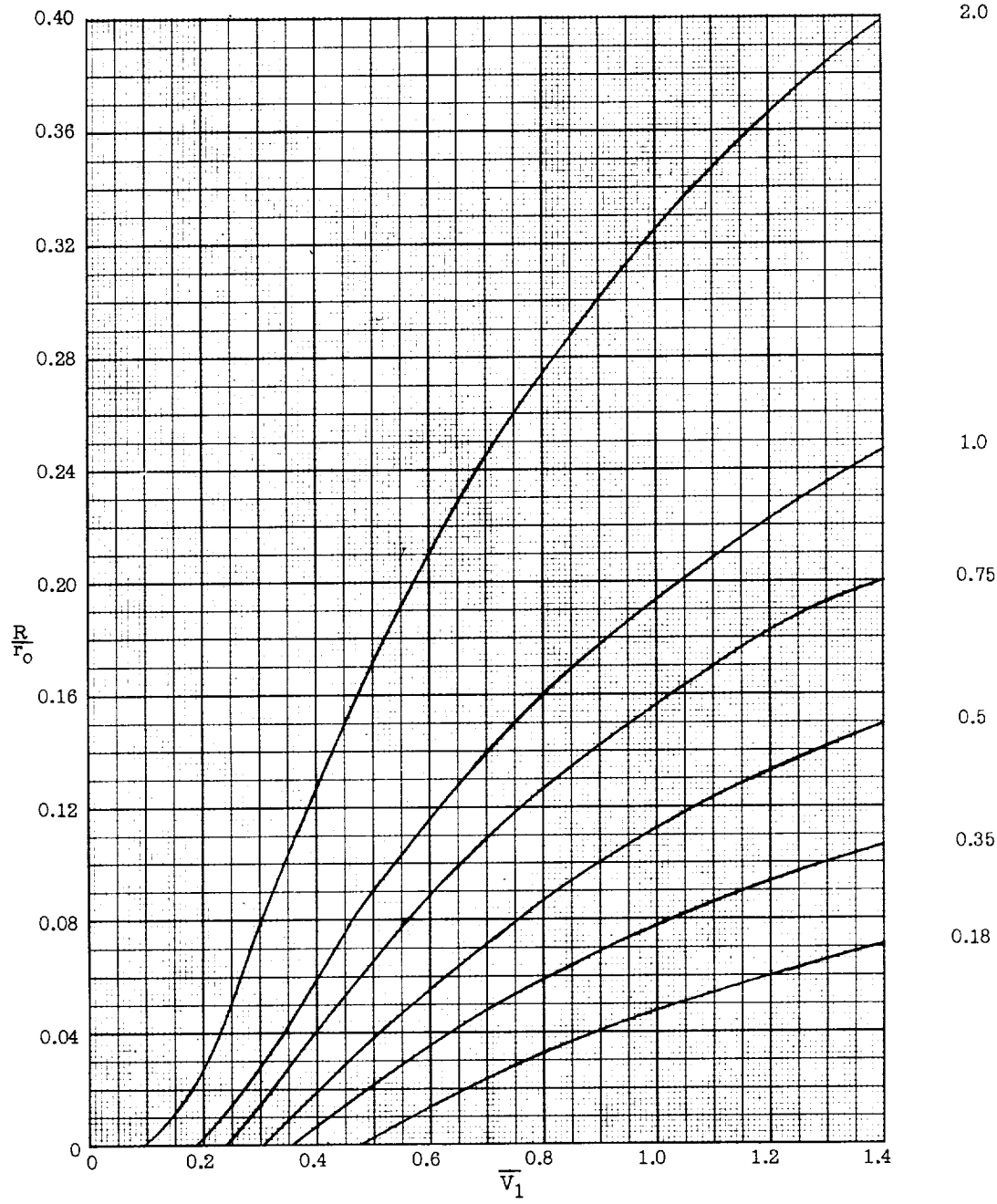
Figure 2.- Concluded.



(a)  $h = 150,000$  feet.

Figure 3.- Effect of velocity of initiation on longitudinal range attainable in constant-altitude maneuver.  $W/C_D A = 50$  pounds per square foot.

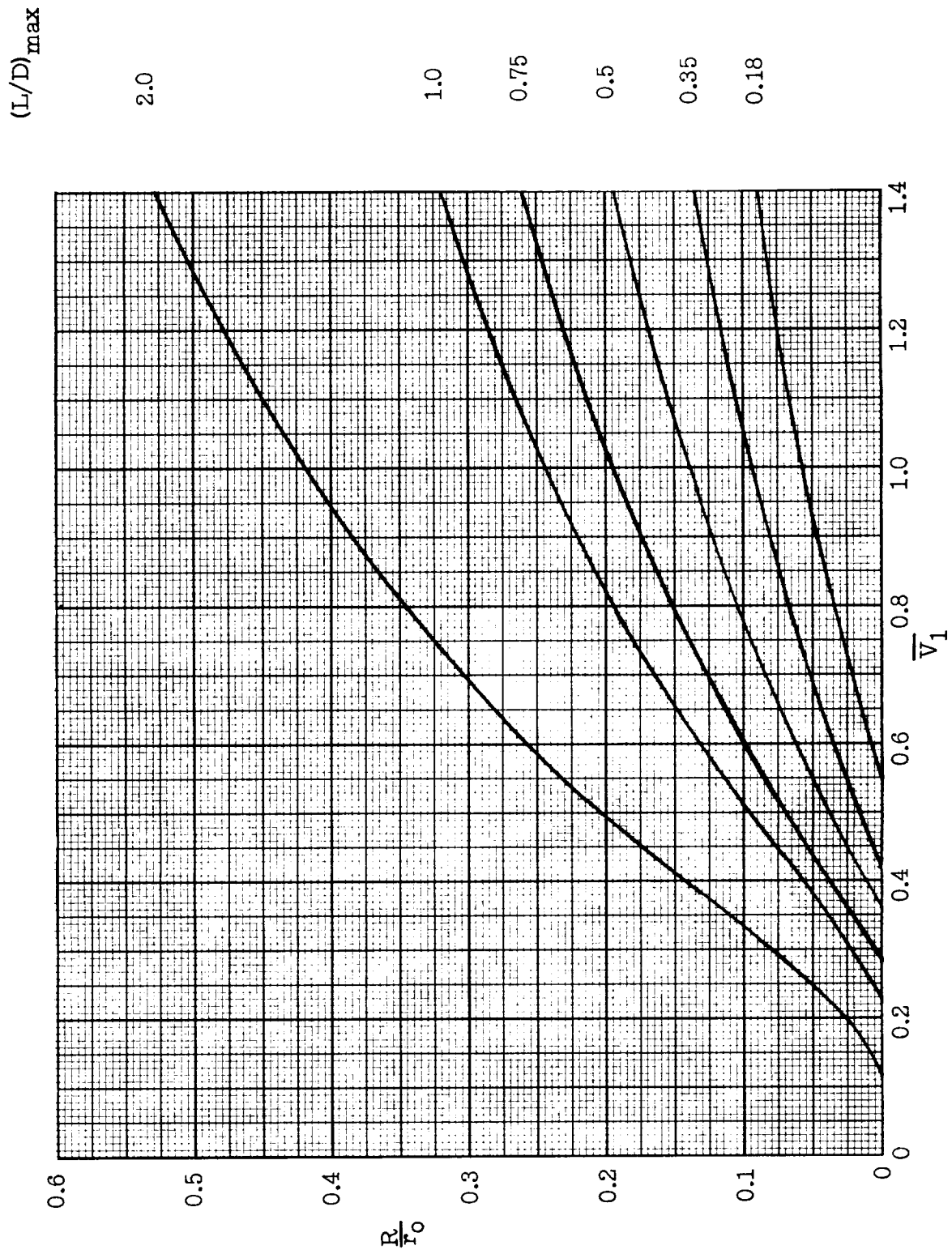
$(L/D)_{\max}$



(b)  $h = 160,000$  feet.

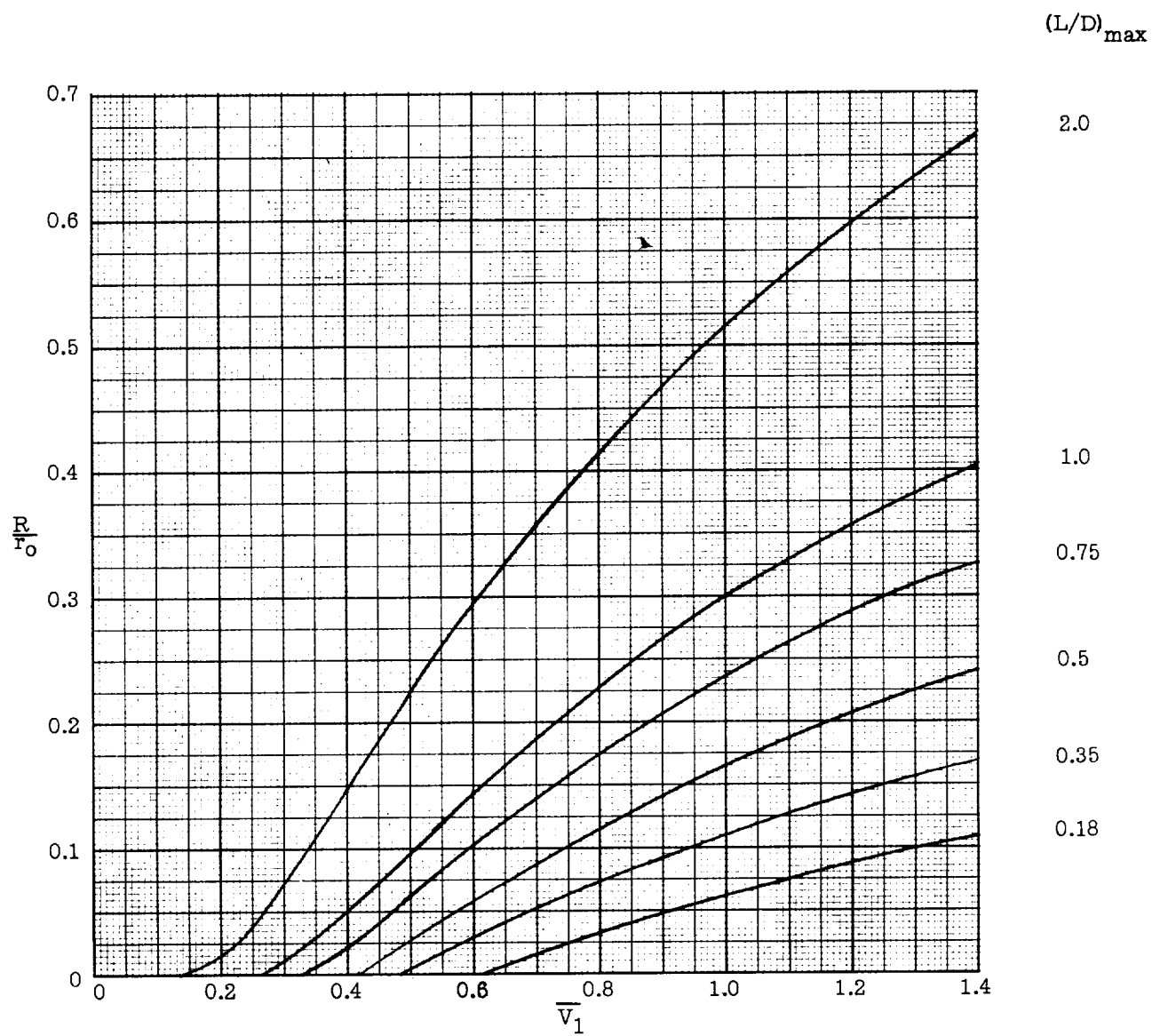
Figure 3.- Continued.





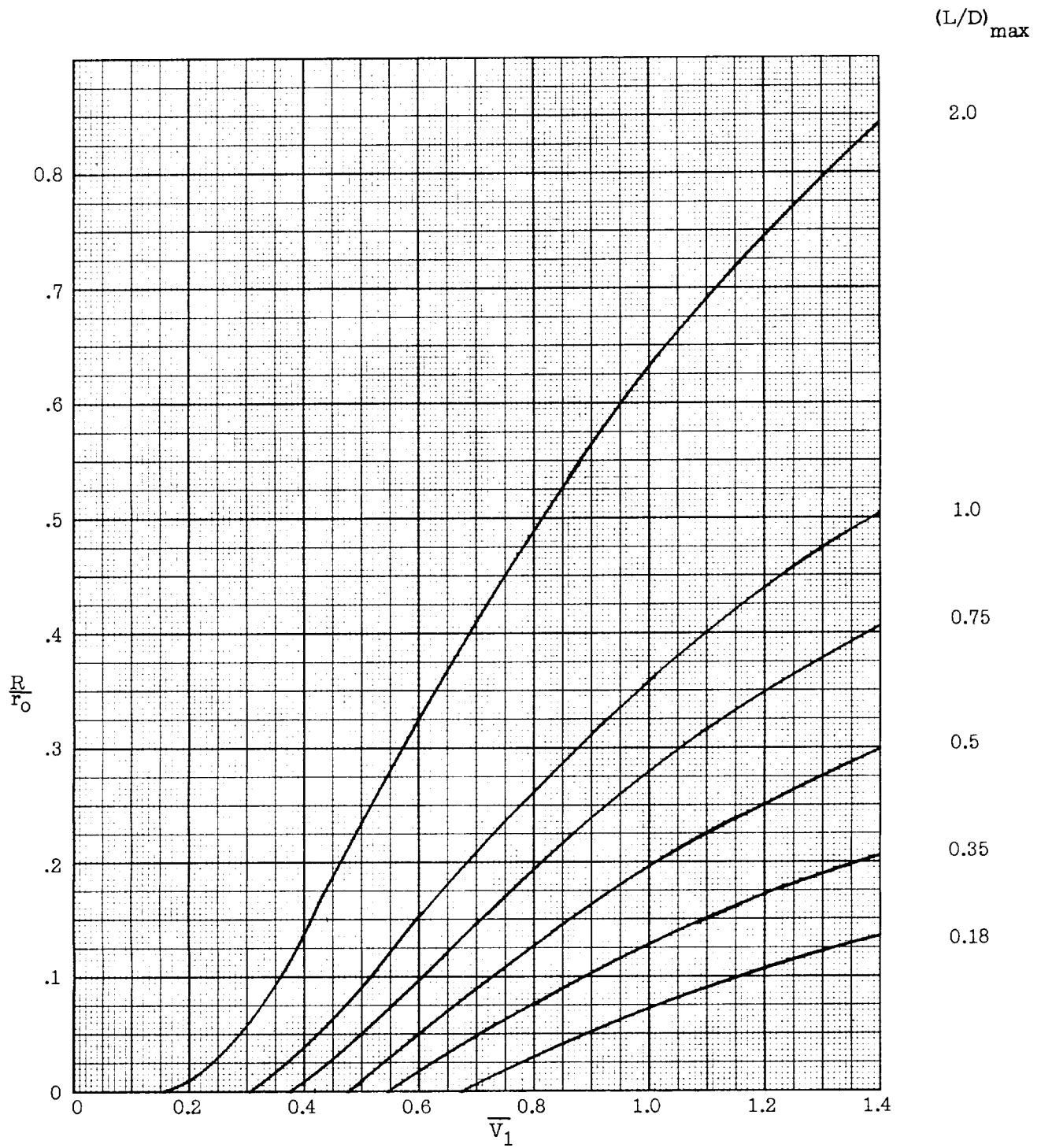
(c)  $h = 170,000$  feet.

Figure 3.- Continued.



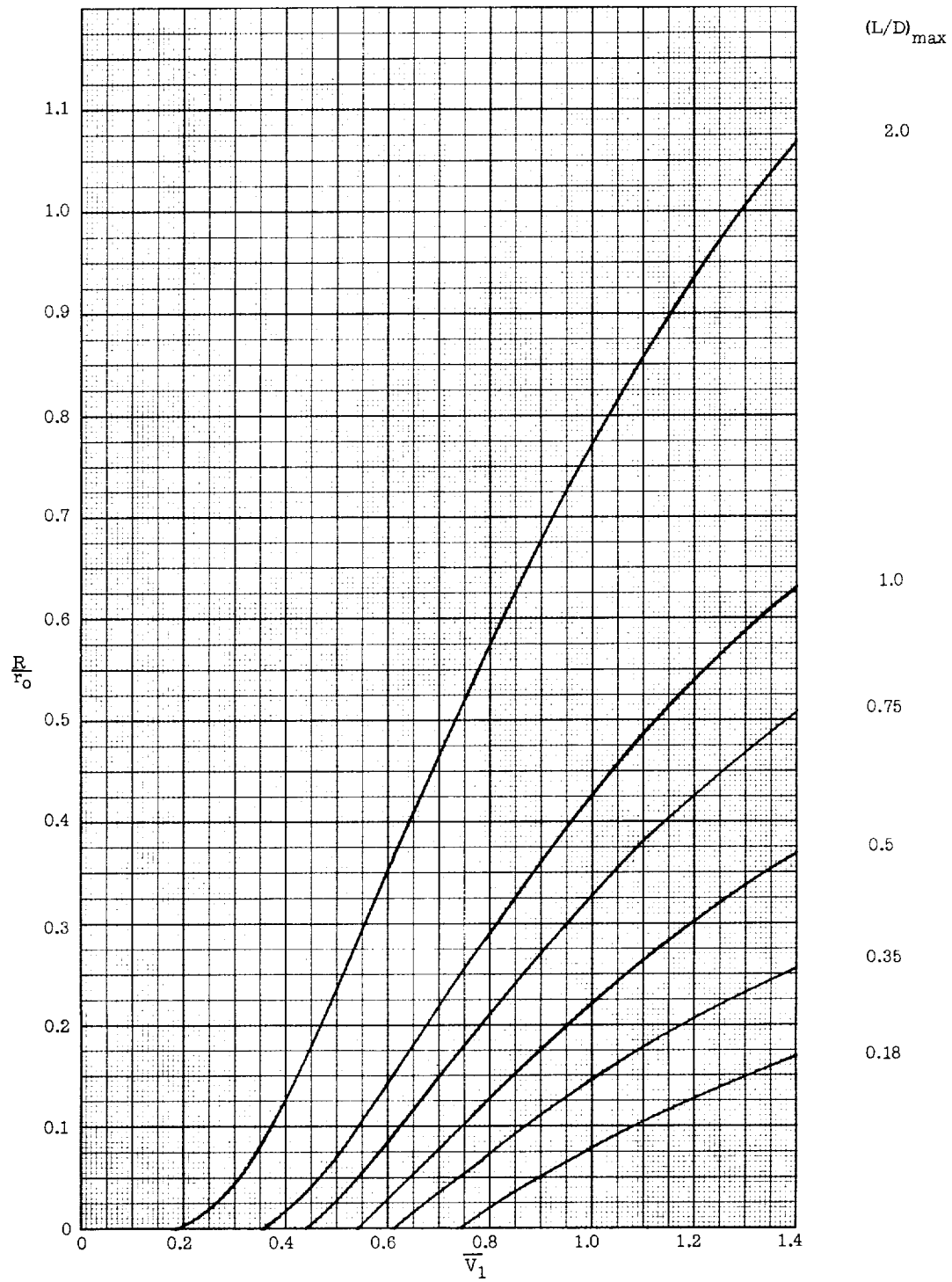
(d)  $h = 180,000$  feet.

Figure 3.- Continued.



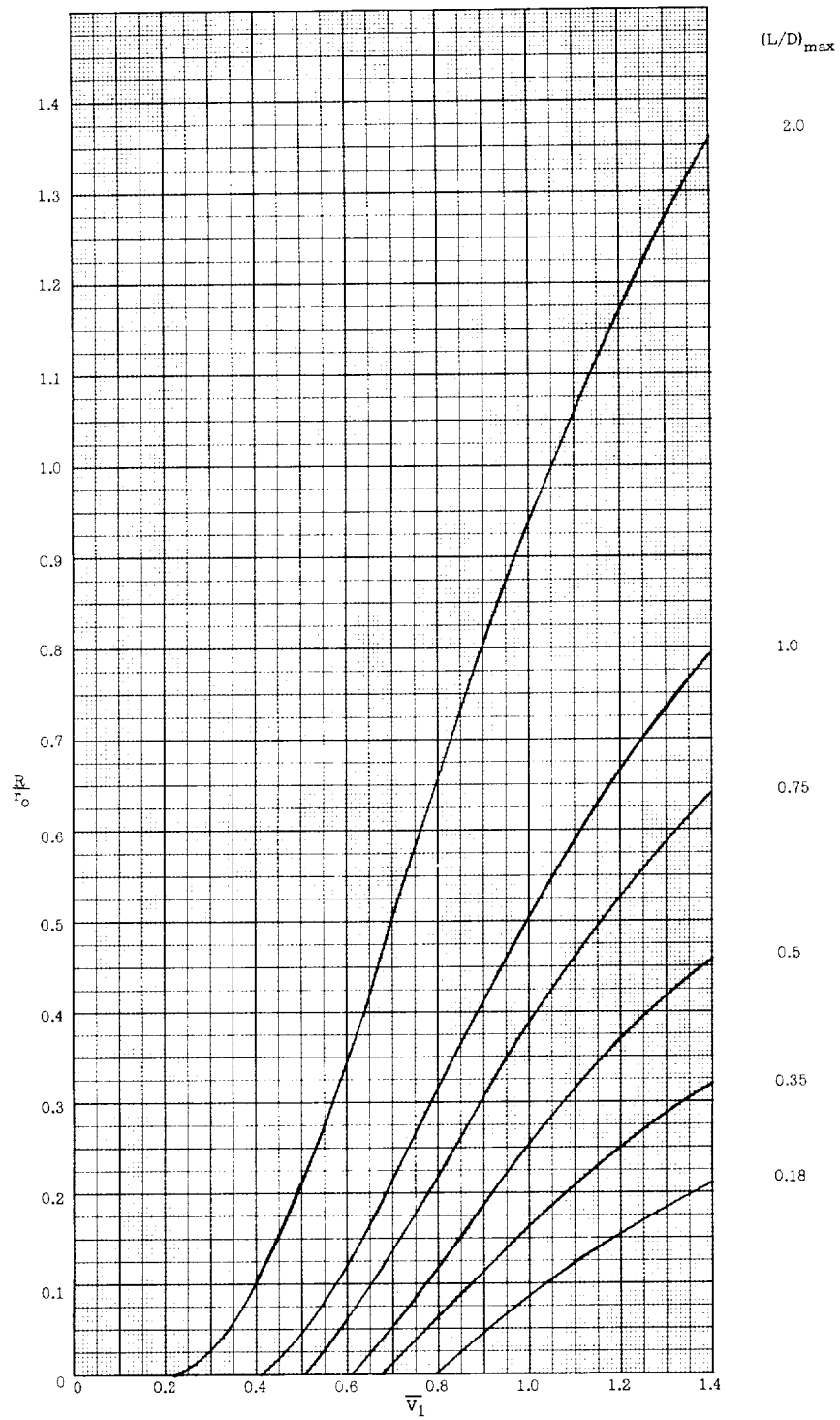
(e)  $h = 190,000$  feet.

Figure 3.- Continued.



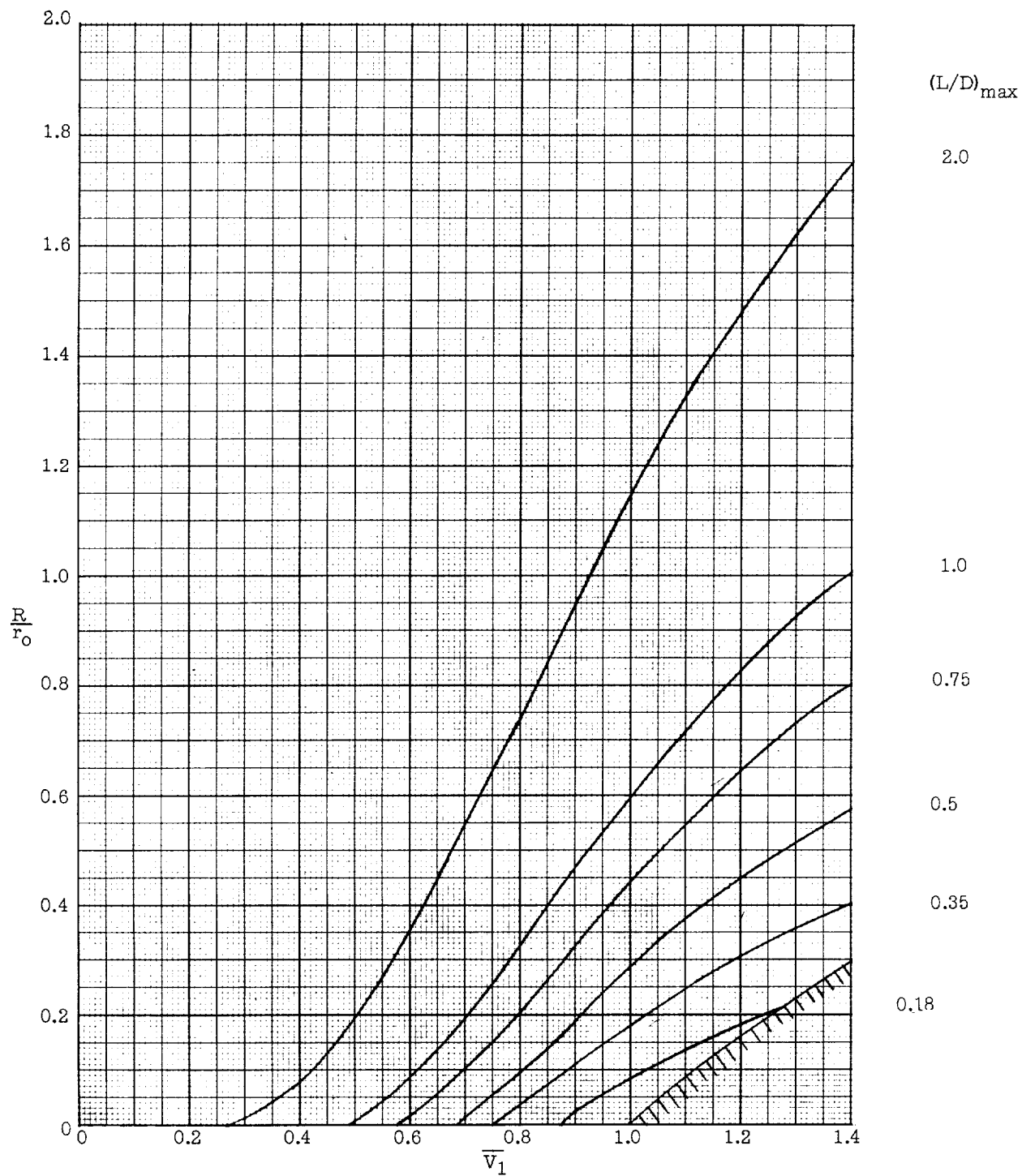
(f)  $h = 200,000$  feet.

Figure 3.- Continued.



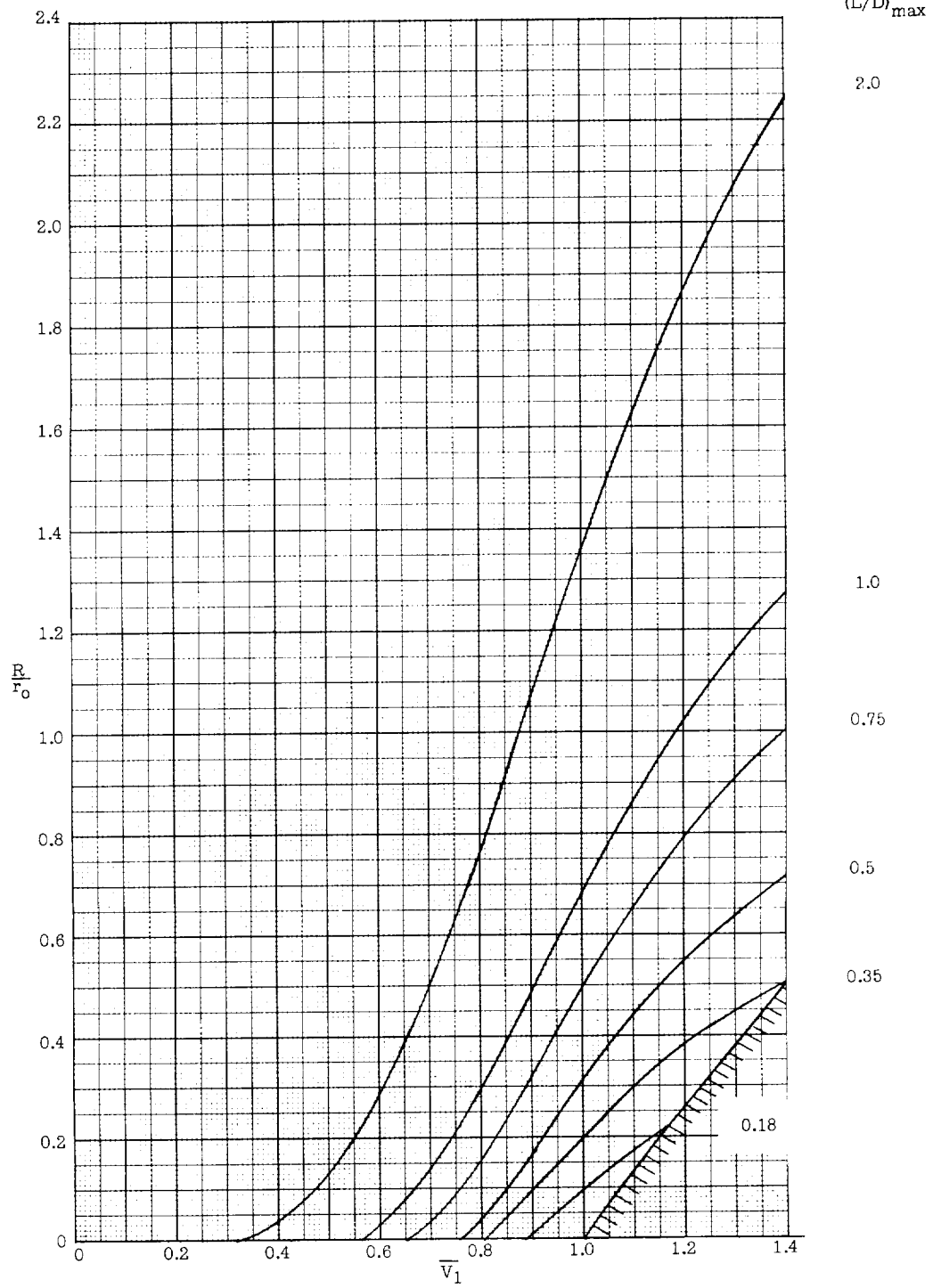
(g)  $h = 210,000$  feet.

Figure 3.- Continued.



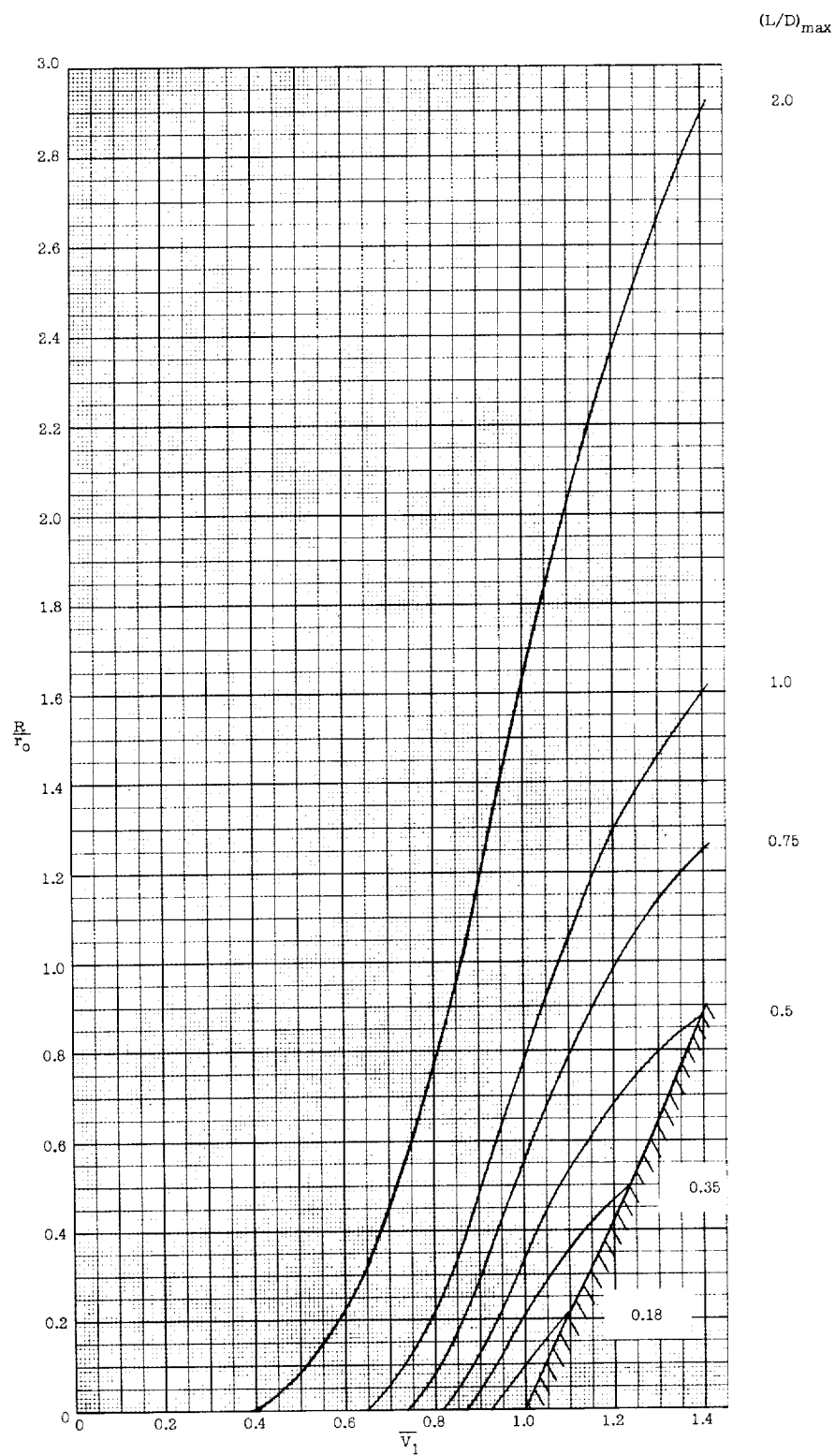
(h)  $h = 220,000$  feet.

Figure 3.- Continued.



(1)  $h = 230,000$  feet.

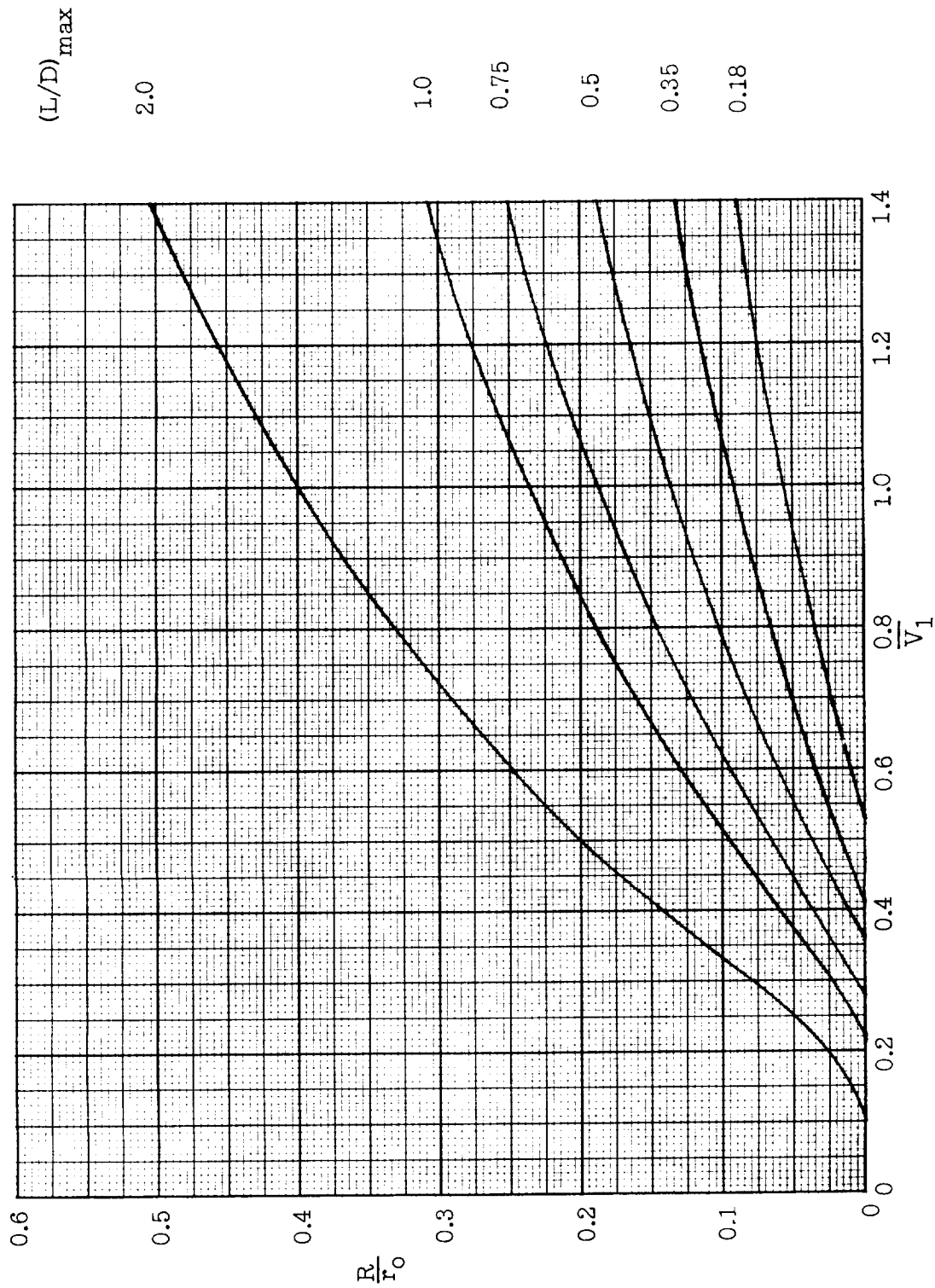
Figure 3.- Continued.



(j)  $h = 240,000$  feet.

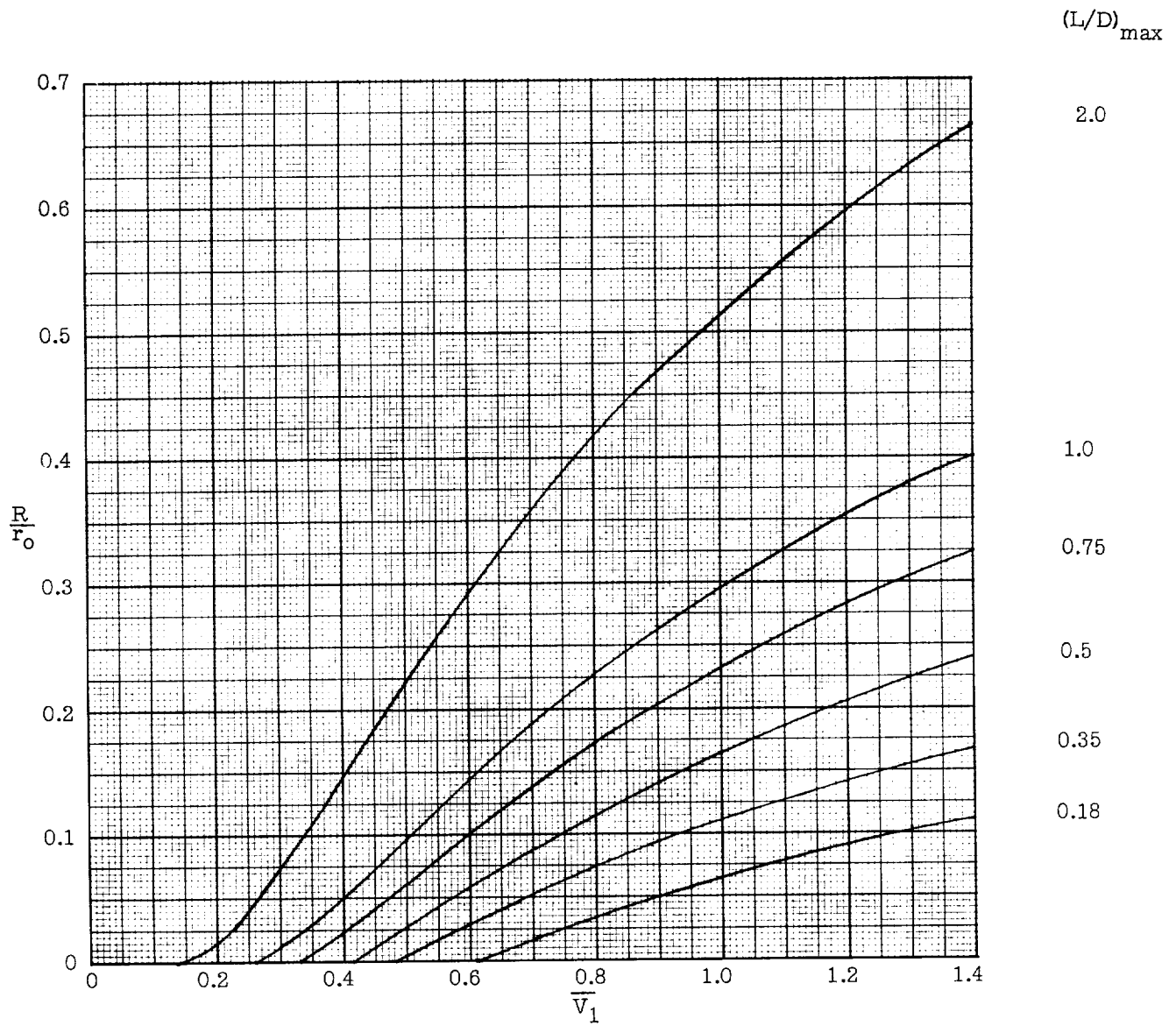
Figure 3.- Concluded.





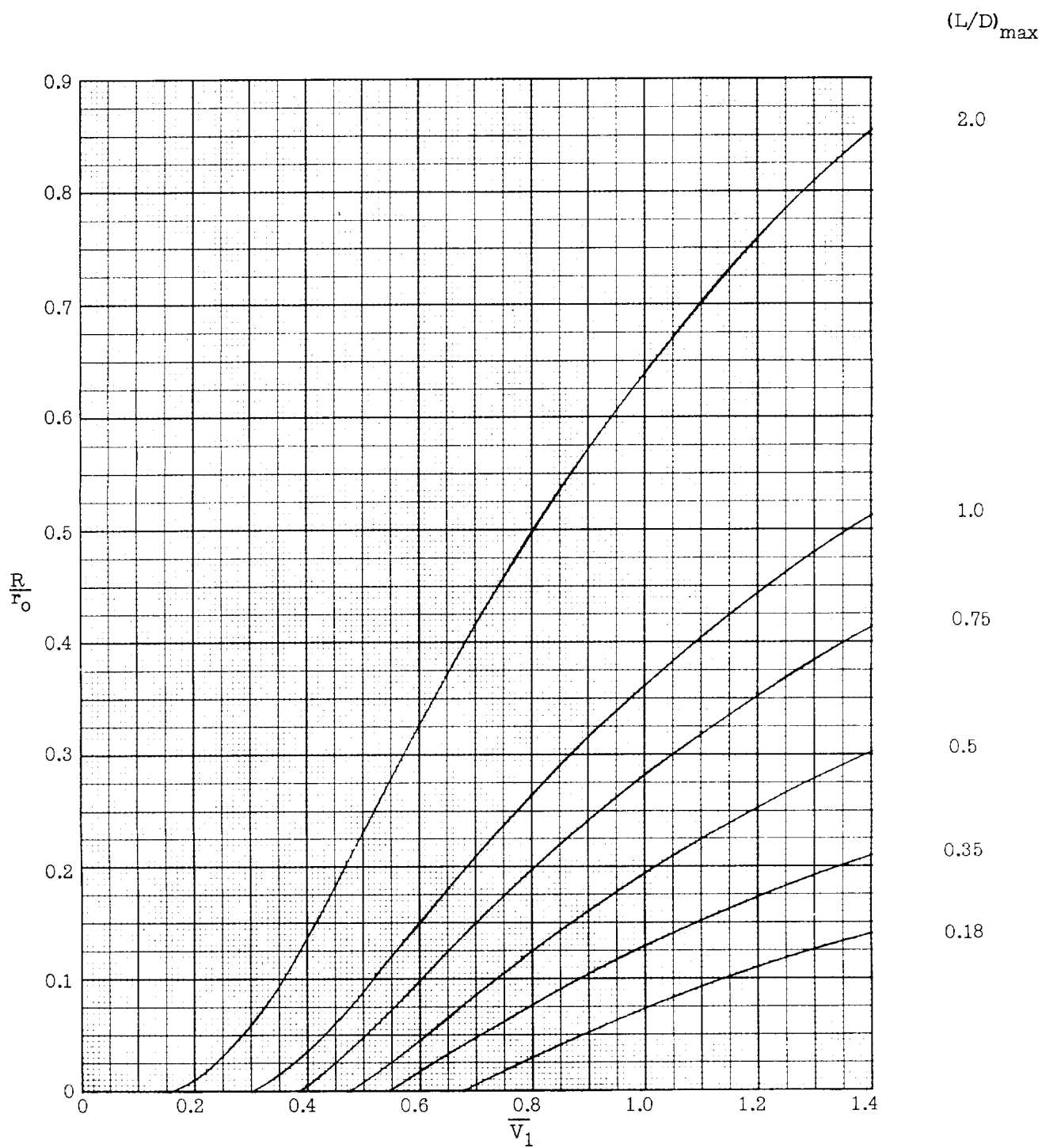
(a)  $h = 150,000$  feet.

Figure 4.- Effect of velocity of initiation on longitudinal range attainable in constant-altitude maneuver.  $w/C_D A = 100$  pounds per square foot.



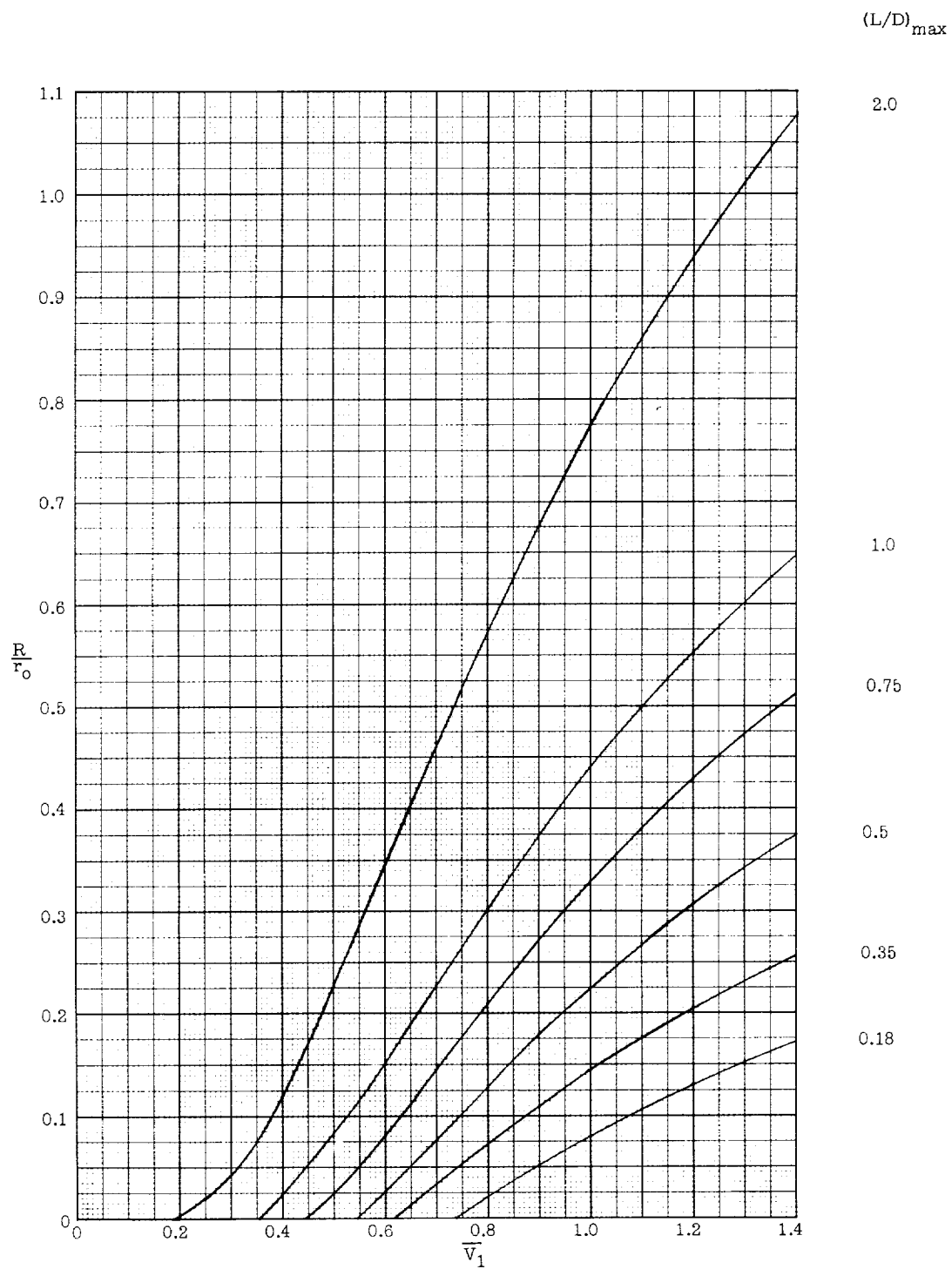
(b)  $h = 160,000$  feet.

Figure 4.- Continued.



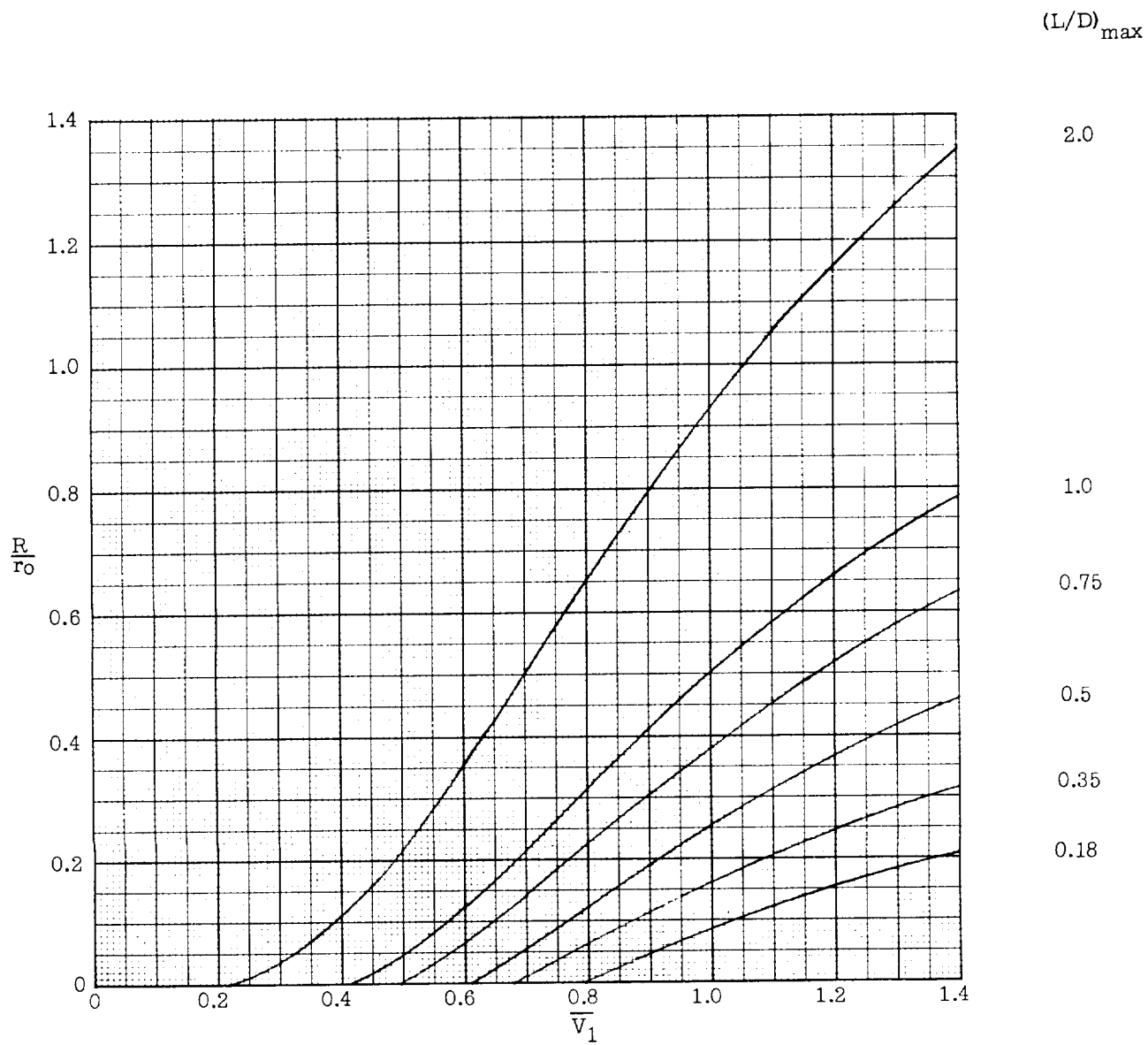
(c)  $h = 170,000$  feet.

Figure 4.- Continued.



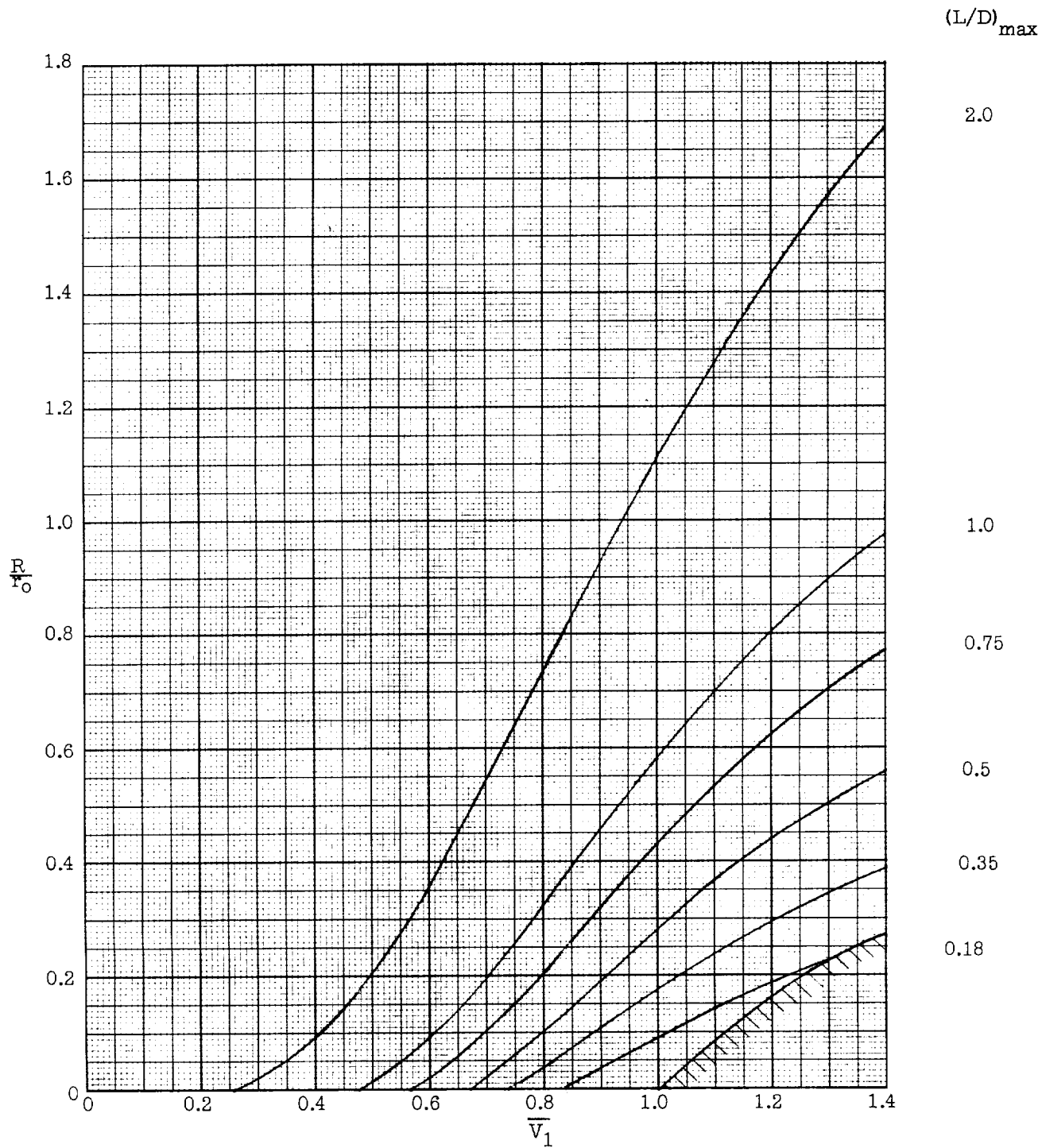
(d)  $h = 180,000$  feet.

Figure 4.- Continued.



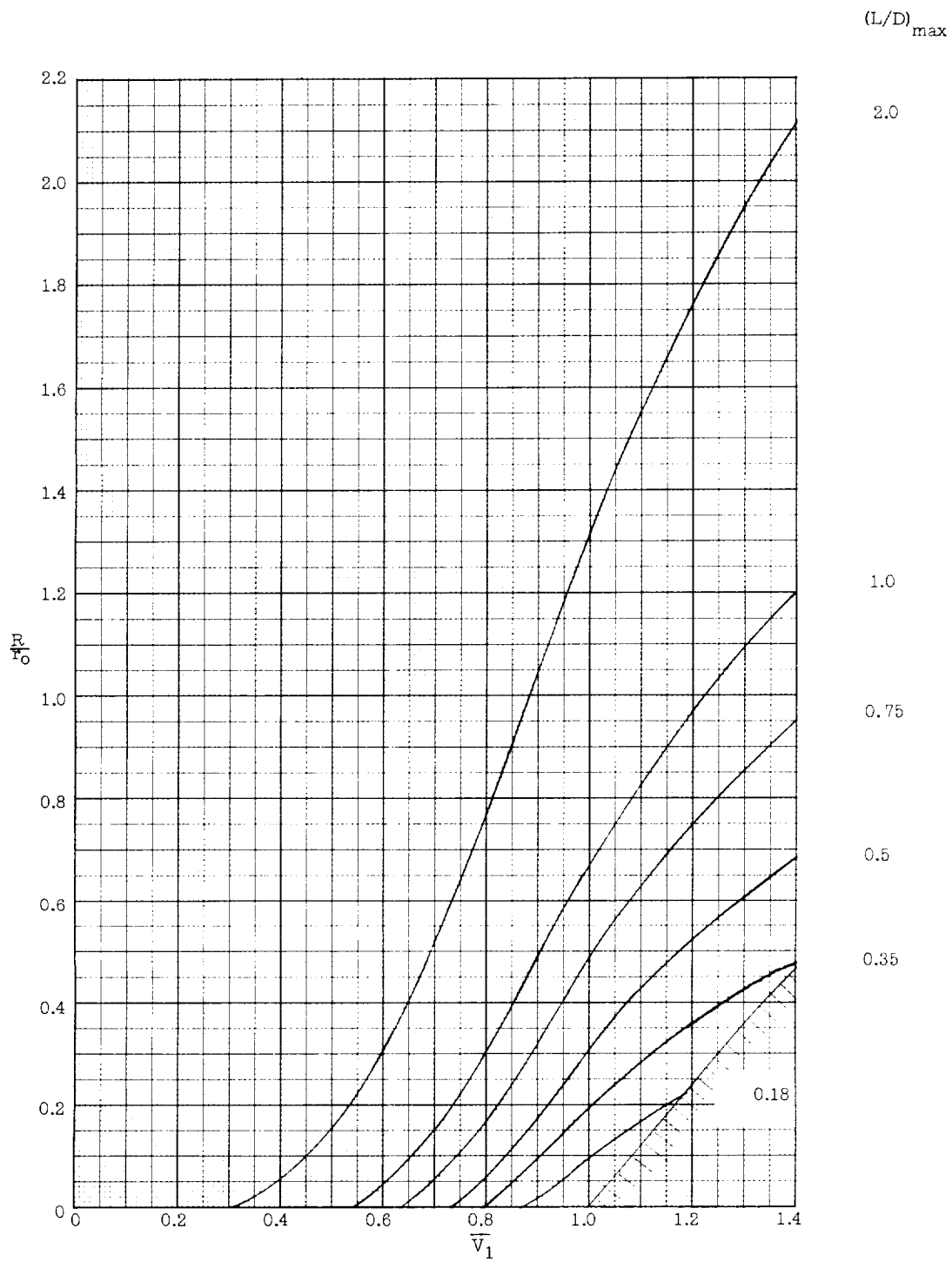
(e)  $h = 190,000$  feet.

Figure 4.- Continued.



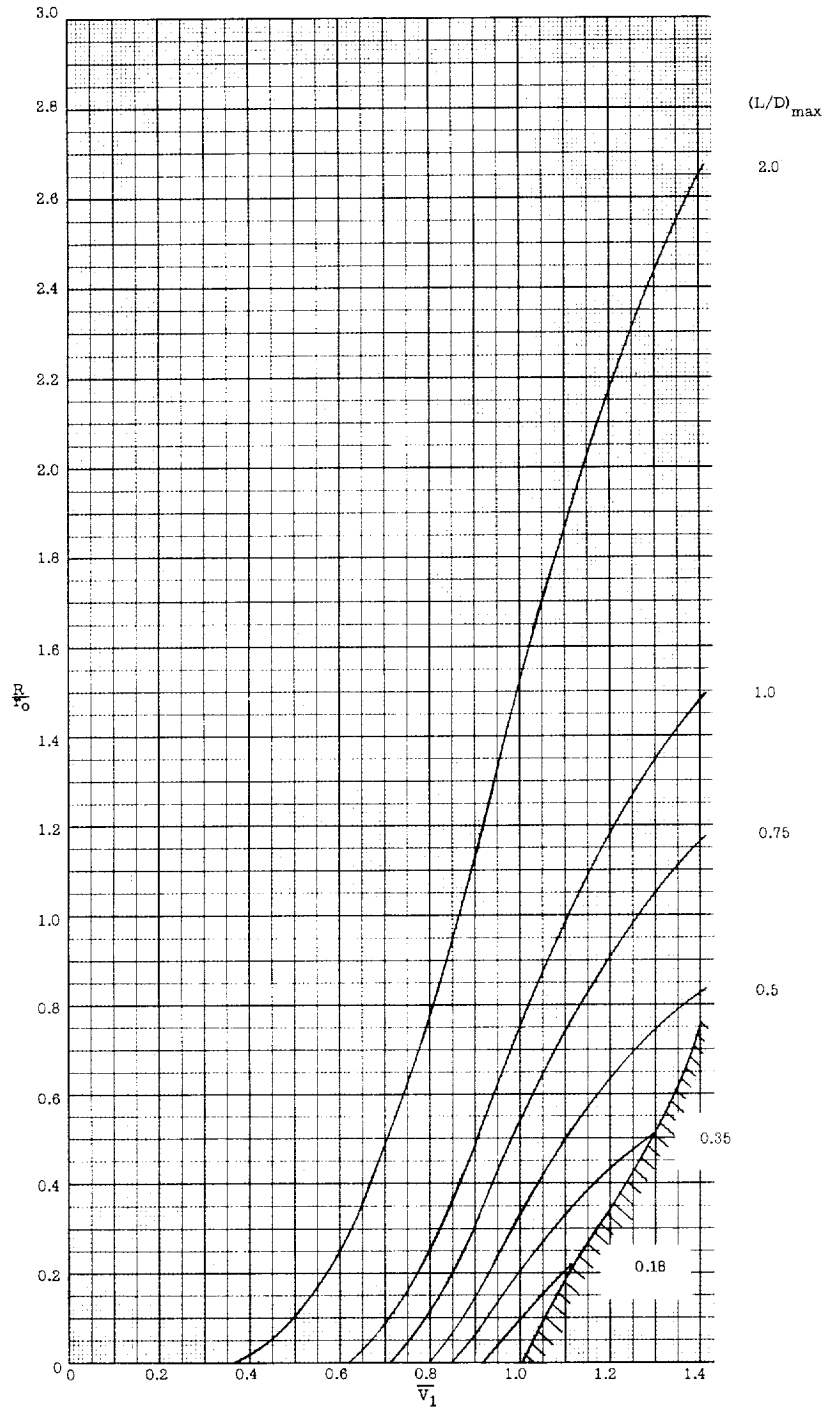
(f)  $h = 200,000$  feet.

Figure 4.- Continued.



(g)  $h = 210,000$  feet.

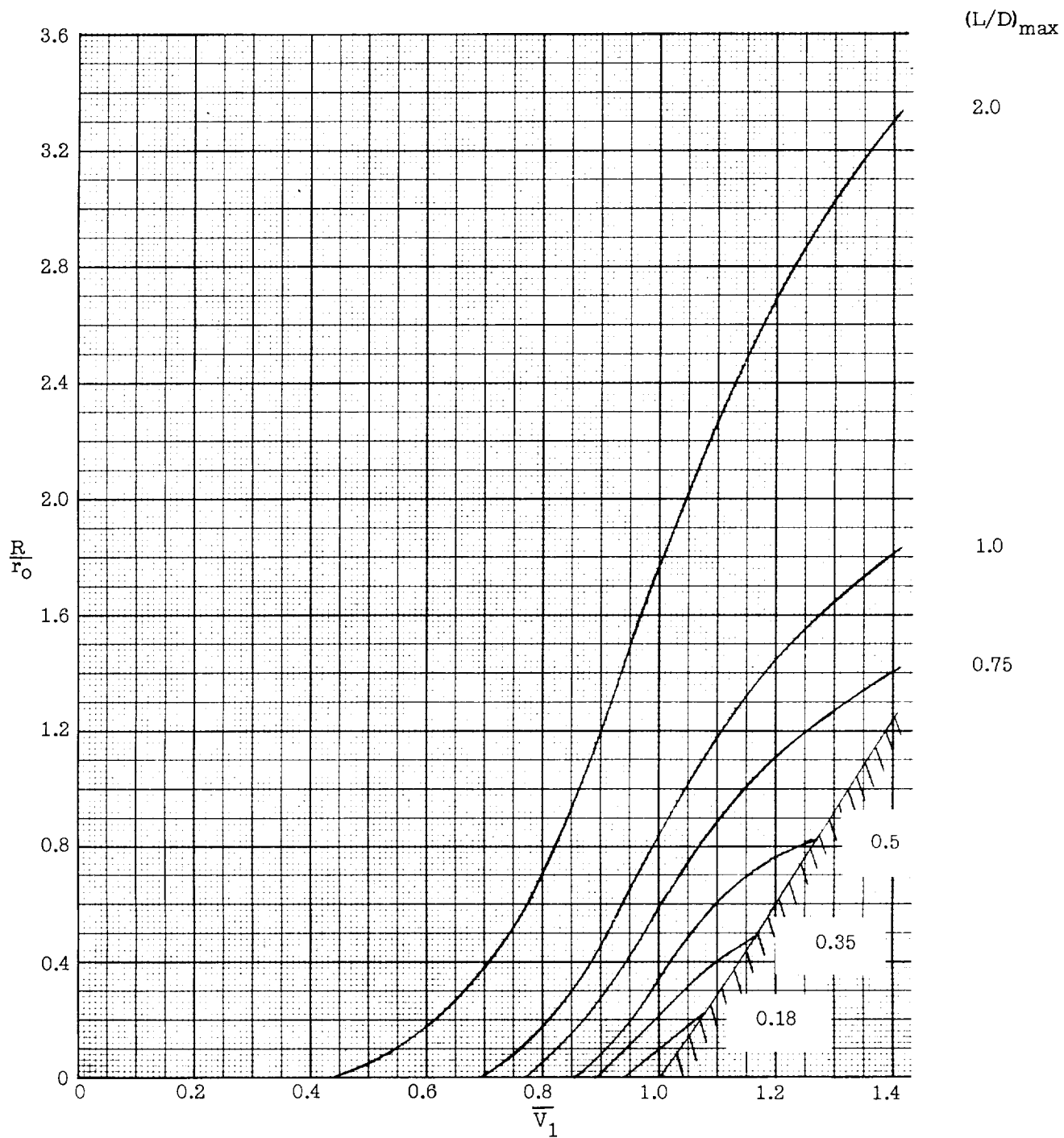
Figure 4.- Continued.



(h)  $h = 220,000$  feet.

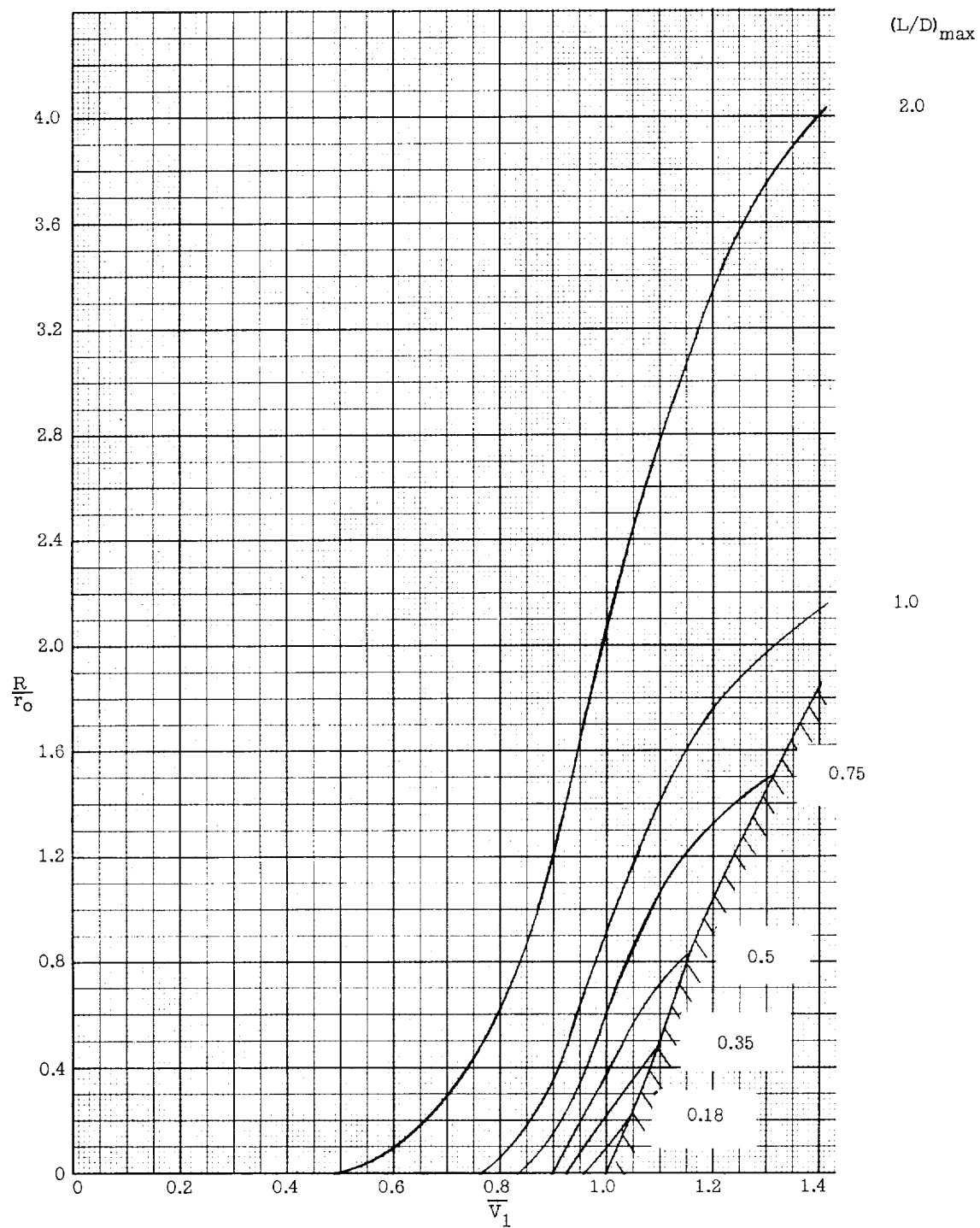
Figure 4.- Continued.





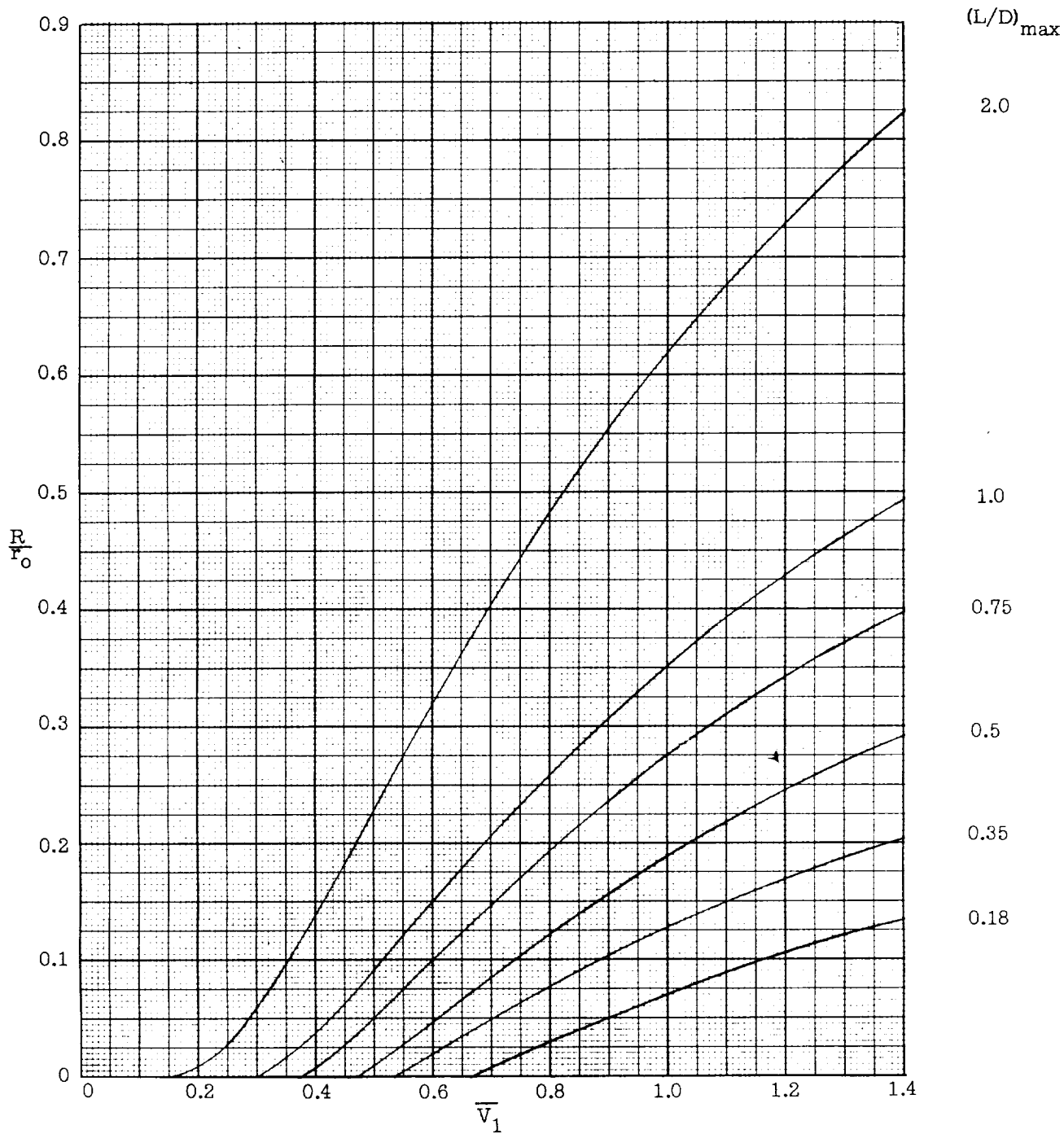
(i)  $h = 230,000$  feet.

Figure 4.- Continued.



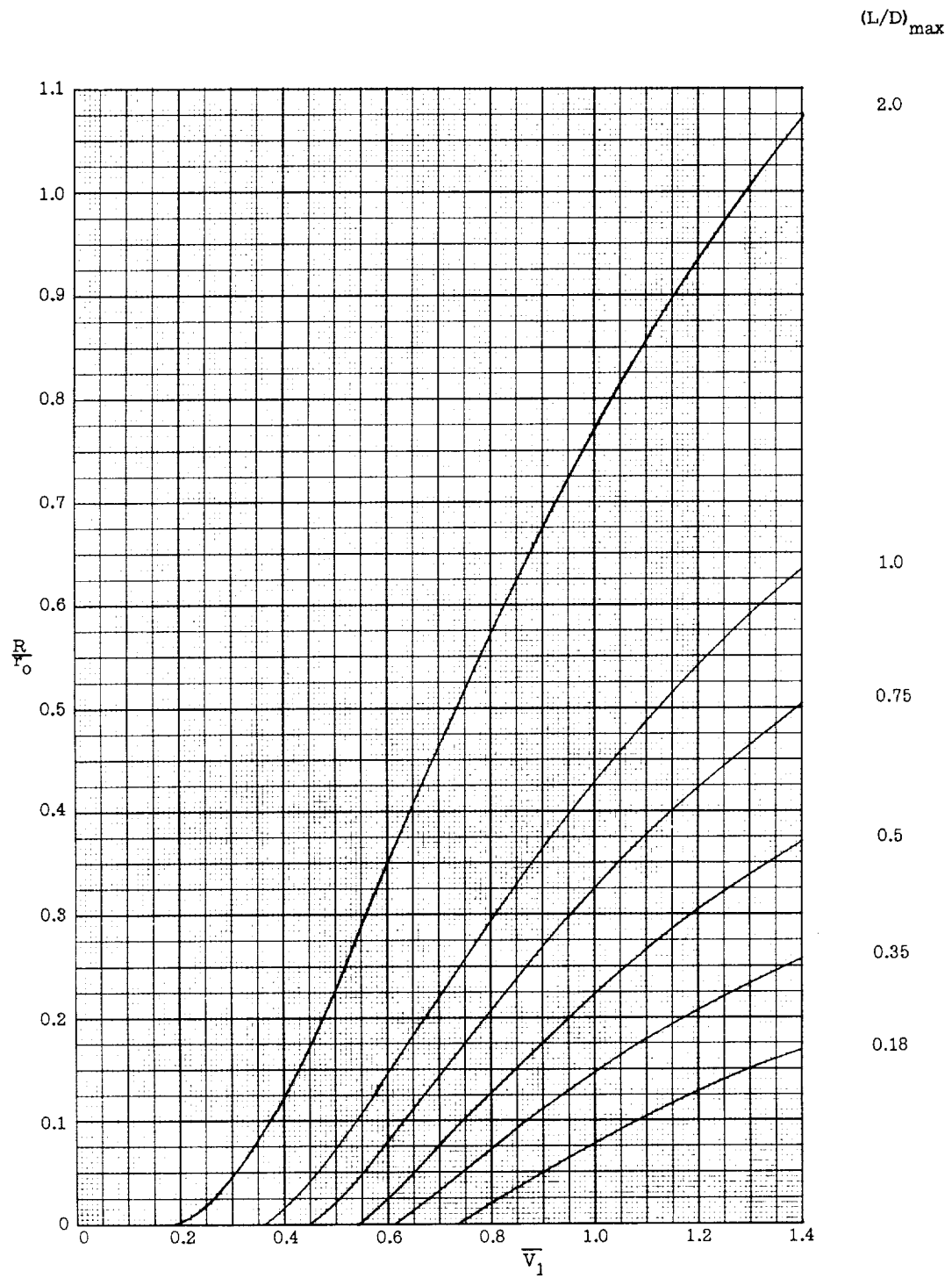
(j)  $h = 240,000$  feet.

Figure 4.- Concluded.



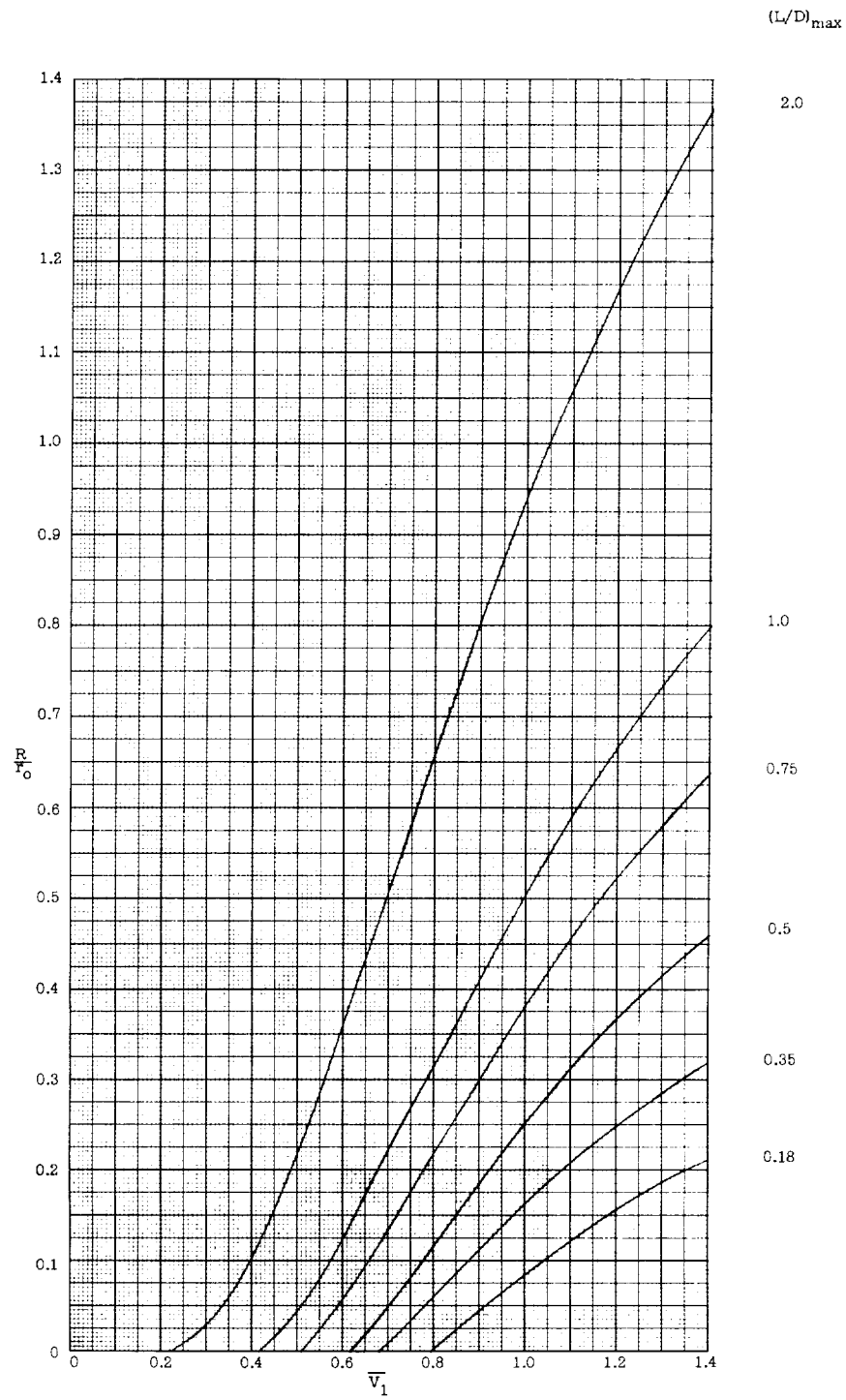
(a)  $h = 150,000$  feet.

Figure 5.- Effect of velocity of initiation on longitudinal range attainable in constant-altitude maneuver.  $W/C_D A = 200$  pounds per square foot.



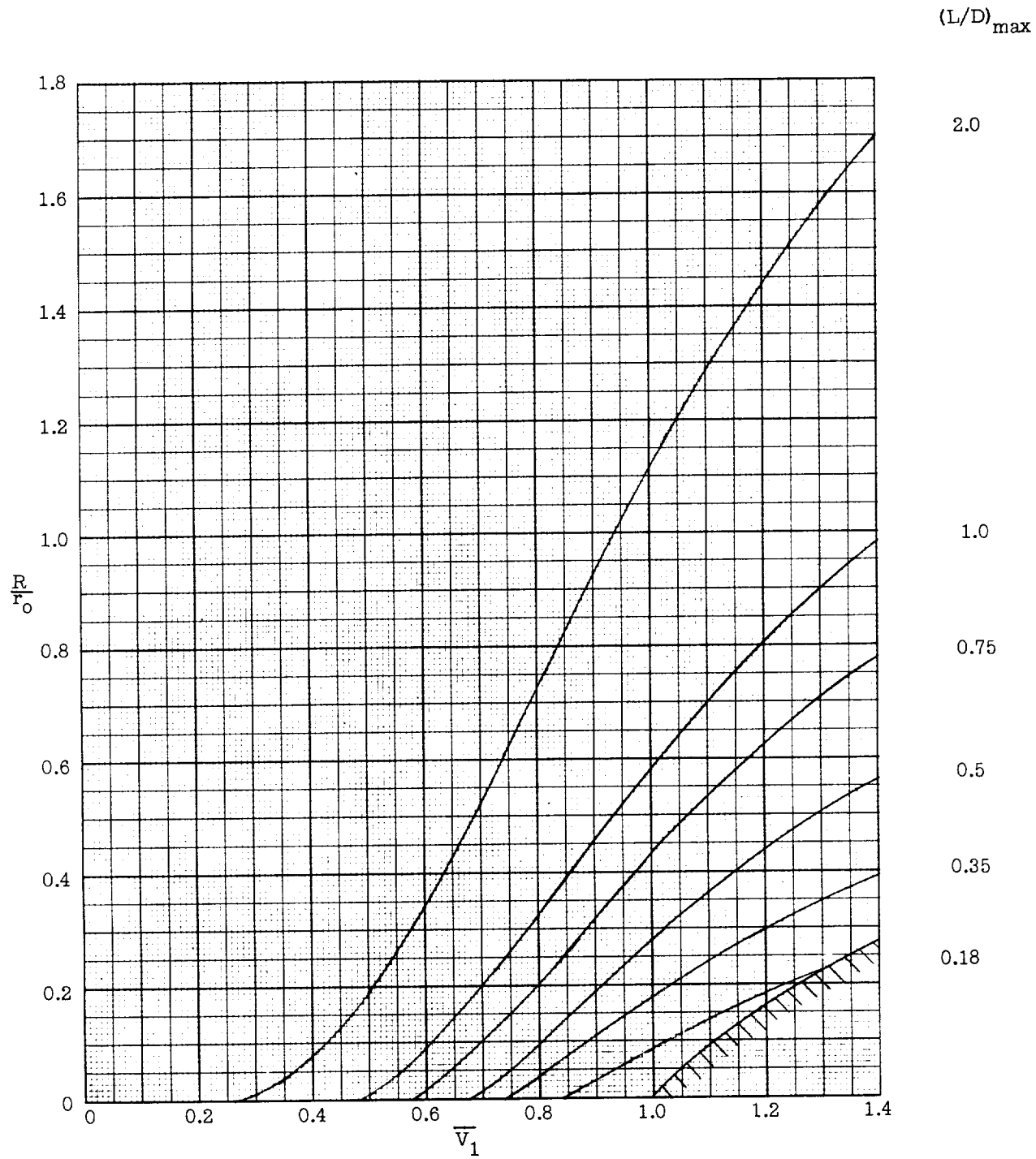
(b)  $h = 160,000$  feet.

Figure 5.- Continued.



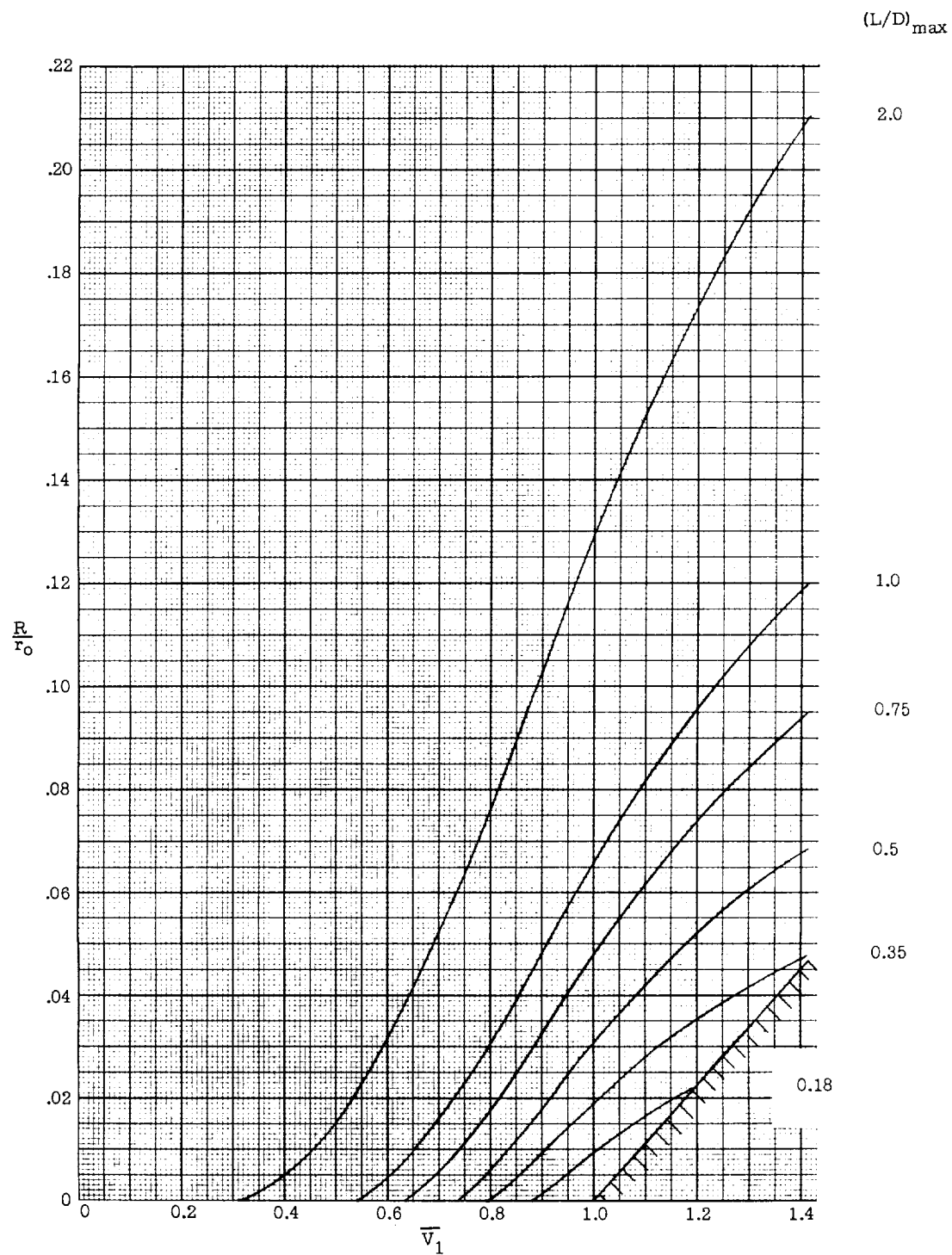
(c)  $h = 170,000$  feet.

Figure 5.- Continued.



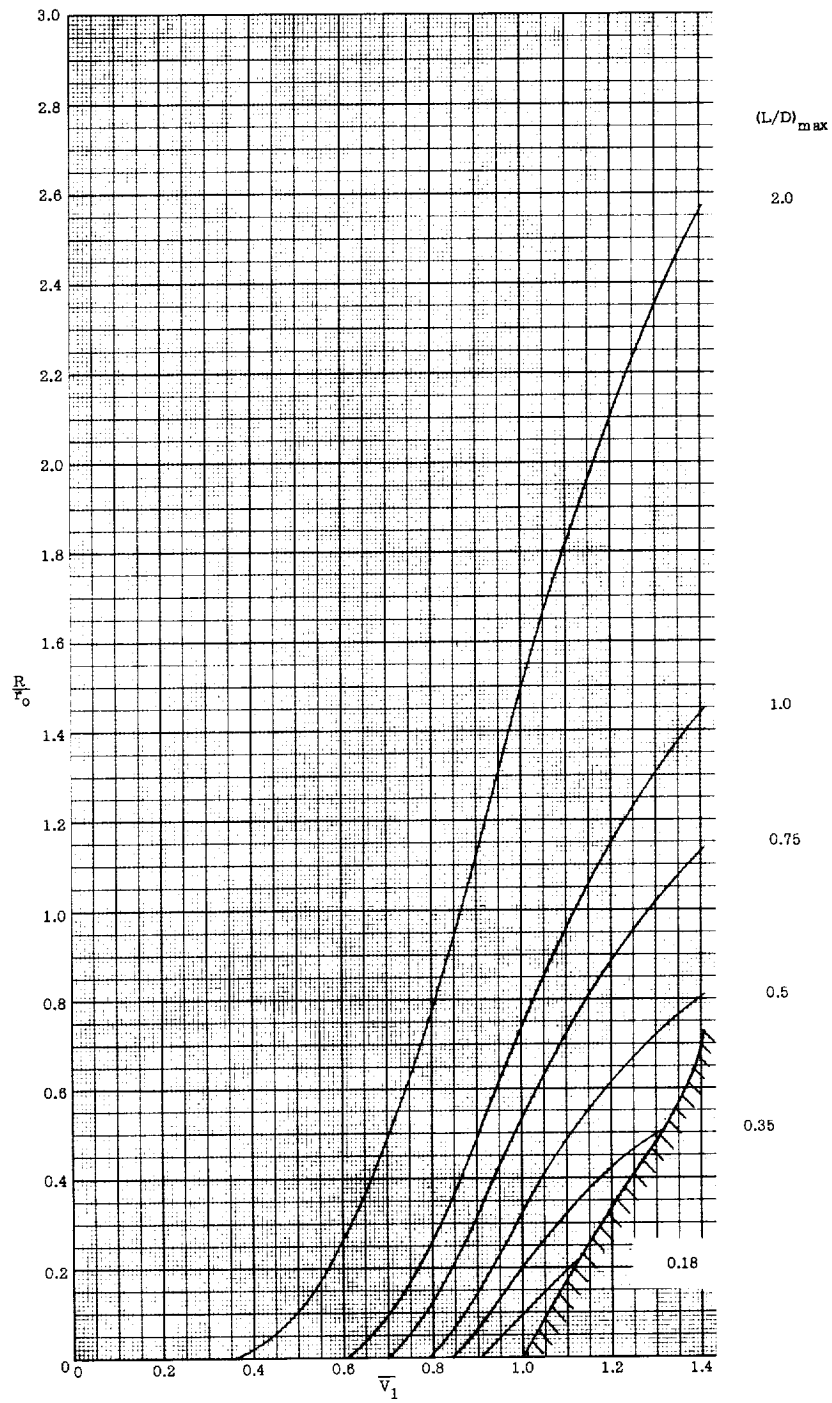
(d)  $h = 180,000$  feet.

Figure 5.- Continued.



(e)  $h = 190,000$  feet.

Figure 5.- Continued.

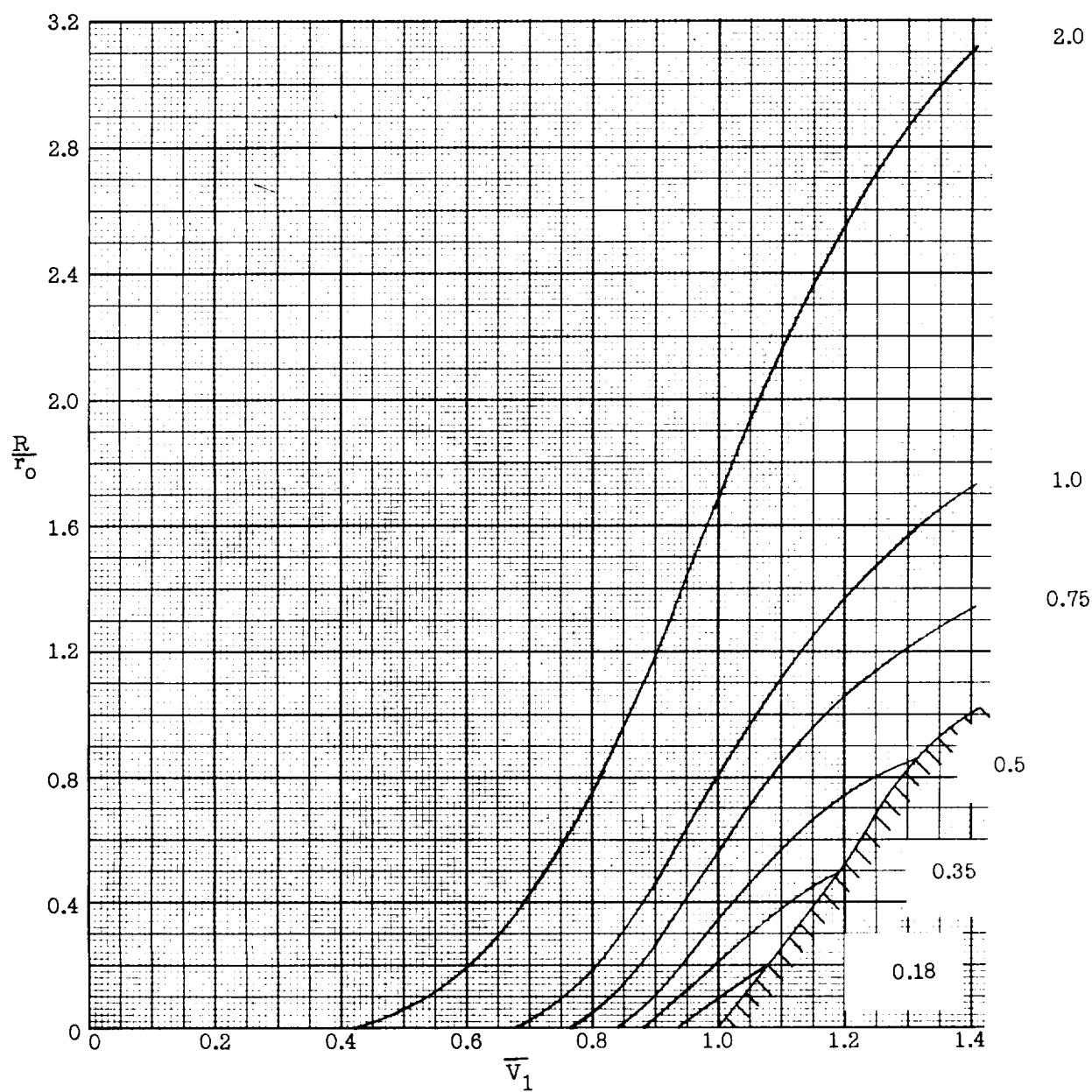


(f)  $h = 200,000$  feet.

Figure 5.- Continued.

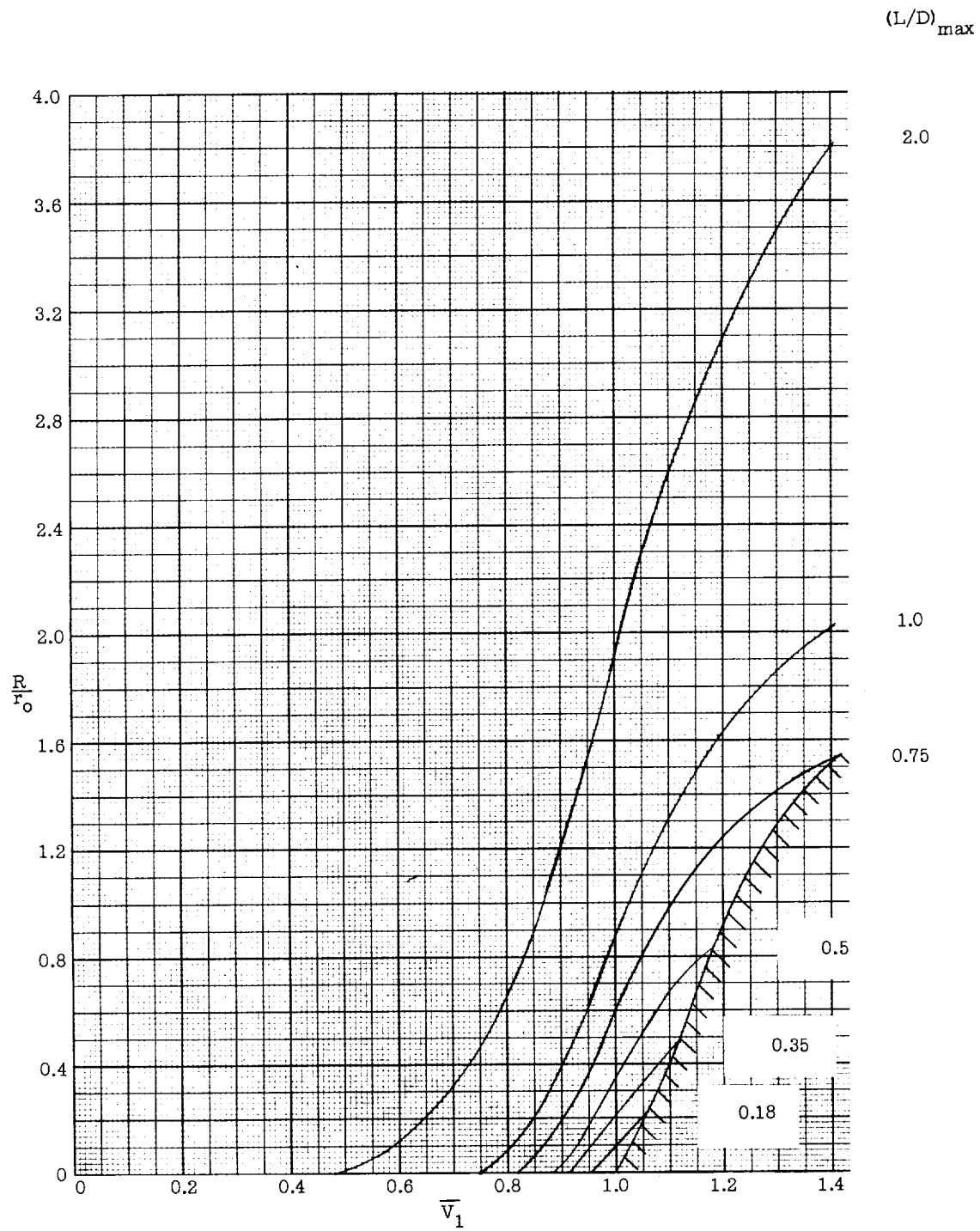


$(L/D)_{\max}$



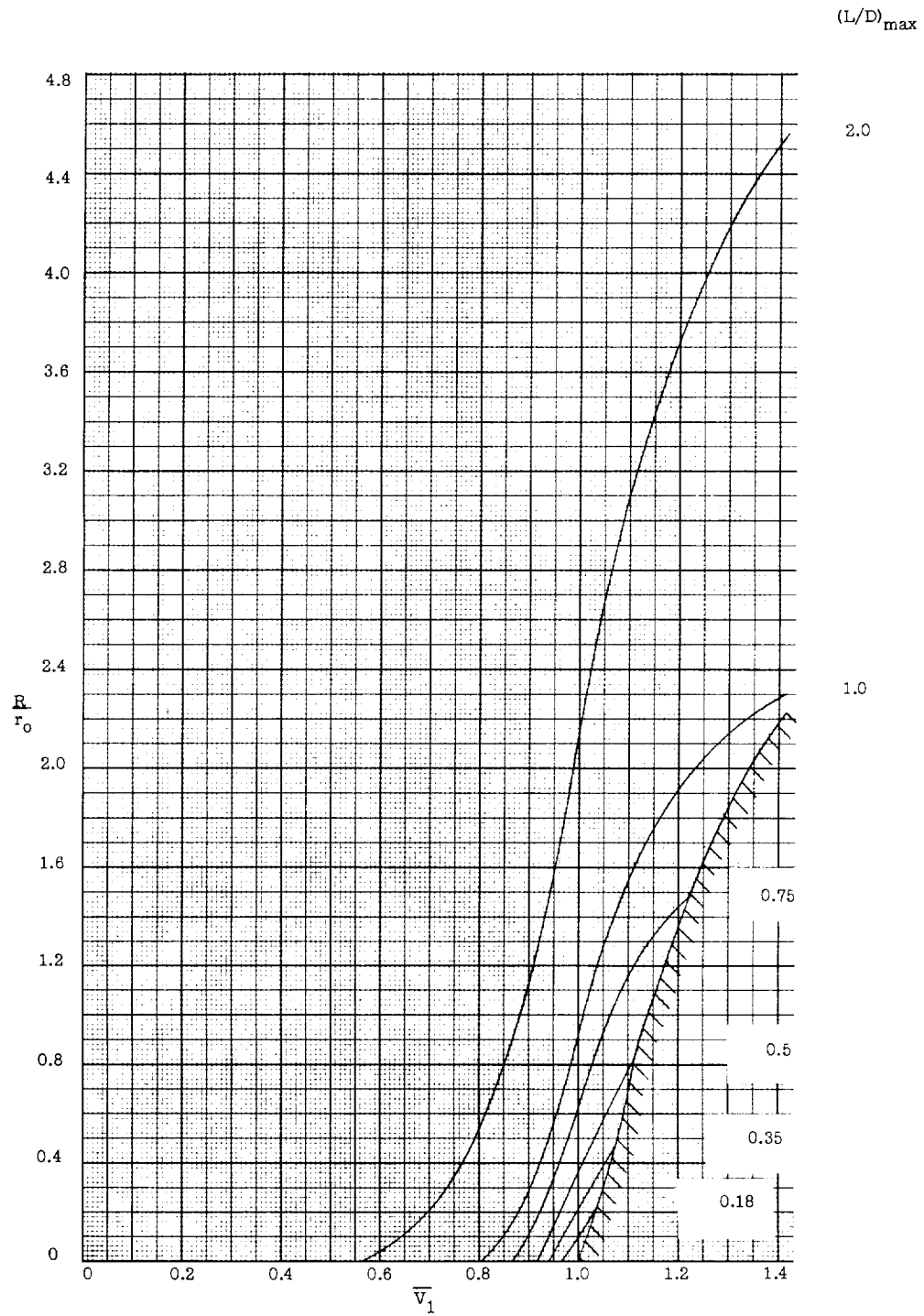
(g)  $h = 210,000$  feet.

Figure 5.- Continued.



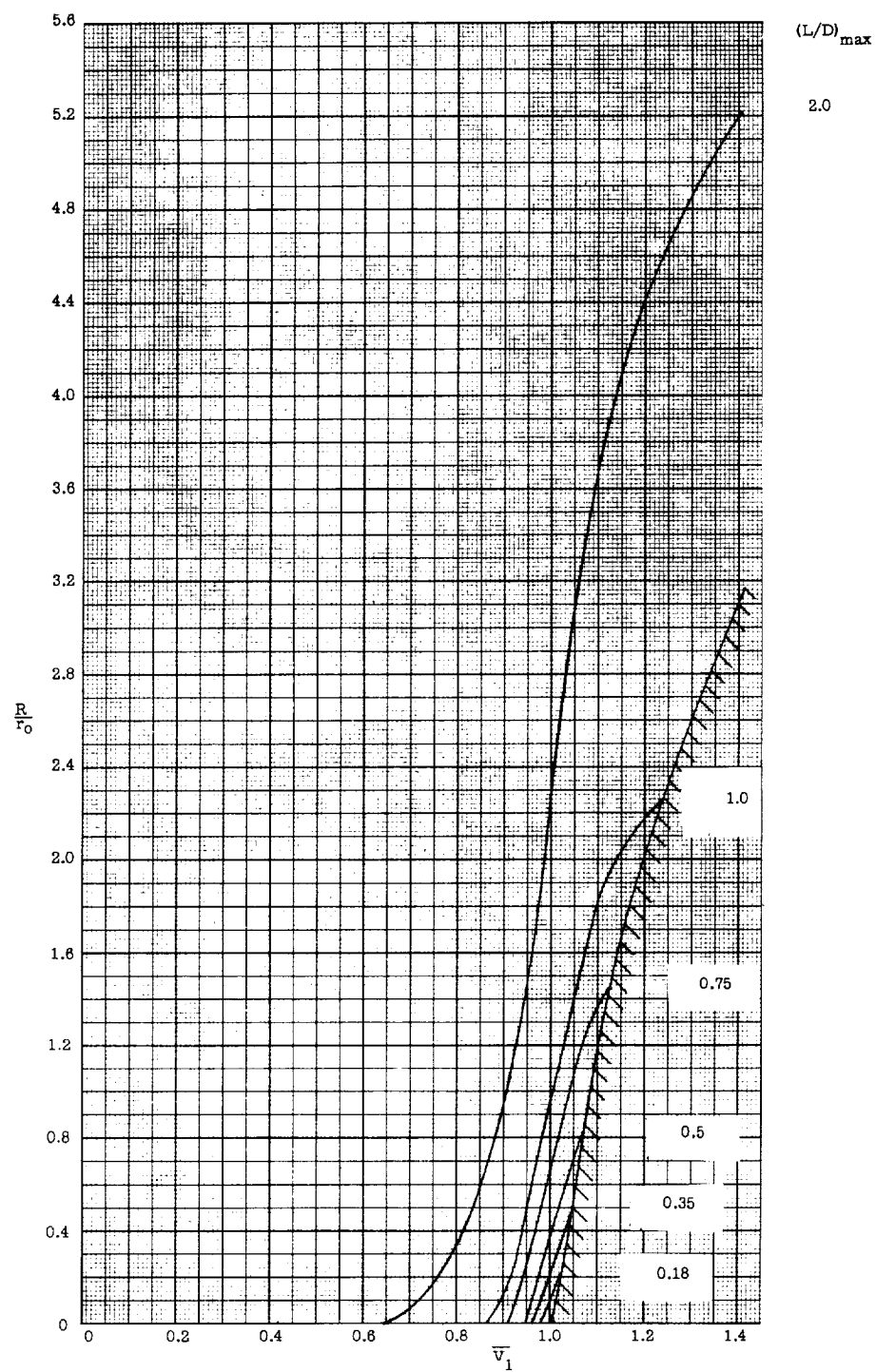
(h)  $h = 220,000$  feet.

Figure 5.- Continued.



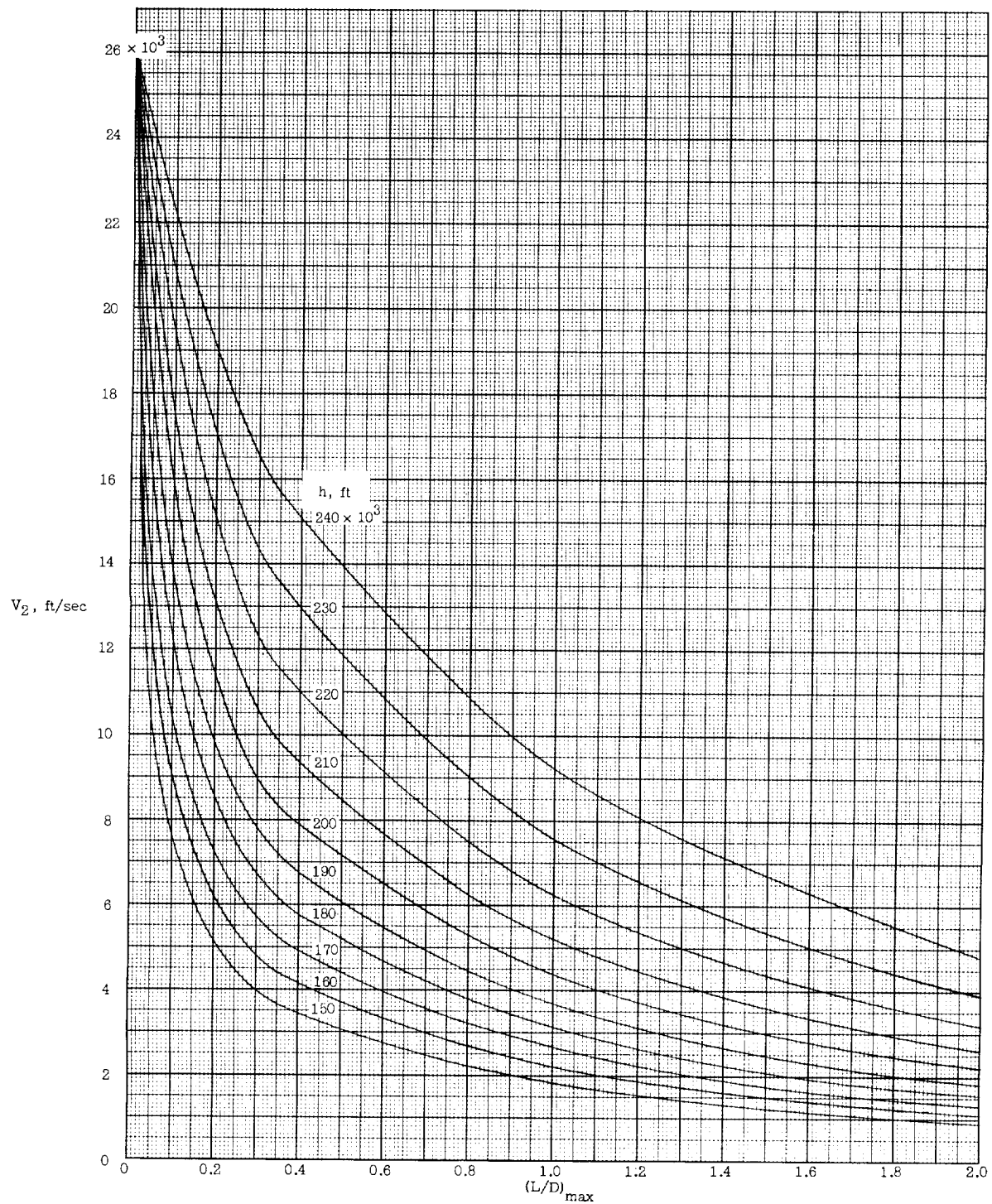
(1)  $h = 230,000$  feet.

Figure 5.- Continued.



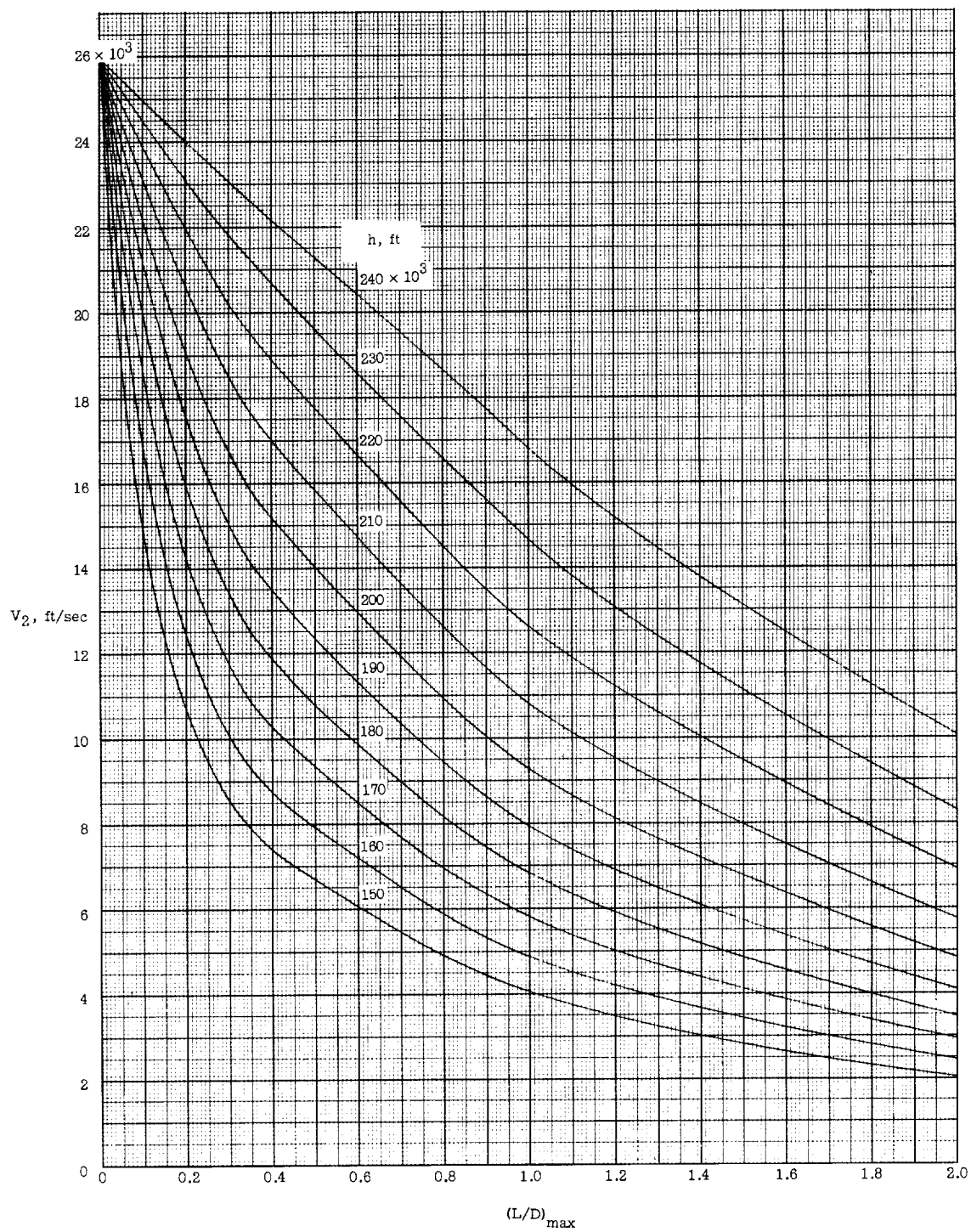
(j)  $h = 240,000$  feet.

Figure 5.- Concluded.



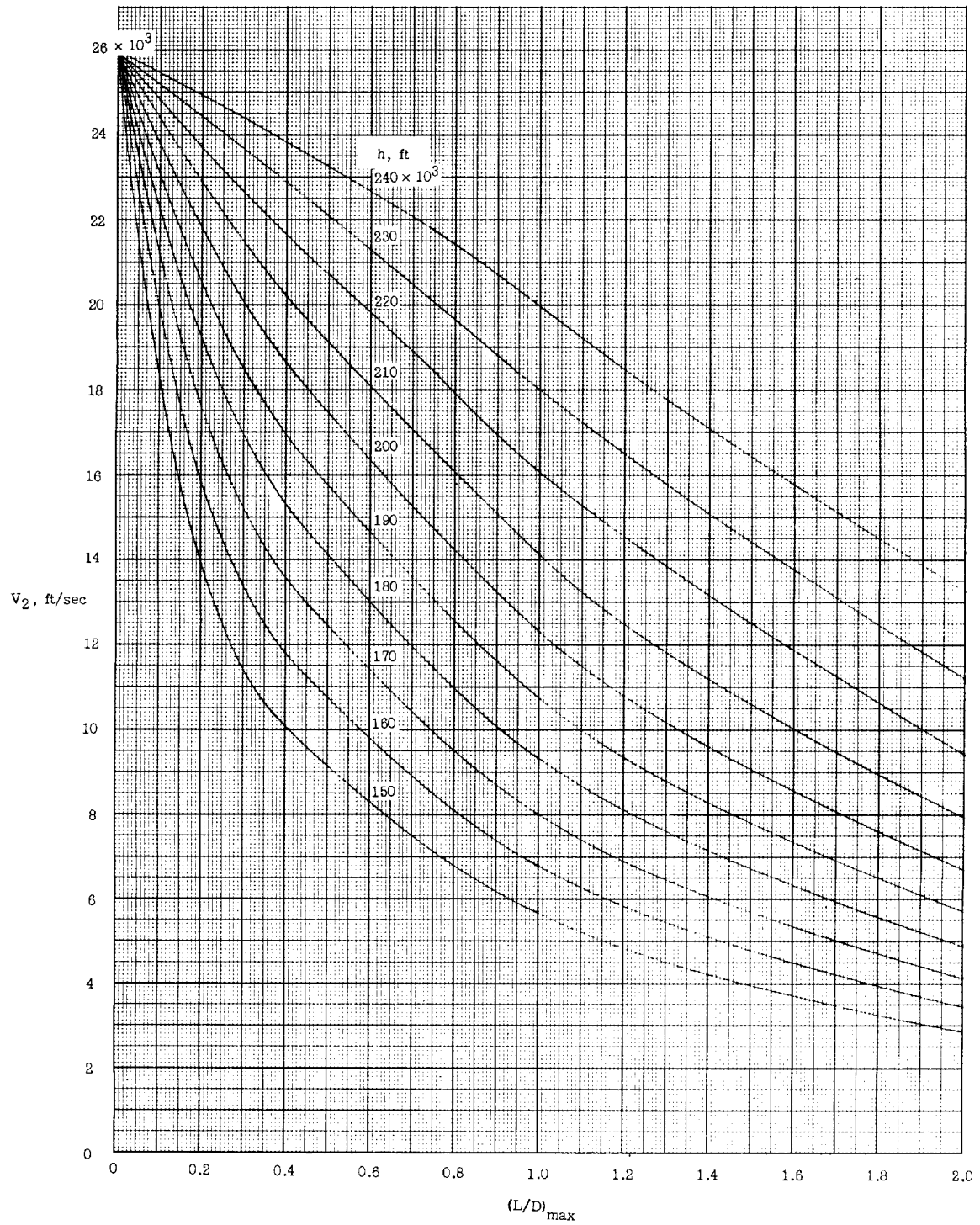
(a)  $\frac{W}{C_D A} = 10$  pounds per square foot.

Figure 6.- Velocity at the end of the constant-altitude maneuver.



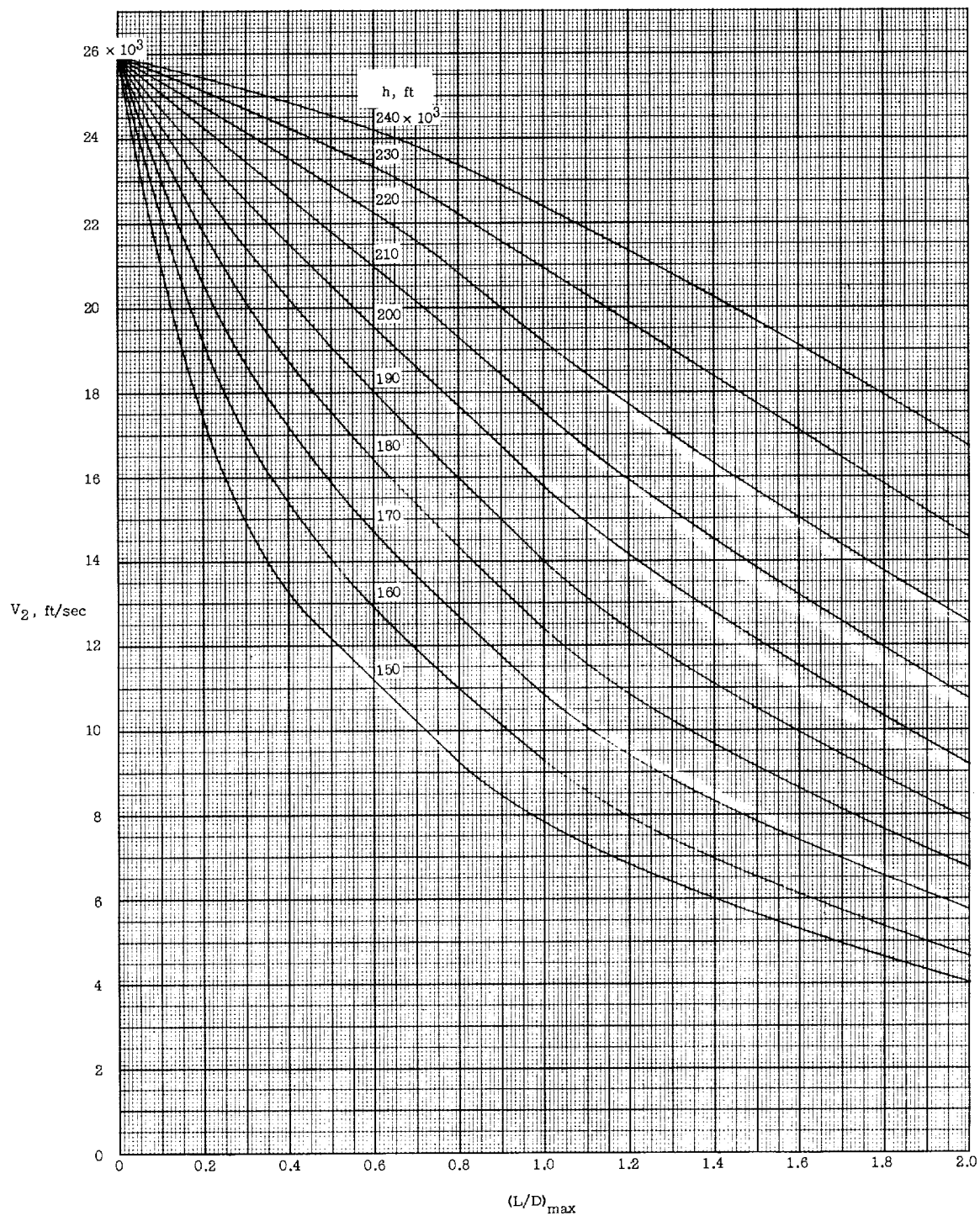
(b)  $\frac{w}{C_D A} = 50$  pounds per square foot.

Figure 6.- Continued.



(c)  $\frac{w}{C_D A} = 100$  pounds per square foot.

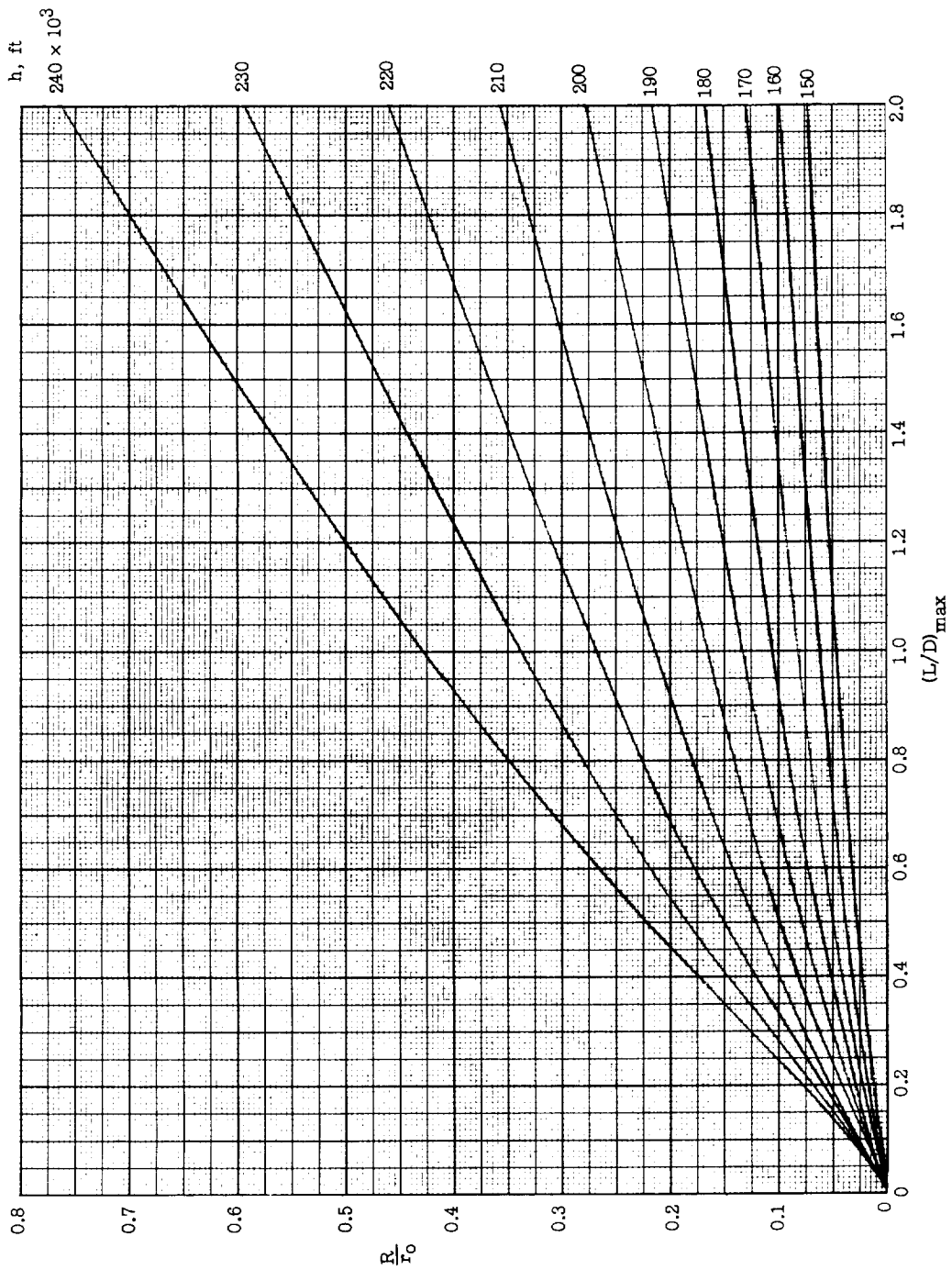
Figure 6.- Continued.



(d)  $\frac{W}{C_D A} = 200$  pounds per square foot.

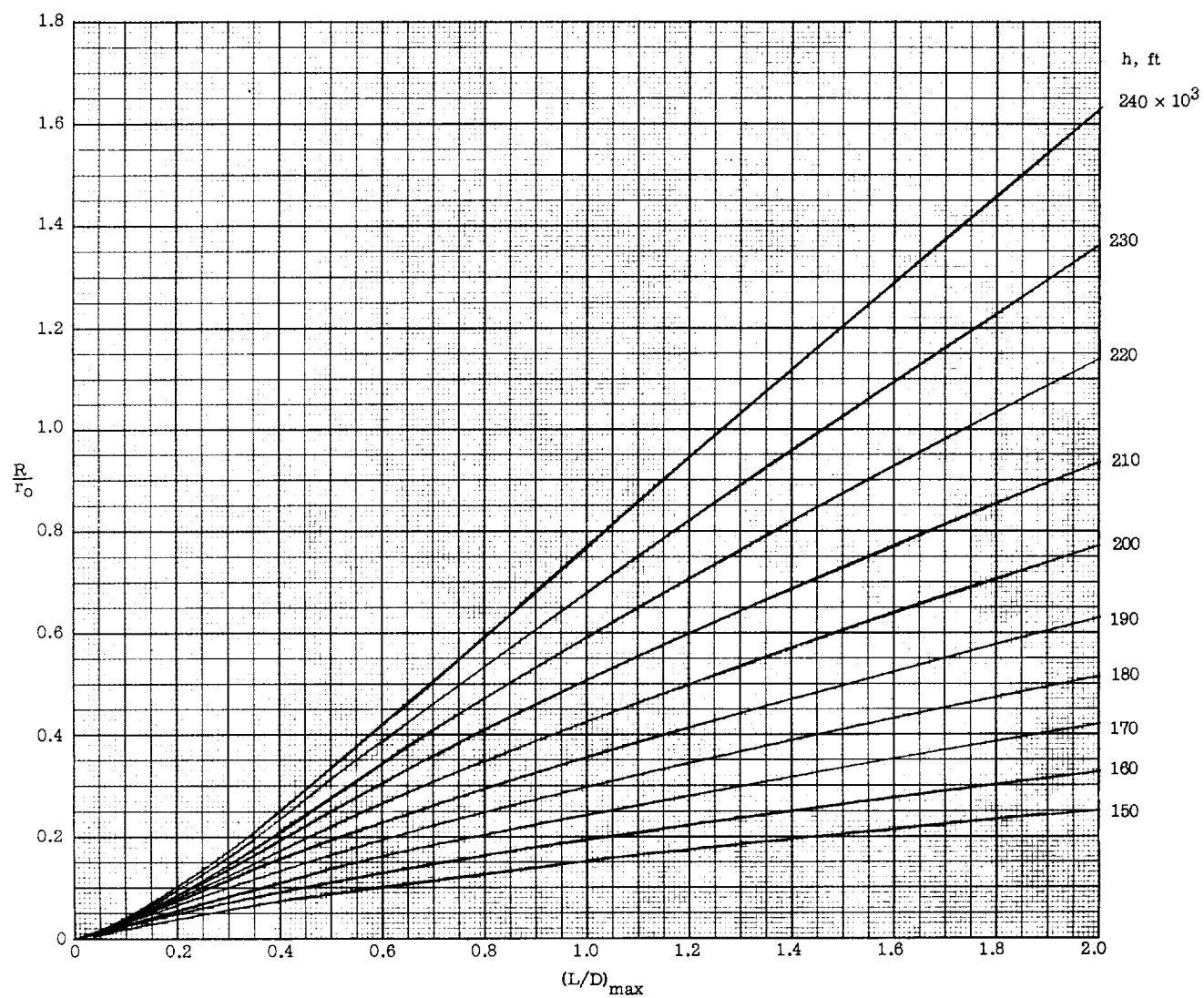
Figure 6.- Concluded.





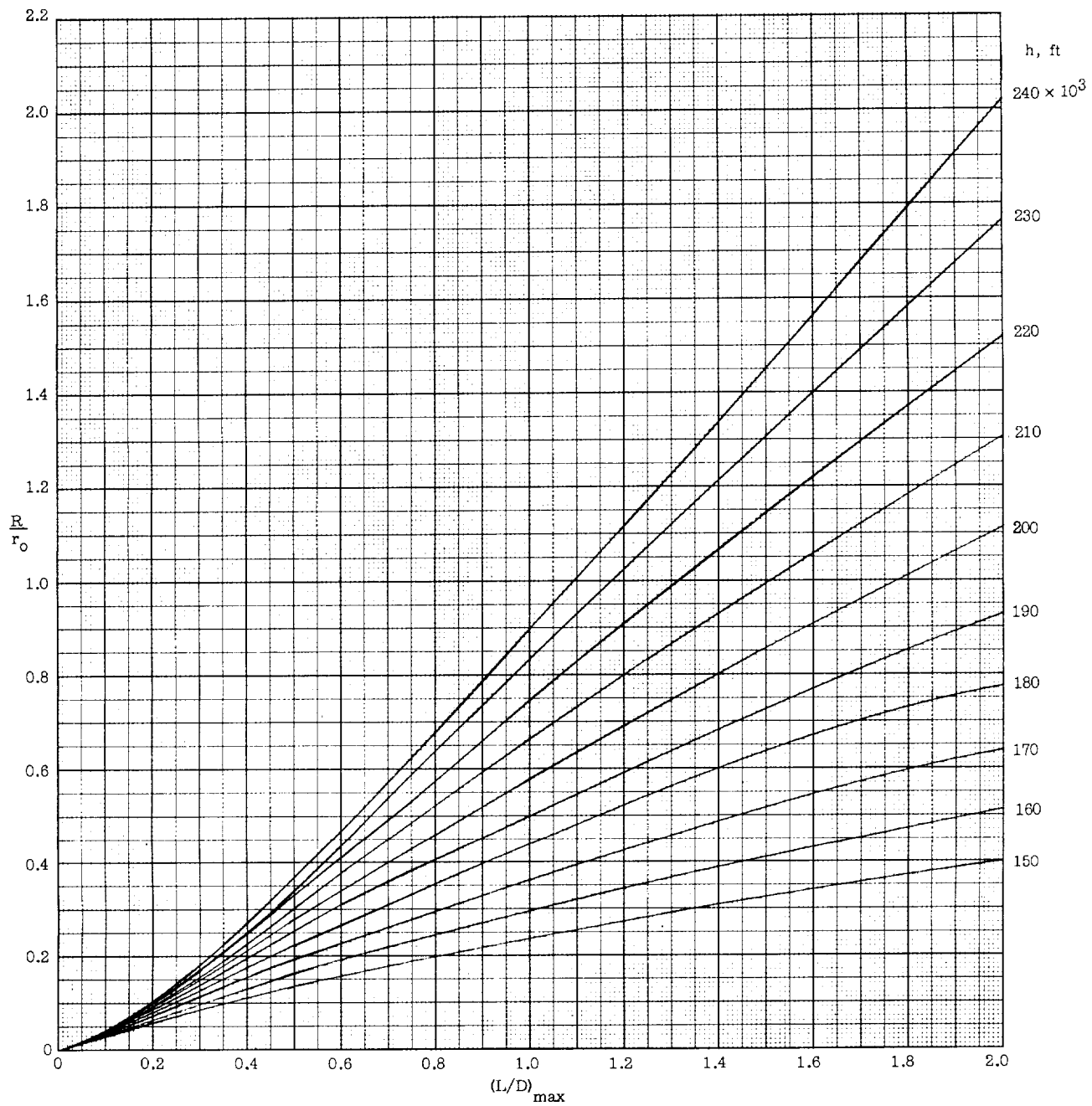
(a)  $\frac{W}{C_D A} = 10$  pounds per square foot.

Figure 7.- Effect of vehicle  $(L/D)_{\max}$  capability on longitudinal range attainable in constant-altitude maneuver.  $\bar{V}_1 = 1.0$ .



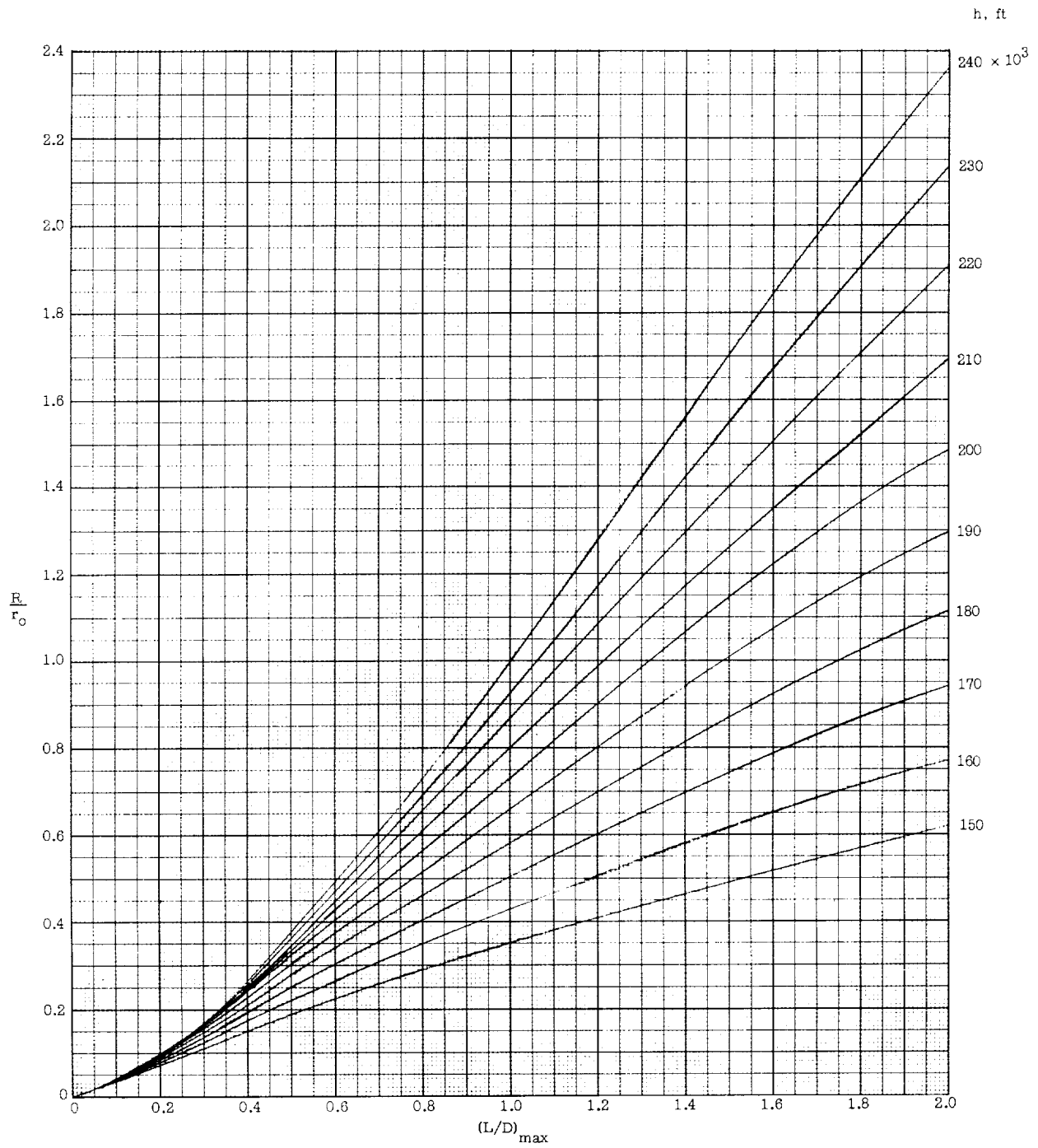
(b)  $\frac{W}{C_D A} = 50$  pounds per square foot.

Figure 7.- Continued.



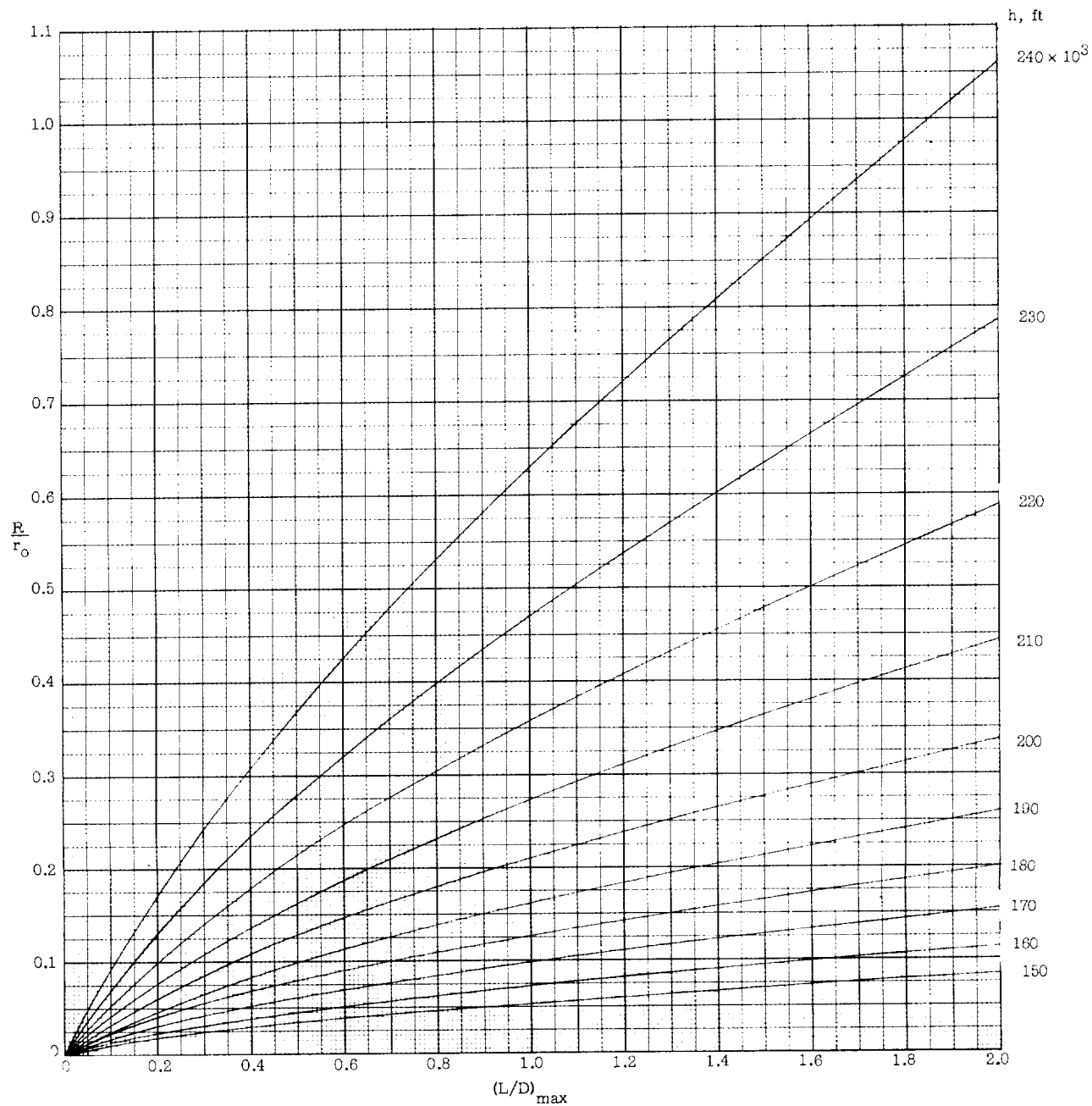
(c)  $\frac{W}{C_D A} = 100$  pounds per square foot.

Figure 7.- Continued.



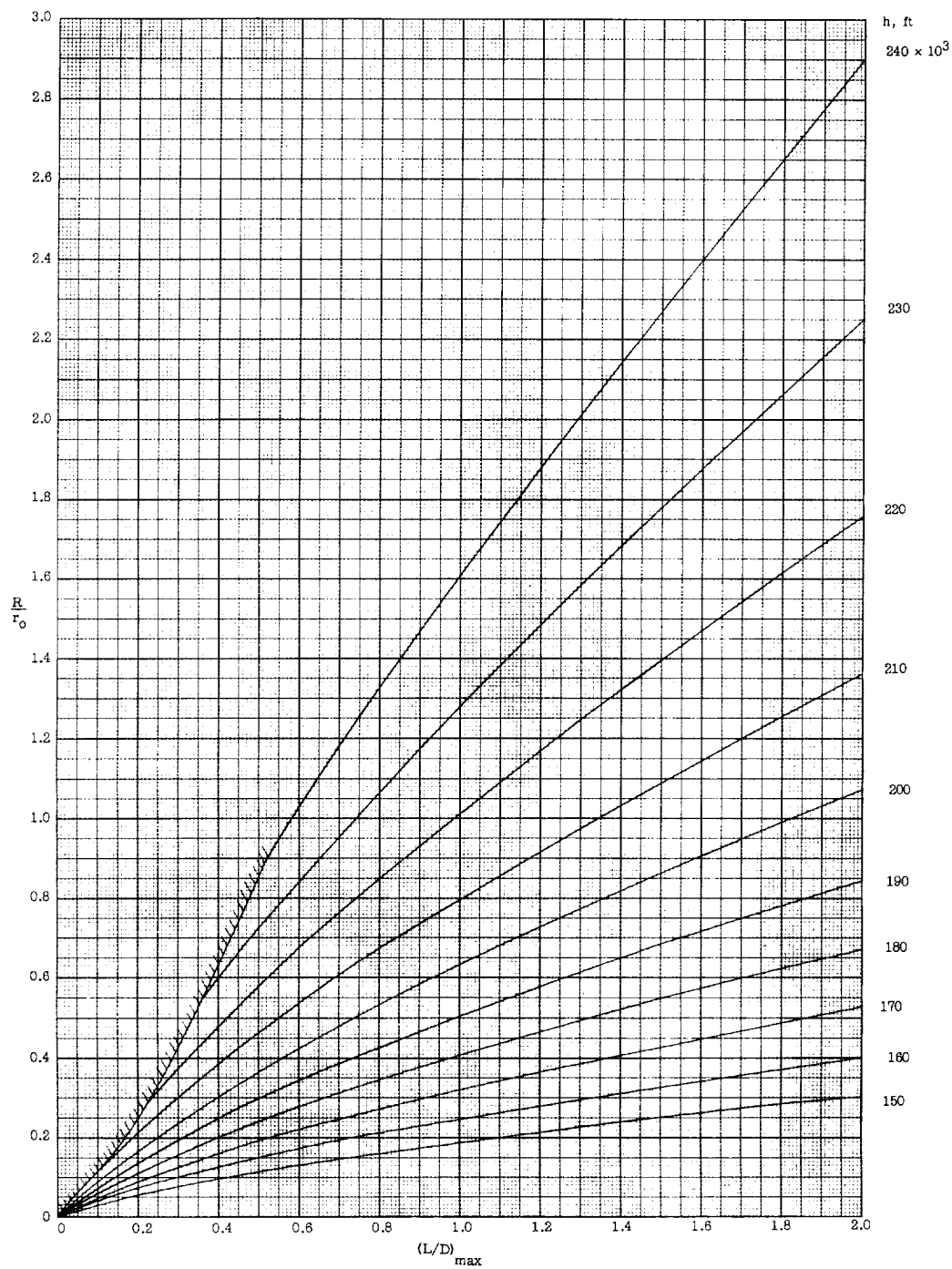
(d)  $\frac{W}{C_D A} = 200$  pounds per square foot.

Figure 7.- Concluded.



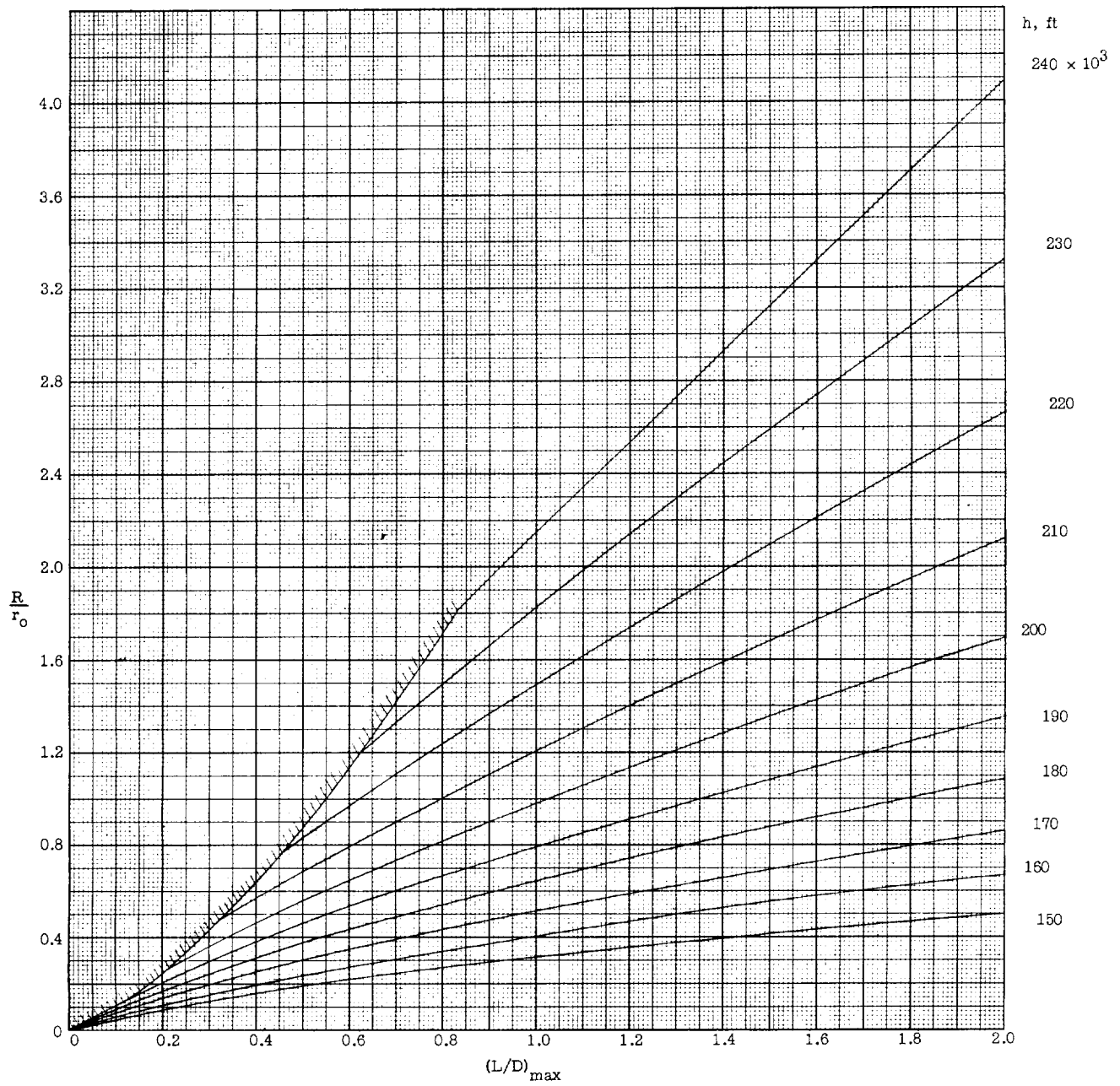
(a)  $\frac{W}{C_D A} = 10$  pounds per square foot.

Figure 8.- Effect of vehicle  $(L/D)_{\max}$  capability on longitudinal range attainable in constant-altitude maneuver.  $\bar{V}_1 = \sqrt{2}$ .



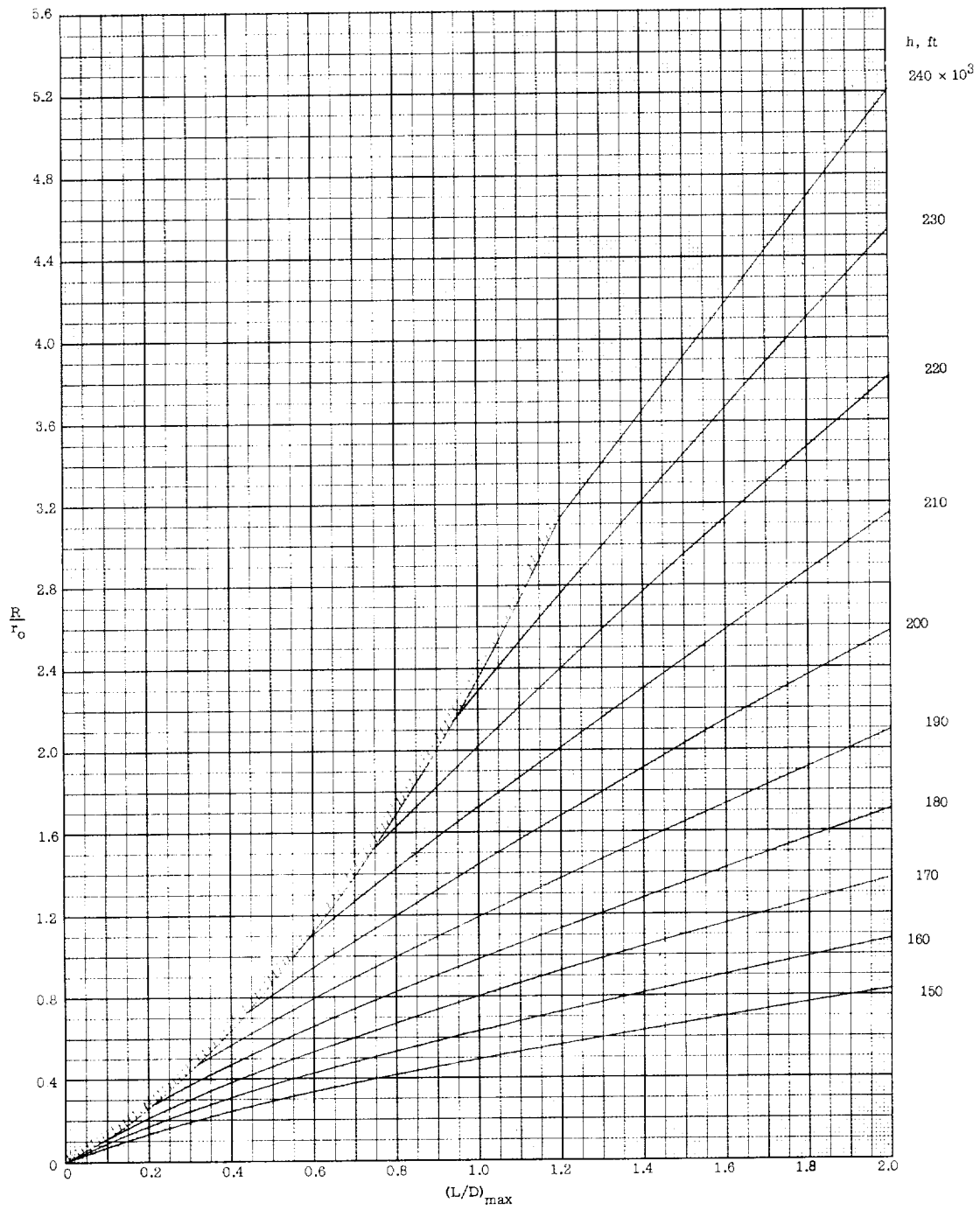
(b)  $\frac{W}{C_{DA}} = 50$  pounds per square foot.

Figure 8.- Continued.



(c)  $\frac{W}{C_D A} = 100$  pounds per square foot.

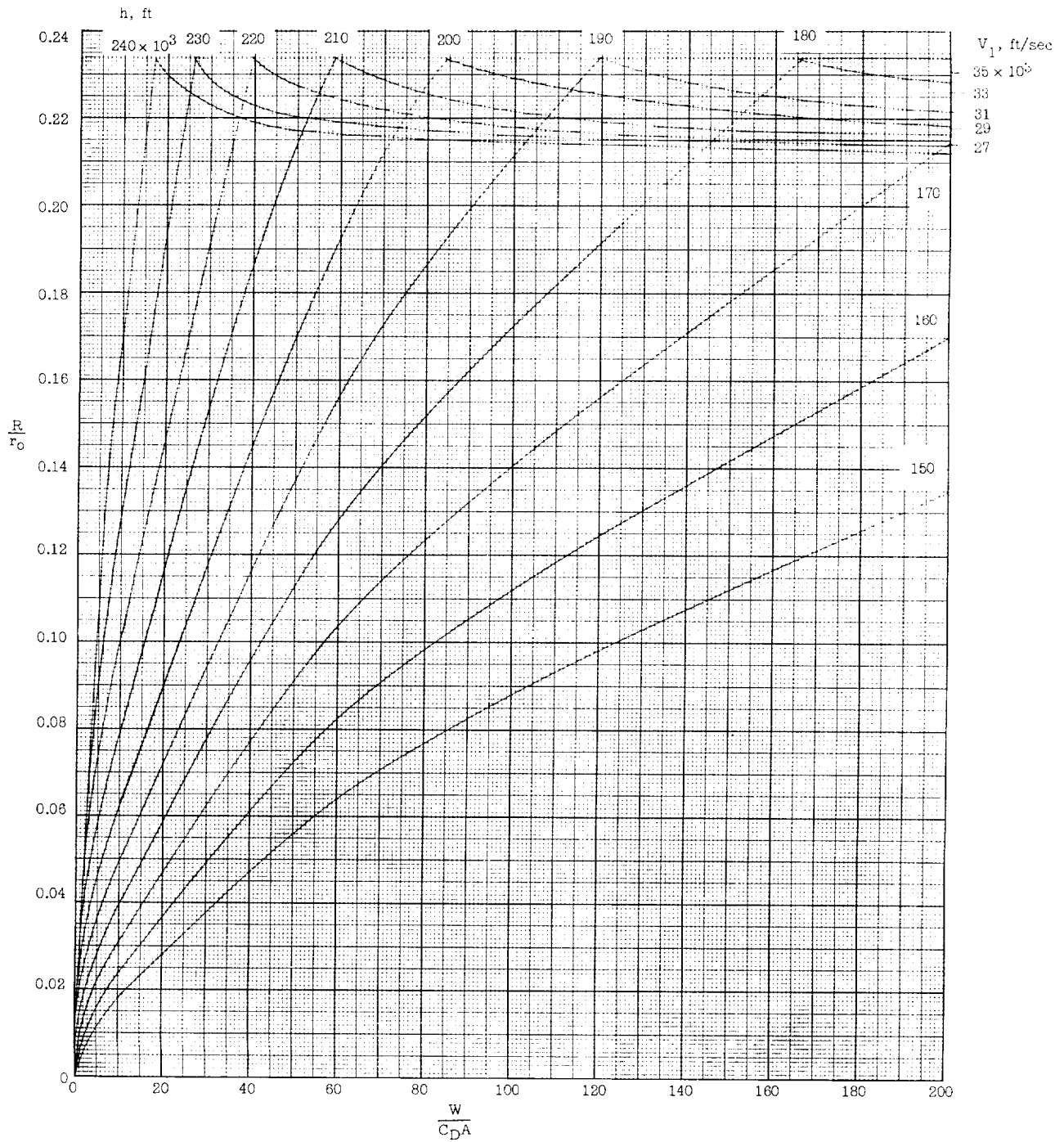
Figure 8.- Continued.



(d)  $\frac{W}{C_D A} = 200$  pounds per square foot.

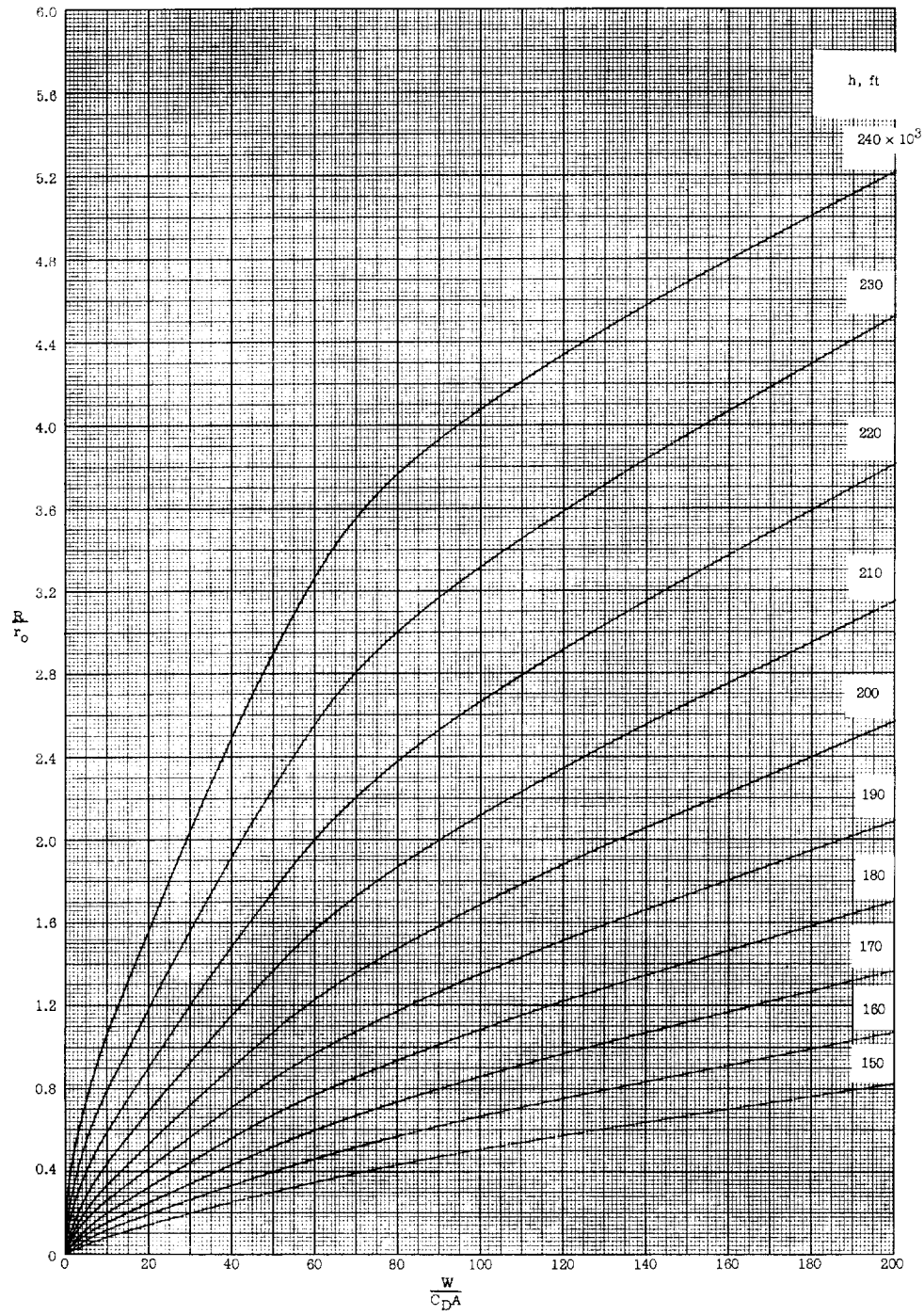
Figure 8.- Concluded.





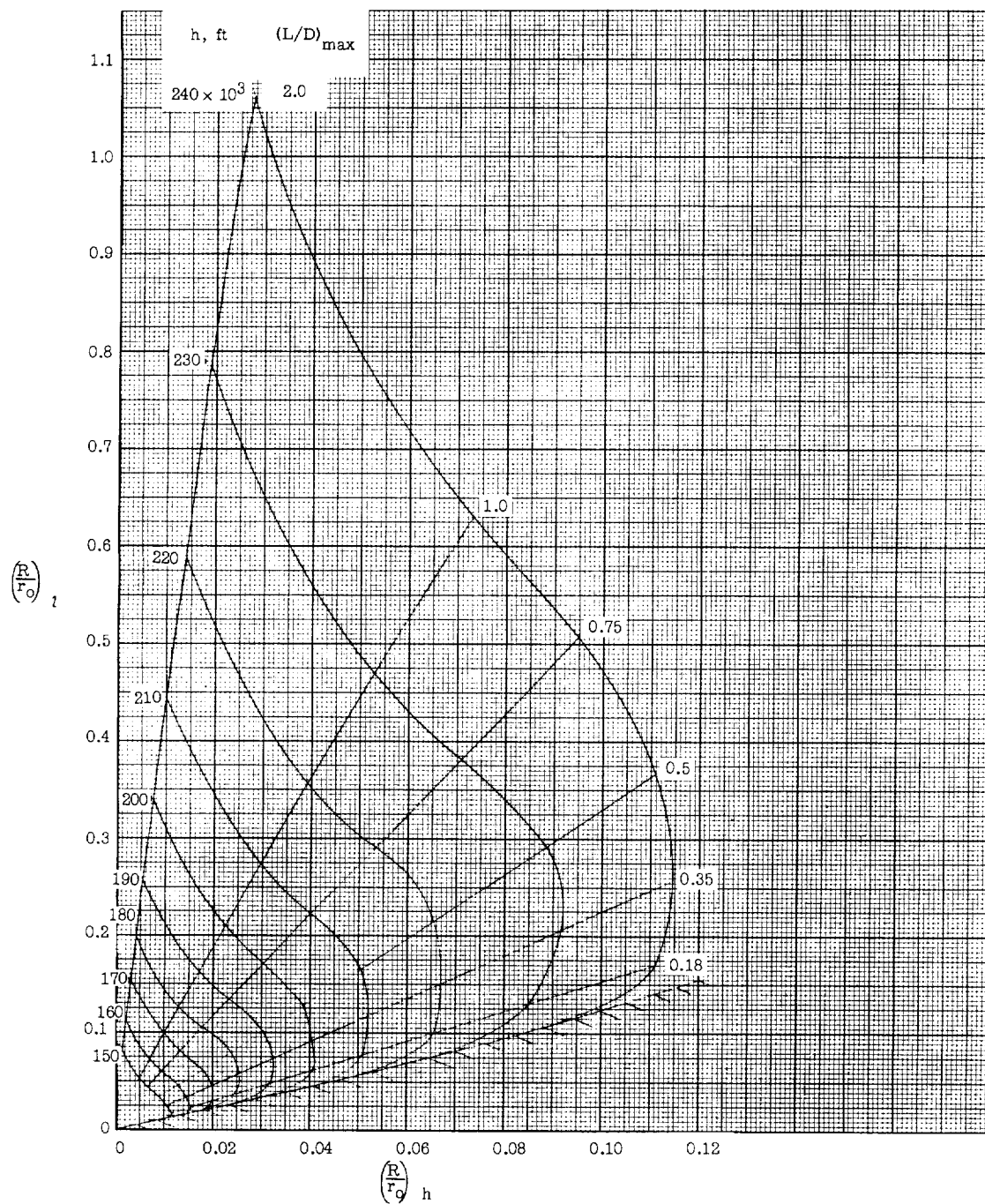
(a)  $(L/D)_{\max} = 0.2$ .

Figure 9.- Effect of vehicle ballistic parameter on attainable longitudinal range for constant-altitude maneuver.



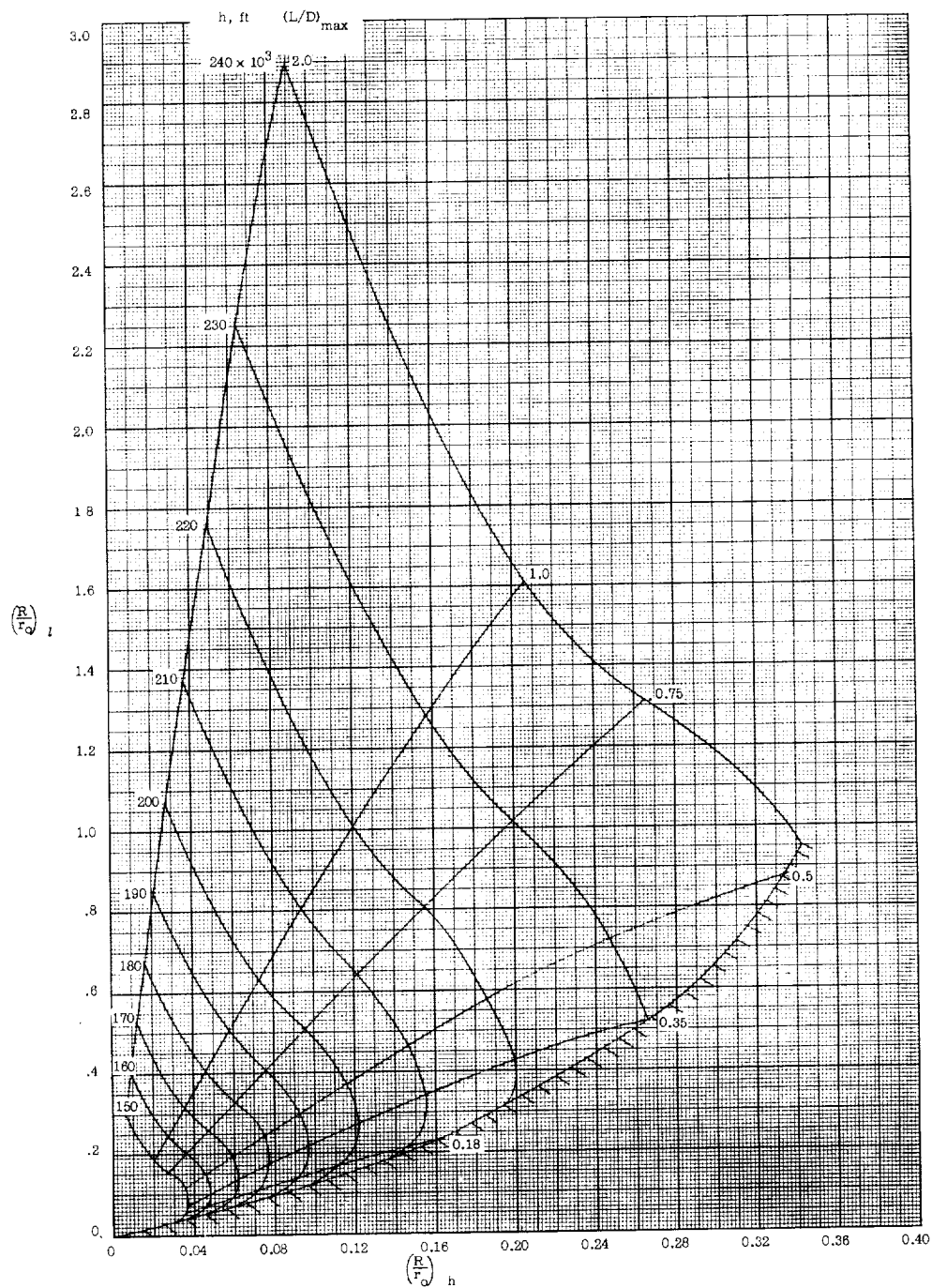
(b)  $(L/D)_{\max} = 2.0$ .

Figure 9.- Concluded.



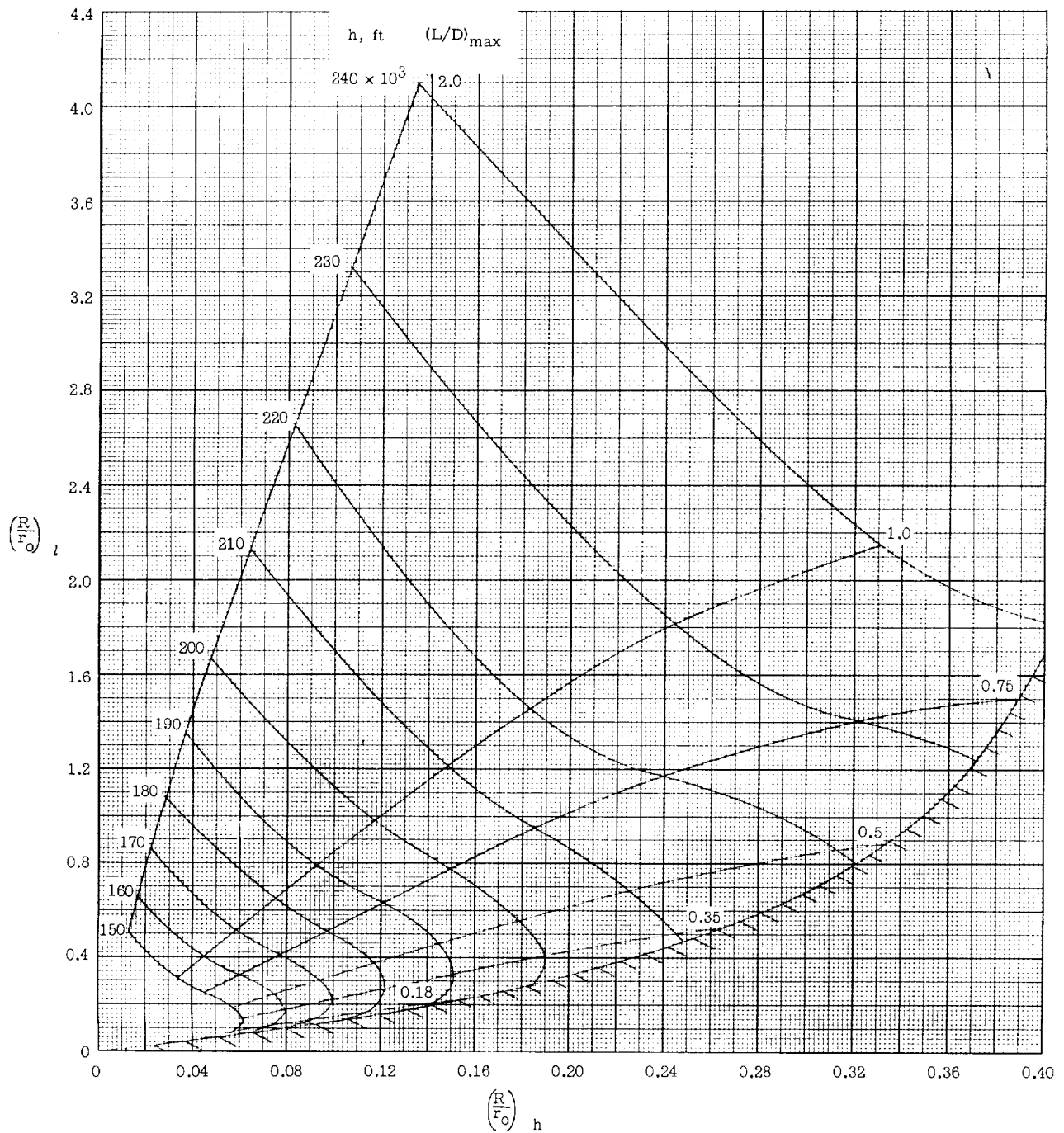
(a)  $\frac{W}{C_D A} = 10$  pounds per square foot.

Figure 10.- Comparison of the longitudinal range attainable by operation on the low-drag side of the drag polar with that attainable by operation on the high-drag side.  $V_1 = 36,500$  feet per second.



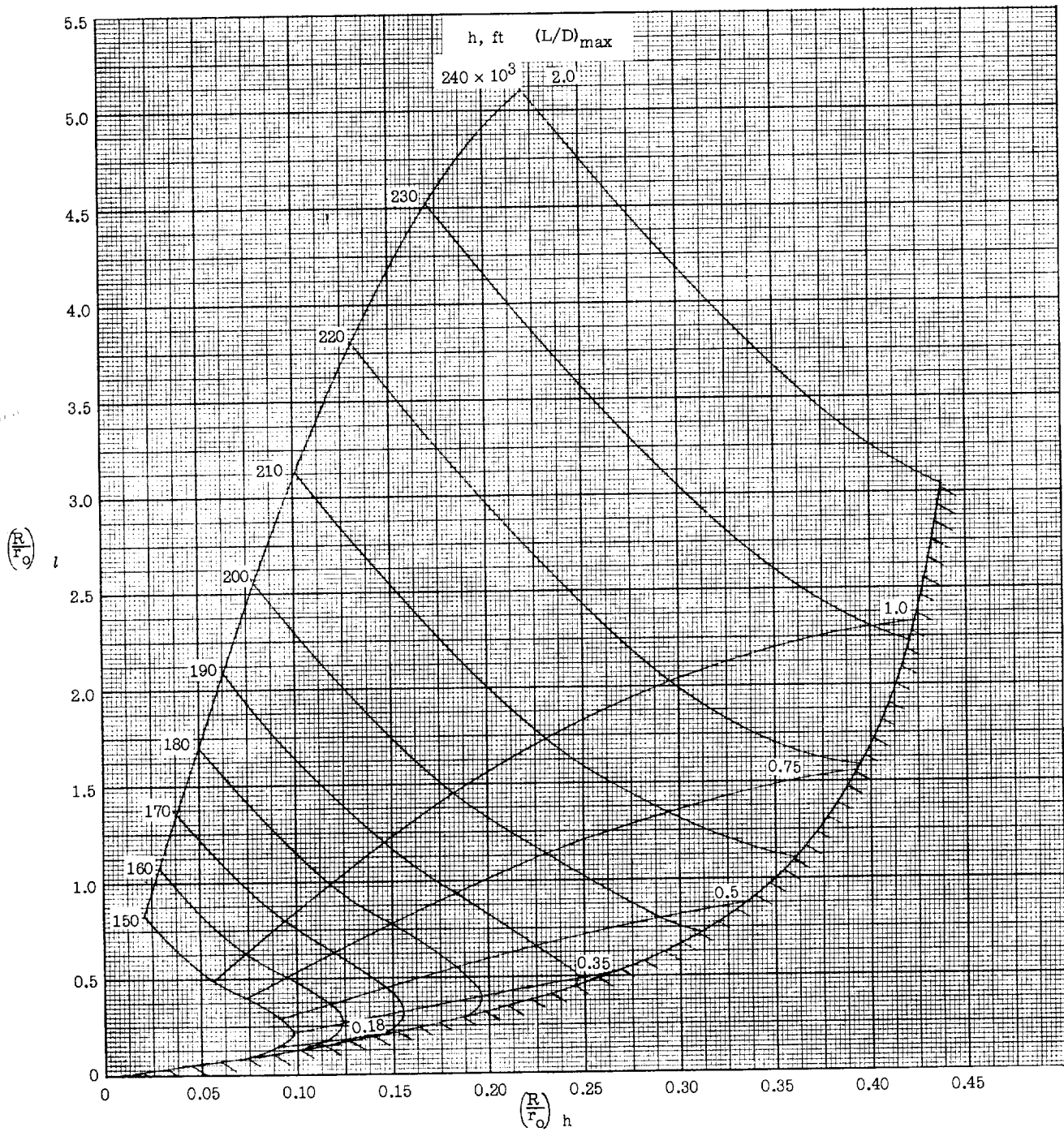
(b)  $\frac{W}{C_D A} = 50$  pounds per square foot.

Figure 10.- Continued.



(c)  $\frac{w}{C_D A} = 100$  pounds per square foot.

Figure 10.- Continued.



(d)  $\frac{W}{C_D A} = 200$  pounds per square foot.

Figure 10.- Concluded.



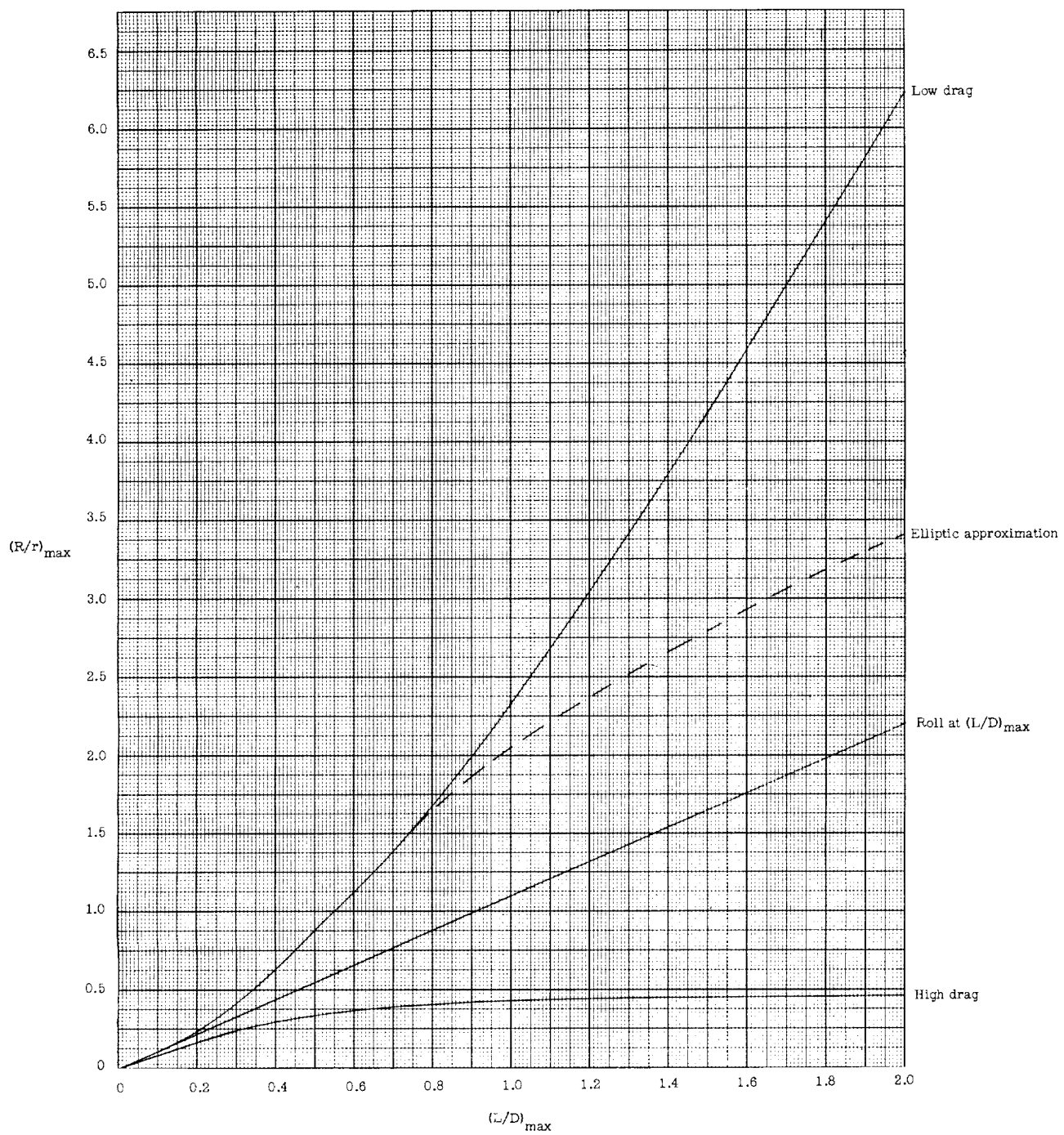


Figure 11.- Maximum range attainable in the constant-altitude maneuver.  $V_1 = 36,500$  feet per second.

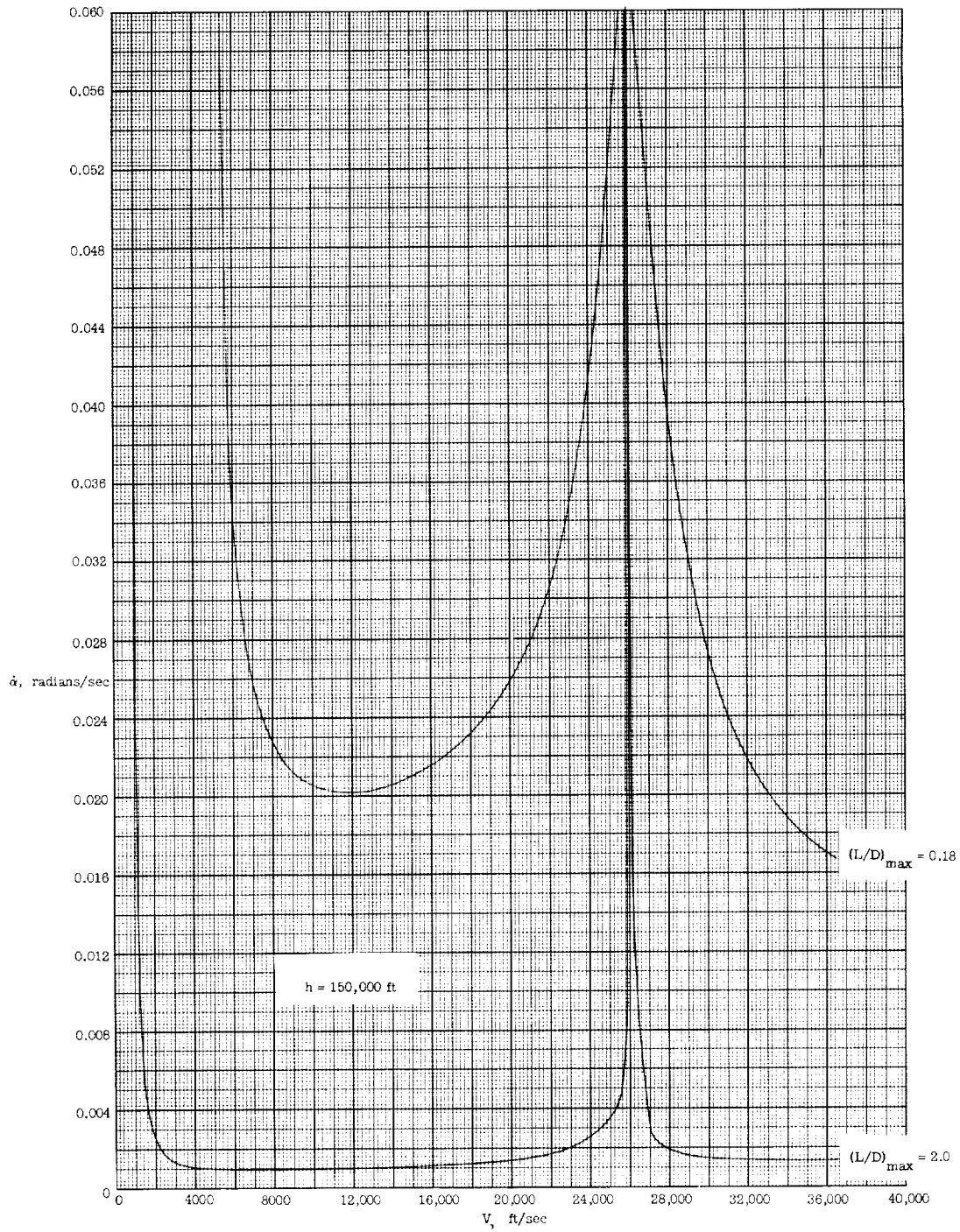


Figure 12.- Typical pitch angle rates associated with the constant-altitude—pitch-controlled maneuver.  $\frac{W}{C_D A} = 10$  pounds per square foot.



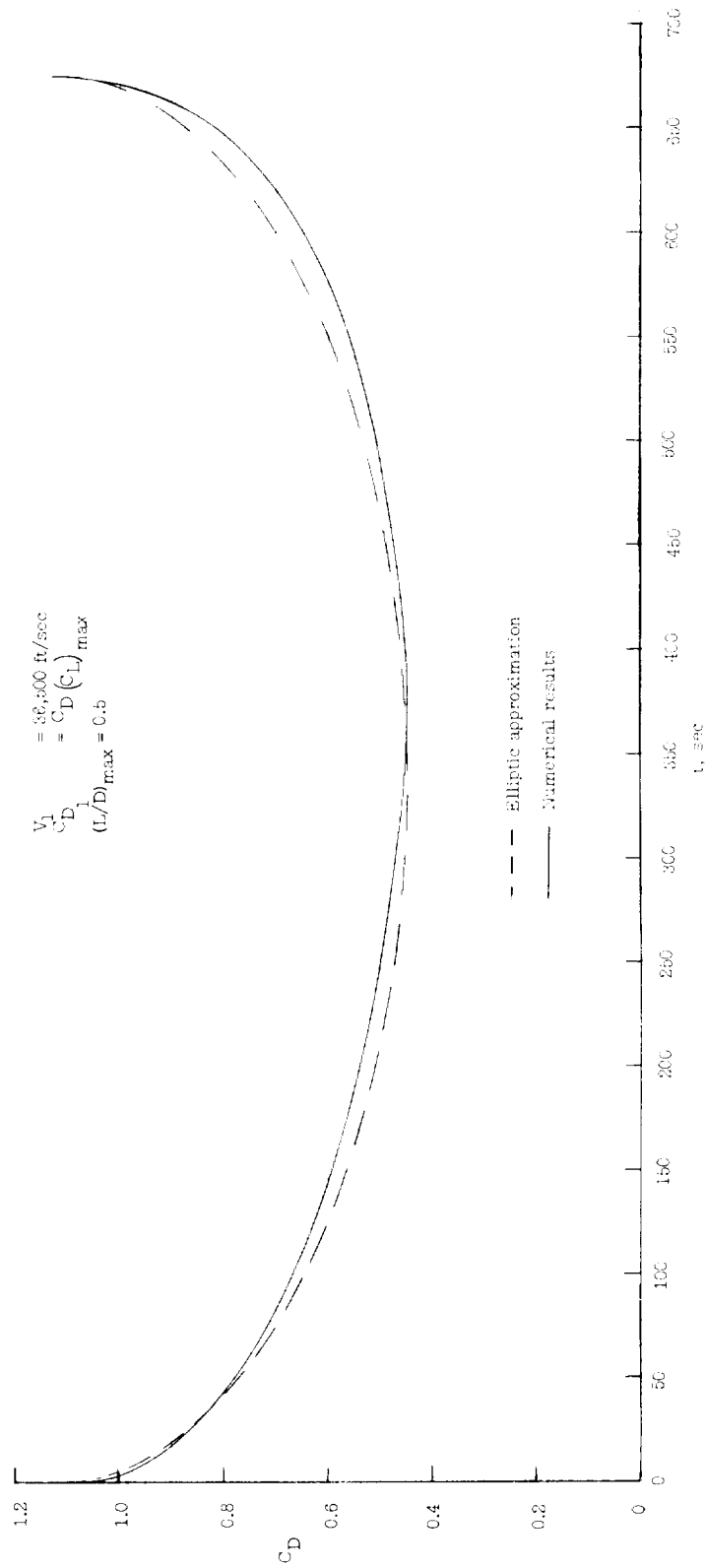


Figure 13.- Comparison of the elliptic approximation to the drag-coefficient--time variation with numerical results.

